RICE UNIVERSITY

Designing Quantum Multicritical and Flat-Band Models via Hamiltonian Engineering

by

Youjiang Xu

A Thesis Submitted
in Partial Fulfillment of the
Requirements for the Degree

Doctor of Philosophy

Approved, Thesis Committee:

Han Pu, Chair
Professor and Chair of Graduate Program
of Physics and Astronomy

Qimiao Si
Harry C. and Olga K. Wiess Professor of
Physics and Astronomy

Junichiro Kono
Karl F. Hasselmann Chair in Engineering,
Professor of Electrical and Computer
Engineering, Chair in Applied Physics,
Professor of Physics and Astronomy,
Professor of Materials Science and
NanoEngineering

Houston, Texas

April, 2021

ABSTRACT

Designing Quantum Multicritical and Flat-Band Models via Hamiltonian Engineering

by

Youjiang Xu

Atomic, molecular, and optical (AMO) systems often feature great controllability. As such, they offer ideal platforms to explore various kinds of quantum phenomena. Designing artificial quantum systems that possess novel and exotic properties is one of the major tasks of theorists working in the AMO field. In this dissertation, we introduce our work on designing novel Hamiltonians which give rise to multicriticality or flat bands.

In the first half of the dissertation, we study the multicriticality. Quantum many-body systems that support multicritical quantum phase transitions are quite rare. However, we find that, in an important generalization of the Dicke model, the superradiant quantum phase transitions can become multicritical. For a subclass of experimentally realizable schemes, multicritical conditions of arbitrary order can be expressed analytically in compact forms. As such, experiments can be readily designed to achieve quantum phase transition of desired order. The phase transition happens both in the thermodynamic limit and the classical oscillator limit. We compare the quantum fluctuation in the two cases by calculating the atom-photon entanglement entropy. We find that the order of the criticality strongly affects the critical entanglement entropy.

In the second half of the dissertation, we propose a powerful and convenient method to systematically design flat-band lattice models. Flat bands often lead to exotic strongly correlated emergent quantum phenomena. We use this method to generate several classes of lattice models, including models with both short- and long-range hoppings, both ordinary and magnetic translational symmetry, both topologically trivial and non-trivial flat bands.

Acknowledgments

My deepest gratitude is for Prof. Han Pu, my most helpful advisor and kindest friend. Han encourages me to develop and pursue my own research interest, and provides as much help as he can. Han is also very considerate in life, and we had great time playing badminton together.

I also want to thank all members in our group, including previous members Li Yang, Lin Dong, Chuanzhou Zhu and Xinghai Zhang, and current members Diego Fallas Padilla and Shah Saad Alam. I am so grateful that Li introduced me to join this group. And it has been a pleasant experience working together with Diego on one of the project covered in this dissertation.

I would like to thank Prof. Frank Geurts who kindly guided me in annual committee reviews and Prof. Kaden Hazzard for his support. Also, I want to thank my doctoral committee members, Prof. Qimiao Si and Prof. Junichiro Kono and our graduate coordinator Rosa Almendarez.

Last but not least, I want to thank my parents and my beloved Chen Chen for their firm support.

Contents

Illustrations

Tables

Chapter 1

Introduction

Atomic, molecular, and optical (AMO) physics is one of the major division of physics, featured by unprecedent level of controllability of the underlying quantum systems. For example, optical atomic clocks have developed to an accuracy level with a systematic uncertainty below 10^{-18} [1], a precision hardly achieved in any other platform. The high controllability means that we can construct artificial quantum systems with atoms, molecules and light, aiming to study or utilize the novel phenomena emerging from such systems. For example, by pushing the temperature to as low as 170 nanokelvins through laser and magnetic cooling, people first observed Bose-Einstein condensate in ultracold rubidium gas in 1995 [2], about seventy years after the phenomenon was predicted. Thus, designing new quantum systems and predicting their novel properties represents one of the major tasks of theoretical physicists working in the field of AMO.

In designing new quantum systems, one important routine is to construct an effective and simplified model that captures the essential physics of a more complex system, and study the properties of the effective model. In general, an effective model arises when there are more degrees of freedom than needed: we do not need three but two numbers to describe the position of a ball rolling on the ground, because the gravity confines the ball to its lowest-energy states, and it will not jump unless it is excited, so its dynamics is effectively two-dimensional rather than three-dimensional. In quantum mechanics, the degrees of freedom equals the dimension of the Hilbert

space, and usually only a small fraction of the whole Hilbert space is needed to effectively describe the physics (thus it is possible to simulate many quantum systems on classical computers, otherwise the dimension of the whole Hilbert space, which grows exponentially when the size of the systems enlarge, will deny classical simulation). Perhaps the most well-known effective model in AMO physics is the two-level atom model. We know that even the simplest atoms, the hydrogens, contain infinite number of electronic configurations. However, when it is close to zero temperature, the atoms will almost always stay in its single lowest-energy state. To make things more interesting, we shine a monochromatic light on the atoms and consider the coupling between the atoms and the light. As long as the frequency of the light is sufficiently close to the energy spacing between the ground state and certain excited state of the atoms, then the possibility of the atom transiting to the other excited states is so small that we can safely neglect these unpopulated states in the effective description of this atom-light system. Consequently, we arrive at the famous semiclassical Rabi model [3], describing the basic form of interaction between an atom and light. Such a two-level simplification of the atoms works well in many applications. Removing redundant degrees of freedom can also be done for the light. An optical lattice uses pairs of counter-propagating lasers to confine the atoms in a lattice-like structure. The mechanism is AC-Stark shift, that is, the atoms absorb a photon from one laser beam and emit a photon to another, in which process, the energy of the atoms is shifted, and the amount of the shifted energy is position-dependent, so the atoms effectively experience a potential resembles a lattice. Finally, in studying the properties of atoms in an optical lattice, we do not consider the possibility that atoms may make transition to other internal states, and the dynamics of the light is ignored, so we effectively arrive at lattice models for atoms resembling those studied in condensed

matter context. In this way, optical lattices, as an effective description of a specific kind of atom-light systems, provide a platform for simulating other quantum systems, taking advantages of great tunability of AMO systems.

Thus, optical lattices, as well as many other platforms and techniques developed in AMO physics, inspire us that novel physics may be explored experimentally if we cleverly design AMO systems whose effective model is of interest. Especially, in this dissertation, we address two types of models we design: 1) Dicke-like models featured by multicriticality associated with superradiant quantum phase transitions, and 2) Lattice models with flat bands. The former can be obtained by manipulating the hyperfine states of atoms through cavity-assisted Raman transitions, and the latter can possibly be realized using optical lattices or synthetic dimension. The basic story line of the dissertation is as follows:

1. In Chapter 1, we introduce the background and motivation of studying multicriticality and flat bands;

2. In Chapter 2, we focus on the multicriticality that occurs in the superradiant phase transitions in the generalized Dicke models. We focus on the multicritical conditions and quantum fluctuations in such models, and study the potential experimental realization;

3. In Chapter 3, we introduce the new protocol for generate all the lattice models whose lowest bands are flat. We show how to apply the protocol to produce some models with finite-range hopping and the Kapit-Mueller model featuring a topological flat band.

Finally, in the last chapter, we provide a summary and discuss possible follow-up research on these topics.

1.1 Multicriticality in AMO physics

Critical phenomena were discovered by Cagniard de la Tour in 1822 [4], who found that when a liquid heated far beyond its boiling point, it becomes indistinguishable from gas, namely entering the supercritical fluid phase. The difference between liquid and gas is marked by the density, which serves as the order parameter of this phase transition. Normally, the density changes discontinuously during a phase transition, however, when we increase the temperature, the density difference between the gas and the liquid becomes smaller and smaller, and finally, when we reach the critical temperature, the densities of the two become the same. Thus, the critical point in this system is the point where the boundary of the discontinuous liquid-gas phase transition terminates.

The physics at the critical point has two major characters: One is the large fluctuation, in the gas-liquid case the large fluctuation in density, which results in critical opalescence [5], and the other is the universal scaling behavior, that is, the physical quantities that deviates a little from their critical values obey some power laws, whose exponents are universal in the sense that phase transitions with different microscopic components may share the same critical exponents.

In the liquid-gas phase transitions, the relevant thermodynamic parameters are temperature and pressure, and there is a single isolated critical point in the two-dimensional phase diagram. When there are more thermodynamic variables, for example, the mole fraction between the two components in a binary fluid mixture, the phase diagram can have larger dimension and the critical point can extend to a critical manifold. In 1970, Griffiths [6] studied the phase transition in He^3-He^4 mixture and found that there were three critical lines in the phase diagram, which intersected at a special point, the tricritical point. It was the first time that a tricritical point

was discovered. In the paper, Griffiths compared the experiment results and the predictions of classical theory, and argued that the discrepancy between them could be explained by a modified scaling formula, suggesting that the tricritical points had its own universality class differing from that of the ordinary critical points. The scaling behavior of a tricritical point is discussed in [7–10]. It is shown that the crossover effect of multiple critical lines makes it necessary to alter the scaling hypothesis at the tricritical point. Later, the concept of tricriticality is generalized to higher-order multicriticality [11–13]. In [11], the order of criticality is defined by deduction, that is, an n^{th} order critical manifold is defined as the intersection of $(n-1)^{\text{th}}$ order critical manifold, with the condition that an ordinary critical point is of second-order. Multicritical points with different orders exhibit different critical behaviors [14, 15], which may provide deeper insight into phase transitions and critical phenomena.

Though multicriticality is an intriguing and important topic in phase transitions, people have rarely found high-order critical points in experiments. The reason is that higher-order critical manifolds have lower dimension, thus more tunable parameters are needed to pinpoint the high-order critical points. Specifically, an n^{th} order critical point usually appears only in phase diagrams of dimension $n-1$ or more. It is also argued that randomness may depress multicriticality [16], which may also be a reason for rare observation of multicriticality.

Because AMO systems provide experimental platforms with a large number of tunable parameters, we naturally expect to realize high-order criticality through carefully designed light-matter interaction. In 2019 [17], we propose a modified Dicke model in which a tricritical point occurs on the boundary of the superradiant quantum phase transitions. The Dicke model [18] describes a single photonic mode interacting with identical two-level atoms, which can be regarded as the many-body version of

the quantum Rabi model. Quantum phase transitions (QPTs) are phase transitions which happen at zero-temperature. As a result, quantum criticality is dominated by quantum fluctuations rather than thermodynamic fluctuations. The Dicke model supports a QPT in the thermodynamic limit: When the atom-photon interaction strength is low, the system is in a normal phase in which the photonic mode is not macroscopically populated; and when the interaction strength increases and exceeds a threshold, the system will enter a superradiant phase in which the number of populated photons will be proportional to the number of atoms. The original superradiant QPT is a second order one with an ordinary critical point at the phase boundary. We show in [17] that if we introduce a staggered magnetic field to the atoms, we can expand the one-dimensional phase diagram to two-dimensional and extend the critical point to a critical line, which terminates at a tricritical point, and the phase diagram is identical to the one discussed by Griffiths in [6], in the sense that the phase diagrams share the same topology. Our work on the tricritical Dicke model was followed by the authors of [19] to achieve fourth-order criticality in Dicke-like systems. For the experimental part, a tricritical point has been found in spin-1 spin–orbit-coupled Bose gases [20].

In our most recent work, we find that arbitrary-order multicritical point can be realized in generalized Dicke models, which includes previously-found multicritical Dicke-like models as special cases. We discuss in detail under what condition multicritical phenomena will happen. And we also study the quantum fluctuation characterized by bipartite von Neumann entanglement entropy. We will introduce the details of this work in Chapter 2.

1.2 Artificial flat-band lattice models

Tight-binding lattice models are powerful simplifications of real physical processes happen in crystals. While an electron in a crystal possesses infinite many degrees of freedom, tight-binding lattice models approximate the real physics by assuming that only a finite number of degrees of freedom are relevant, like the assumption made in two-level atoms. The tight-binding lattice models capture the essential physics while being simple, and are widely used in condensed matter physics. In AMO physics, optical lattice [21], synthetic dimension [22], and other techniques, provide platforms of artificial lattices.

The simplest lattice models consider only single-particle processes without taking interactions into account. With the discrete translational symmetry of the lattice, the single-particle eigenstates of the models are Bloch waves, taking the pseudo-momentum as their quantum number, grouping the eigenenergies into several bands, and the number of bands equals the degrees of freedom per lattice cell. When a band is dispersionless, i.e., the energy is independent of the momentum, we say the band is flat.

Flat bands can occur naturally, leading to quantum magnetism [23], or be constructed from artificial lattices with specially designed lattice structures [24]. We are curious about the latter. A flat band contains massively degenerate eigenstates. The massive degeneracy of a flat band has two major consequences: 1). The band has no intrinsic energy scale and could be sensitive to even the weakest perturbation and produce rich physics, and 2). Because the Bloch waves in the band share the same energy, it is possible to superimpose them to build localized states which remain as eigenstates on the same band. The sensitivity of flat bands to perturbation is one of the most important motivation of studying flat-band models. For example, when the

perturbation is disorder causing Anderson localization, the flatness may modify the localization length [25], create 'inverse' Anderson transition [26], or generate disorder-induced topological phase transitions [27], etc. When the perturbation is interaction, strongly correlated phases may be produced [28–30]. And one of the most well-known novel physics emerged from flat band is the fractional quantum Hall effect [31–33] that is the result of the combination of degenerate Landau levels and interactions between electrons.

Because of the amazing properties of flat bands and the growing capability of fabricating lattice models in lab, it is worth figuring out a systematic way of designing flat-band models. People have tried various method for building flat bands [34–38], most of them utilizing the so-called compact localized states (CLSs). As we mentioned earlier, flat bands support localized states as their eigenstates, and a CLS is a state among the various localized eigenstates that minimizes the number of cells occupied by the states. The flat-band Hamiltonian is the parent Hamiltonian of the CLSs, in the sense that the CLSs resides in the null space of the Hamiltonian, up to a constant energy shift (i.e., shift the energy of the flat band to zero). Given a CLS, we may be able to construct a flat-band model by solving an inverse eigenvalue problem.

Though the CLS method successfully generate all kinds of flat-band models in one-dimensional lattices [34], it faces some major difficulties, particularly for higher spatial dimensions. For an arbitrary localized state on a given lattice, its parent Hamiltonian may not exist, because the corresponding inverse eigenvalue problem that may not have a solution. Moreover, the inverse problem is in general computationally cumbersome, particularly for spatial dimensions larger than one. Another drawback of the CLS method is that information about the band spectrum cannot be obtained readily. In particular, one cannot know a priori whether the flat band is

a ground or an excited band, while it is often preferred that the flat bands are the lowest bands if the model is realized by superconducting networks [24].

With these considerations in mind, we propose a new protocol of generating flat band models utilizing a simple mathematic object in linear algebra, the Gram matrix. We will introduce the protocol in Chapter 3, and it can be seen that all the difficulties faced by the traditional CLS method can be overcome.

Another feature of our new protocol is the capability of generating topological flat bands. Through the Gram matrix method, we reproduce the Kapit-Mueller model [39–41], which supports massively degenerate ground states with non-trivial Chern number that can be regarded as Landau levels on discrete lattices. Our method reveals the universal scaling of the degeneracy of the flat band in the Kapit-Mueller models, which is closely related to the completeness of some subsets of coherent states and is applicable to infinite many different models that do not share the discrete Landau level description.

Chapter 2

Multicriticality in generalized Dicke models

2.1 Dicke model and superradiant phase transitions

In 1954, Dicke [18] discovered that two-level atoms trapped within a small volume can emit photons coherently and constructively, leading to amplified radiation named superradiance. Ever since then, the Dicke model has attracted extensive attention and become one of the most iconic models in quantum optics and quantum many-body physics. The Dicke Hamiltonian is given by

$$H_{\text{Dicke}} = \omega a^\dagger a + \frac{g\left(a + a^\dagger\right)}{2\sqrt{N}} \sum_{k=1}^{N} \sigma_x^{(k)} + \epsilon \sum_{k=1}^{N} \sigma_z^{(k)}, \tag{2.1}$$

which describes an ensemble of two-level atoms interacting with a quantized photonic mode. In Eq. (2.1), the two-level atoms are depicted by Pauli matrices σ_x and σ_z where the upper index distinguishes different atoms. The bare atomic term $\epsilon\sigma_z$ gives the energy spacing 2ϵ between the two levels. The total number of atoms is N. The photonic mode is represented by bosonic annihilation and creation operators a and $a^\dagger$, and the light frequency is ω. The atoms and photons couple through the dipole moment represented by σ_x, and the dipole interaction strength is given by g. The Hamiltonian processes a Z_2 symmetry such that H_{Dicke} is invariant when adding minus signs to the photonic and atomic operators simultaneously: $a \to -a$, $\sigma_x \to -\sigma_x$.

Hepp and Lieb [42] studied the properties of the Dicke model in thermal equilibrium. In the thermodynamic limit $N \to \infty$, it is found that, when the interaction between atoms and photons is weak, the system is in its normal phase, in which the

number of photons does not grow with N. By contrast, when the interaction is strong, the system will enter the superradiant phase, in which the number of photons will be proportional to N. The phase transition is continuous with a critical point at the phase boundary. At zero-temperature, the location of the phase boundary is determined by a single parameter $\kappa := \omega\epsilon g^{-2}$, which can be obtained from the mean-field theory.

The mean-field Hamiltonian is obtained by ignoring the commutator $\left[a, a^\dagger\right] = 1$ as done in [43], and replacing the bosonic operators by a real number $\sqrt{N}\phi\epsilon/g$ that represents the photonic degrees of freedom with neglected quantum fluctuation:

$$h_{\mathrm{MF}} := \epsilon\left(\kappa\phi^2 + \phi\sigma_x + \sigma_z\right). \tag{2.2}$$

The replacement is equivalent to assuming the system being in a direct-product state, of atoms and photons, $|\mathrm{atom}\rangle \otimes \left|\sqrt{N}\phi\epsilon/g\right\rangle$, where $|\mathrm{atom}\rangle$ represents an atomic state where all the atoms share the same orientation, and $\left|\sqrt{N}\phi\epsilon/g\right\rangle$ represents a photonic coherent state. No entanglement between the atoms and photons is included in the mean-field approximation.

The ground state energy of the mean-field Hamiltonian can be easily calculated:

$$\epsilon_{\mathrm{MF}}\left(\phi\right) = \epsilon\left(\kappa\phi^2 - \sqrt{\phi^2+1}\right). \tag{2.3}$$

At zero-temperature, there is no thermal fluctuation, and the photonic coherent state will take a specific value of ϕ which minimizes the ground-state energy, and this value of ϕ is considered as the order parameter of the model in the framework of the Landau theory of phase transition. When $\kappa > 1/2$, ϵ_{MF} has a single minimum located at $\phi = 0$, which means there is no photon, $\left\langle a^\dagger a\right\rangle = 0$, and the system is in the normal phase. When $\kappa < 1/2$, ϵ_{MF} has two global minimums located at $\phi = \pm\sqrt{\frac{1}{4\kappa^2} - 1}$, accordingly $\left\langle a^\dagger a\right\rangle = Ng^2\left(\frac{1}{4} - \kappa^2\right)/\omega^2$, which means the system

enters the superradiant phase. Because the order parameter is a continuous function of κ, so the phase transition is second-order and the phase boundary $\kappa = 1/2$ is a critical point. The phase transition can also happen at finite temperature, but here we focus on quantum phase transitions only.

The mean-field result is only an approximation because of the neglected quantum fluctuation. In particular, the mean-field result is independent from N, predicting that the phase transition occurs no matter how many atoms there are, which is not correct. Without quantum fluctuation, there is an abrupt change in the photon number from $\left\langle a^\dagger a\right\rangle = 0$ to $\left\langle a^\dagger a\right\rangle = Ng^2\left(\frac{1}{4} - \kappa^2\right)/\omega^2$, whereas quantum fluctuation can smear out the singularity when N is finite. In fact, the bare vacuum state satisfying $\left\langle a^\dagger a\right\rangle = 0$ will never be the true ground state of the Dicke model as long as the interaction is turned on, which can be seen by simple variational argument. Suppose no more than one photon can appear and no more than one atom can be excited, then the restricted Hilbert space will have dimension four. In the restricted Hilbert space, the expectation value of the Dicke Hamiltonian H_{Dicke} can be represented by the expectation value of some Pauli matrices:

$$\langle H_{\text{Dicke}}\rangle = \left\langle \frac{\omega}{2}\sigma_z^{(0)} + \frac{g}{2}\sigma_x^{(0)}\sigma_x^{(1)} + \epsilon\sigma_z^{(1)}\right\rangle + \frac{\omega}{2} - (N-1)\,\epsilon.$$

It can be shown that $\left\langle a^\dagger a\right\rangle = \left\langle \sigma_z^{(0)} + 1\right\rangle > 0$ for the ground state of $\frac{\omega}{2}\sigma_z^{(0)} + \frac{g}{2}\sigma_x^{(0)}\sigma_x^{(1)} + \epsilon\sigma_z^{(1)}$ as long as $g \neq 0$. Therefore, we can always find a photon in the dressed vacuum due to quantum fluctuation, and the difference between the number of photons between the $\kappa > 1/2$ region and the $\kappa < 1/2$ region can be significant only when $Ng^2/\omega^2 \gg 1$ according to the mean-field results. Hence, the phase transition should be understood asymptotically in terms of a large Ng^2/ω^2, otherwise there will not exist distinct phases due to quantum fluctuation. The expression Ng^2/ω^2 suggests that not only can the superradiant phase transition happen in the thermodynamic limit

$N \to \infty$, but it can also happen in another limit, $\omega/g \to 0$ for any finite N, which is called the classical oscillator limit [44]. We will only consider the thermodynamic limit in this section, and introduce the classical oscillator limit in the next section.

In the thermodynamic limit, the effect of quantum fluctuation can be investigated through the Holstein-Primakoff transformation [45]. The Dicke Hamiltonian in Eq. (2.1) can be cast into another form through the collective spin operators $J_{x,z} := \frac{1}{2}\sum_{k=1}^{N} \sigma_{x,z}^{(k)}$:

$$H_{\text{Dicke}} = \omega a^\dagger a + \frac{g}{\sqrt{N}}\left(a + a^\dagger\right) J_x + 2\epsilon J_z. \tag{2.4}$$

The Holstein-Primakoff transformation represents J_x and J_z by new bosonic operators b and $b^\dagger$

$$\begin{aligned} J_x &= \frac{1}{2} b^\dagger \sqrt{N - b^\dagger b} + h.c., \\ J_z &= b^\dagger b - \frac{1}{2} N. \end{aligned}$$

In the large N limit, where $N \gg \left\langle b^\dagger b \right\rangle, \left\langle a^\dagger a \right\rangle$, Eq. (2.4) can be written as

$$H_{\text{Dicke}} = \omega a^\dagger a + 2\epsilon b^\dagger b + \frac{g}{2}\left(a + a^\dagger\right)\left(b + b^\dagger\right) - \epsilon N + o\left(1\right). \tag{2.5}$$

This model can be interpreted as a two-dimensional harmonic oscillator with the effective position and momentum operators given by

$$\begin{aligned} X_1 &:= \frac{1}{\sqrt{2\omega}}\left(a + a^\dagger\right), \\ X_2 &:= \frac{1}{2\sqrt{\epsilon}}\left(b + b^\dagger\right), \\ P_1 &:= i\sqrt{\frac{\omega}{2}}\left(a^\dagger - a\right), \\ P_2 &:= i\sqrt{\epsilon}\left(b^\dagger - b\right). \end{aligned}$$

Thus, the Dicke Hamiltonian becomes

$$H_{\text{Dicke}} = \frac{1}{2}\left(\sum_{j,k=1}^{2} P_j \delta_{jk} P_k + X_j \Omega_{jk}^2 X_k\right) - \epsilon N + o(1). \tag{2.6}$$

where

$$\Omega^2 := \begin{pmatrix} \omega^2 & \sqrt{2\omega\epsilon}g \\ \sqrt{2\omega\epsilon}g & 4\epsilon^2 \end{pmatrix}.$$

The eigen-frequencies λ_+, λ_- of the two-dimensional harmonic oscillator are given by the square roots of the eigenvalues of the matrix Ω^2:

$$\lambda_\pm^2 = \frac{\omega^2 + 4\epsilon^2}{2} \pm \sqrt{2\omega\epsilon g^2 + \left(\frac{\omega^2 - 4\epsilon^2}{2}\right)^2}, \tag{2.7}$$

and consequently the eigenvalues of H_{Dicke} take the form

$$E(n_-, n_+) = \left(n_- + \frac{1}{2}\right)\lambda_- + \left(n_+ + \frac{1}{2}\right)\lambda_+ - \epsilon N + o(1), \tag{2.8}$$

where n_- and n_+ are two non-negative integers that must be much less than N, in order for the conditions $N \gg \left\langle b^\dagger b \right\rangle, \left\langle a^\dagger a \right\rangle$ to hold. Obviously, for this result to make sense, the smaller eigenvalue of Ω^2, λ_-^2, cannot be negative. Therefore, the condition $\lambda_- = 0$ marks a phase transition. It can be easily verified that $\lambda_- = 0$ coincides with the mean-field phase boundary $\kappa = 1/2$. In other words, the mean-field theory gives the exact phase diagram in the thermodynamic limit.

The success of the classical mean-field theory in predicting the phase boundary does not mean that the phase transition is classical. When λ_- approaches zero, the characteristic length of the two-dimensional harmonic oscillator goes to infinity. As a result, the ground state of the oscillator contains a great amount of quantum fluctuation, breaks the conditions $N \gg \left\langle b^\dagger b \right\rangle, \left\langle a^\dagger a \right\rangle$, and thus invalidates the large-N expansion of the Dicke Hamiltonian. The diverging quantum fluctuation indicates that the point $\kappa = 1/2$ is indeed associated with quantum criticality. People have

calculated the atom-photon von Neumann entanglement entropy to characterize the quantum fluctuation and the critical behavior [46–48]. We will calculate the entanglement entropy to characterize the multicriticality in the generalized Dicke models we propose later.

2.2 Superradiant phase transition in the classical oscillator limit

In the previous section, we mentioned that the mean-field theory suggests that the superradiant quantum phase transition in the Dicke model occurs not only in the thermodynamic limit $N \to \infty$, but also in the limit $\omega/g \to 0$. The latter is named classical oscillator limit because when ω is small, the quantum oscillator $\omega a^\dagger a$ behave like a classical one. The classical oscillator limit will not alter the mean-field result, giving the same mean-field phase diagram as that in the thermodynamic limit. However, the two limit show qualitatively different behaviors in terms of quantum fluctuation, as we will illustrate in this section. We set $N = 1$ for simplicity, which reduces the Dicke model to the quantum Rabi model, whose exact eigenenergies can be solved iteratively [49].

First, because the superradiant phase transition is understood asymptotically, we need to determine the order of magnitude of ϵ, given $\omega/g \to 0$ in the classical oscillator limit. This can be done by noticing that the parameter $\kappa = \omega\epsilon g^{-2}$ determining the phase diagram should be finite, $\kappa \sim 1$. Consequently, $\epsilon \sim g^2/\omega$, which can also be verified by equating the order of magnitude of each term in Eq. (2.1). In the superradiant phase, the mean-field analysis tells us $\langle a \rangle \sim g/\omega$, so

$$\left\langle \omega a^\dagger a \right\rangle \sim \left\langle \frac{g\left(a + a^\dagger\right)}{2} \sigma_x \right\rangle \sim g^2/\omega.$$

As a result, the last term $\langle \epsilon \sigma_z \rangle$ should have the same order of magnitude, which yields $\epsilon \sim g^2/\omega$. Without loss of generality, we take $\epsilon \sim 1$, and g and ω are regarded as first-order and second-order infinitesimal, respectively.

Because ϵ is much larger than the rest of energy scales, in the ground state, the atom will almost be fixed to its lower-energy state, leaving the photonic mode the only degree of freedom. It is possible to map the whole Hamiltonian in Eq. (2.1) to the lower-energy manifold of the atom, neglecting the atom-photon entanglement and derive an effective Hamiltonian for the photons, which is accurate to the lowest order [44]:

$$H_{\text{eff}} = \omega \left(a^\dagger a - \frac{1}{8\kappa} \left(a + a^\dagger \right)^2 \right). \tag{2.9}$$

Again, this effective Hamiltonian is valid only when the fluctuation in the photon mode $\langle a^\dagger a \rangle$ is finite. Using Bogoliubov transformation, the effective Hamiltonian can be diagonalized and further simplified to $H_{\text{eff}} = \omega_{\text{CO}} b^\dagger b$, where b is a new bosonic annihilator that is a linear combination of a and $a^\dagger$, and the dressed frequency $\omega_{\text{CO}} := \sqrt{1 - \frac{1}{2\kappa}}\omega$. The dressed frequency vanishes when $\kappa = 1/2$ and becomes imaginary when $\kappa < 1/2$, which again confirms the mean-field result that the superradiant phase transition happens at the critical point $\kappa = 1/2$, just like in the thermodynamic limit.

We have seen that either in the thermodynamic limit $N \to \infty$ or in the classical oscillator limit $\omega/g \to 0$, the phase diagram and the position of the critical point are exactly determined by the mean-field theory despite the presence of quantum fluctuation, which is shown later to be a general property of the family of Dicke-like models with superradiant phase transitions. Because the mean-field theory in the Dicke-like models is equivalent to the single-parameter Landau theory of phase transition with Z_2 symmetry, we are going to study the geometry of the phase diagrams in the Landau theory, and, more importantly, find those multicritical manifolds.

2.3 Multicriticality in the single-parameter Landau theory of phase transition with Z_2 symmetry

The Landau theory of phase transitions is the basic theoretical framework to describe phase transitions involving spontaneous symmetry breaking. In the case of the Dicke model, it is the Z_2 symmetry described under Eq. (2.1) that gets broken in the superradiant quantum phase transition. In the normal phase, the single non-degenerate ground state remains invariant under the transformation $a \to -a$ and $\sigma_x \to -\sigma_x$. In the superradiant phase, the ground states are two-fold degenerate, and we can properly choose the two basis vectors of the ground state manifold such that the two state vectors exchange under the transformation mentioned above. In the Landau theory, the spontaneous symmetry breaking is described by the change of the order parameters. In the case of the Dicke model, the single order parameter ϕ is chosen to be proportional to $\langle a \rangle$, which would be zero in the normal phase, and would take two non-zero values with opposite signs in the superradiant phase. The value of the order parameter should minimize the free energy, which coincides with the ground-state energy in a zero-temperature quantum phase transition. In general, for phase transitions breaking a Z_2 symmetry with a single order parameter ϕ, the free energy F is an even function of the order parameter, analytic at $\phi = 0$, expressed by a Taylor series containing only the even power terms:

$$F(\phi) = \sum_{n=0}^{\infty} c_n \phi^{2n}. \tag{2.10}$$

We are going to analyse the phase diagram given the free energy in Eq. (2.10).

With Eq. (2.10), the order parameter ϕ may change singularly around some point $\phi \neq 0$. For example, certain free energy F could have four local minimums whose locations are $\{\phi_1, -\phi_1, \phi_2, -\phi_2\}$ where $\phi_1, \phi_2 \neq 0$, then the order parameter changes

abruptly from ϕ_1 to ϕ_2 when the parameters c_n's in Eq. (2.10) change in a way such that it turns $F(\phi_1) < F(\phi_2)$ into $F(\phi_1) > F(\phi_2)$ while keeping the locations of the local minimums unchanged. Though being singular, this kind of transitions does not involve symmetry breaking, so we will only focus on the case where a zero ϕ changes to some non-zero values which happens when the Dicke-like models enter the superradiant phase from the normal phase.

The superradiant phase transition can be either continuous or discontinuous. Although the discontinuous phase boundary can rarely be obtained analytically, the critical points, including the multicritical points we are interested in, always reside on the continuous phase boundary where $\phi = 0$, thus we can use the Taylor series Eq. (2.10) to derive the equations on the parameters c_n's which specify the critical and multicritical manifolds.

First, the simplest case that is frequently discussed in text books is that all c_n's ares zero except c_1 and c_2. In this case, the free energy is quadratic in terms of ϕ^2 so the minimums can be easily calculated. It is required that F has a global minimum to make the system stable, so we must have $c_2 > 0$. Now, F can be written as

$$F = c_2 \left(\phi^2 + \frac{c_1}{2c_2}\right)^2 - \frac{c_1^2}{4c_2},$$

which has two global minimums at $\phi = \pm\sqrt{-\frac{c_1}{2c_2}}$ if $c_1 < 0$, or has one global minimum at $\phi = 0$ if $c_1 > 0$. Therefore, the equation determining the critical manifold, where two global minimums merge into one, is given by $c_1 = 0$. Because c_1 is a function of the thermodynamic variables, the equation $c_1 = 0$ gives a critical manifold in the phase space whose dimension is one less than the dimension of the phase diagram.

Is there a high-order critical point when F is quadratic in ϕ^2? The answer is no. As we introduced in Chapter 1, an n^{th}-order critical manifold is the intersection of

$(n-1)^{\text{th}}$ critical manifolds. In the case that F is quadratic in ϕ^2, there is at most two global minimums. When the two minimums merge into one, they produce the only critical manifold specified by the equation $c_1 = 0$, which cannot intersect with another critical manifold to produce a tricritical point. Note that the values of c_0 and c_2 do not affect the phase diagram, because either adding or multiplying a constant to F does not change the location of the minimums.

Therefore, to have two or more critical manifolds that intersect, we must have at least three minimums. The simplest F that support three minimums is a cubic function in ϕ^2. To guarantee the existence of a lower bound of the free energy, the coefficient c_3 must be positive. One of the three local minimums must be located at $\phi = 0$ due to the symmetry. When $\frac{dF}{d\phi^2}\Big|_{\phi=0} > 0$, $\phi = 0$ must be a local minimum. We know

$$\frac{dF}{d\phi^2} = c_1 + 2c_2\phi^2 + 3c_3\phi^4,$$

so when $c_1 > 0$, $\phi = 0$ is a local minimum. F may also have two local minimums at $\phi = \pm\phi_0$, where $\phi_0^2 > 0$ is the larger solution of the equation $\frac{dF}{d\phi^2}\Big|_{\phi^2=\phi_0^2} = 0$. Thus,

$$\phi_0^2 = \frac{\sqrt{c_2^2 - 3c_1c_3} - c_2}{3c_3},$$

with the condition $c_3 > 0$. To make $\phi_0^2 > 0$, it is required that, either $c_1 < 0$, or $c_2 < 0$ and $c_2^2 \geq 3c_1c_3$. In addition, when $c_1 = 0$ and $c_2 \geq 0$, $\phi = 0$ is a minimum. In conclusion, the free energy F has:

1. A single local minimum at $\phi = 0$, which is also the global minimum, if $c_1 > 0$ and $c_2^2 < 3c_1c_3$, or $c_1 \geq 0$ and $c_2 \geq 0$;

2. Double local minimums at $\phi = \pm\phi_0$, which are also the global minimums, if $c_1 < 0$, or $c_1 = 0$ and $c_2 < 0$;

3. Three local minimums at $\phi = 0, \pm\phi_0$, if $c_1 > 0$ and $c_2 < 0$ and $c_2^2 \geq 3c_1c_3$.

In the third case above, to determine where the global minimum is, we need to evaluate F at $\phi = 0$ and $\phi^2 = \phi_0^2$, respectively. The calculation can be simplified by noticing that when F has three global minimums, it must take the form

$$F = c_0 + c_3\phi^2\left(\phi^2 - \phi_0^2\right)^2.$$

By identifying this formula with the Taylor expansion of F, we get

$$-2\phi_0^2 c_3 = c_2,$$

or

$$c_2 + 2\sqrt{c_1c_3} = 0.$$

In the phase diagram, this equation specify the triple line, where three phases coexist. When $c_2 + 2\sqrt{c_1c_3} > 0$, the single global minimum locates at $\phi = 0$, and when $c_2 + 2\sqrt{c_1c_3} < 0$, the double global minimums locate at $\phi = \pm\phi_0$.

With all of the discussion above, we can establish the phase diagram (see Fig. 2.1 (a)) in the two-dimensional parameter space spanned by c_1 and c_2. There is a continuous phase transition boundary, which is also the critical line, whose shape is determined by the equation $c_1 = 0$ and $c_2 \geq 0$, and there is a discontinuous phase transition boundary, which is also the triple line, whose equation is $c_2 + 2\sqrt{c_1c_3} = 0$ and $c_2 < 0$. The two boundaries smoothly join together at the point $c_1 = c_2 = 0$, in the sense that the derivative $\frac{dc_1}{dc_2}$ approaches zero when we approach the point $c_1 = c_2 = 0$ along either line. The boundary divides the phase diagram into two half plane. The half plane contains the region $c_1 < 0$ represents the symmetry-breaking phase and the other plane represents the symmetry-preserving phase.

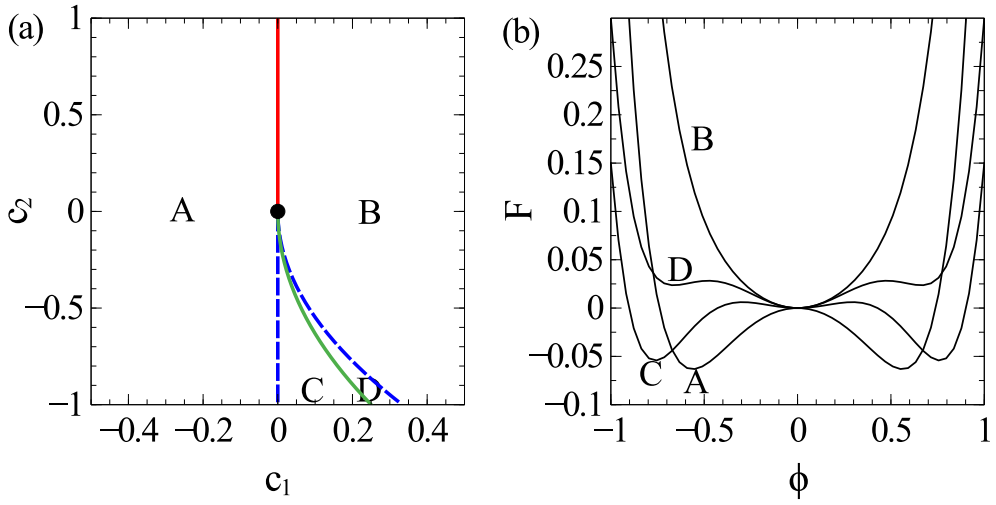

Figure 2.1 : (a) The phase diagram associated with a free energy F that is a cubic polynomial in ϕ^2. The solid lines are the phase boundaries. The region to the left of the boundary marked by A and C is the symmetry breaking phase and the right marked by B and D is the symmetry preserving phase. The red solid line in the region $c_2 > 0$ is the critical line. The green solid line in the region $c_2 < 0$ is the triple line where three global minimums coexist. The region C and D within the blue dashed line has three local minimums in the free energy. The black dot in the center is the tricritical point. (b) Typical plots of F against ϕ for different regions shown in panel (a).

We see the phase diagram has the same structure as the one given by Griffiths in [6], where a tricritical point appears at the intersection of the continuous phase transition boundary and the discontinuous phase transition boundary. So, is the point $c_1 = c_2 = 0$ in the current phase diagram also a tricritical point? The answer is yes. But we see only one critical line in Fig. 2.1 (a), so where are the other critical lines that it intersect with? Like the case studied by Griffiths, the other critical lines do not reside in the accessible phase space subjecting to the Z_2 symmetry. They are visible in the three-dimensional phase diagram, in which the additional axis represents the variable conjugate to the order parameter. In this case, the free energy is modified by an additional term $c_{1/2}\phi$ which breaks the Z_2 symmetry. With such a linear term in

the free energy, it becomes difficult to write down the analytical expressions for the minimums of F, but we can still analyse the geometry of the phase diagram. First, the maximum number of the local minimums of F is still three, because a liner term would only shift the function $\frac{dF}{d\phi}$ by a constant. Then, let us mark the locations of the three local minimums by α, β, and γ if they exist, with the condition $\alpha < \beta < \gamma$. Now, with the Z_2 symmetry broken, β is not necessarily zero, and α may be different from $-\gamma$. By properly adjusting $c_{1/2}$, it is possible either to make α and β the global minimums that merge into one minimum at a critical line, or to make β and γ the global minimums that merge at another critical line. These two new critical lines will join the critical line on the Z_2-symmetric surface at the point $c_1 = c_2 = 0$, where the three global minimums merge simultaneously. Thus, in the extended phase diagram including the conjugate variable $c_{1/2}$, it is manifested that the point $c_1 = c_2 = 0$ is indeed the tricritical point. We plot the phase boundaries of the extended phase diagram in Fig. 2.2.

Next, we consider the case where F is a polynomial of ϕ^2 with degree p. Again, to ensure the stability, the coefficient $c_p > 0$. In general, it is impossible to write down the analytical expressions for the minimums of F, however, it is possible to gain insight into the topology of the minimums, that is, how the minimums merge and split, which gives rise to the critical and multicritical points. In the cubic case, the third-order critical point is the point where three global minimums merge. Similarly, in general, *the n^{th}-order critical point should be the point where n global minimums merge*, if we are allowed to break the Z_2 symmetry. This definition is consistent with the previous one, because when we have n global minimums, we can select n groups of $(n-1)$ minimums to merge into $(n-1)^{\text{th}}$ order critical manifolds, and the intersection of these n lower-order critical manifolds is the point where all of the n

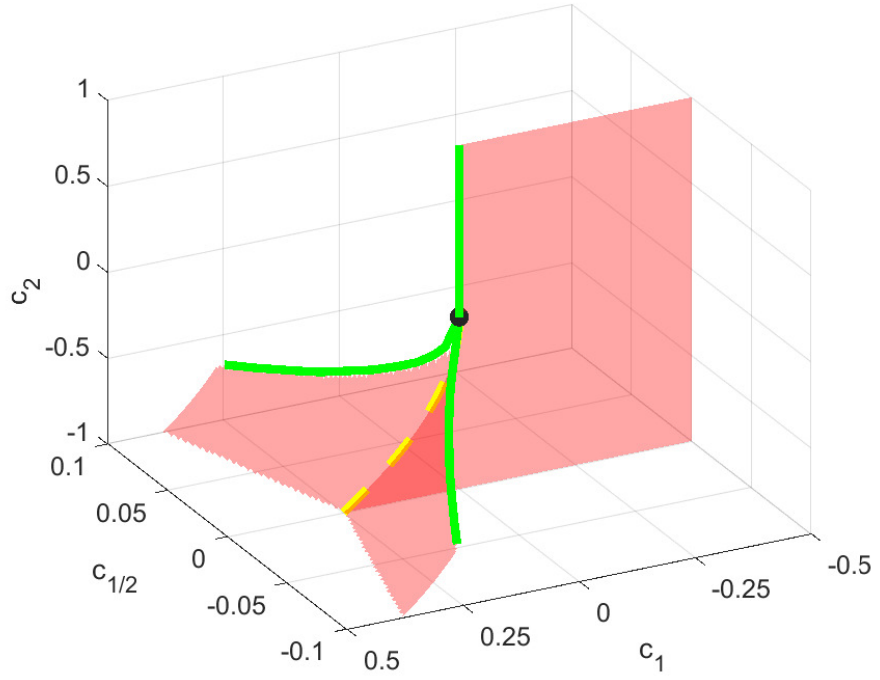

Figure 2.2 : The phase diagram associated with a free energy F that is a cubic polynomial in ϕ^2 plus a linear term $c_{1/2}\phi$ breaking the Z_2 symmetry. The three critical lines are marked by green solid lines, which intersect at the tricritical point, the black dot, in the center. The triple line is marked by a yellow dashed line. The discontinuous phase transition boundaries are marked by red surfaces.

minimums merge, giving rise to the n^{th}-order critical point. F has at most p global minimums, so the highest order critical point it can support is of p^{th} order. When a general polynomial F' (where the prime is to denote the broken Z_2 symmetry) of ϕ with degree $2p$ has $n \leq p$ global minimums, it can always be cast into the form

$$F' = \prod_{k=1}^{n} (\phi - a_k)^2 \prod_{l=1}^{p-n} (\phi - b_l)(\phi - b_l^*) + F_0', \tag{2.11}$$

where a_k's are the locations of the n minimums, b_l's are some complex numbers with non-vanishing imaginary part, and F_0' is the value F' takes at the minimums. When the n minimums in Eq. (2.11) merge, the a_k's approach the same value a_0

simultaneously, and as a result F' takes the form

$$F' = (\phi - a_0)^{2n} \prod_{l=1}^{p-n} (\phi - b_l)(\phi - b_l^*) + F_0'.$$

Therefore, we derive another criteria for the multicriticality, that is, around an n^{th}-order critical point $\phi = a_0$, the free energy should be a power function of $\phi - a_0$ to the $2n^{\text{th}}$, or $F' - F_0' \propto (\phi - a_0)^{2n}$. In the case $a_0 = 0$, we have

$$F = \phi^{2n} \prod_{l=1}^{p-n} \left(\phi^2 + \left|b_l^2\right|\right) + F_0'.$$

Accordingly, the equations to determine the n^{th} order critical manifold in the phase diagram is

$$c_1 = c_2 = \cdots = c_{n-1} = 0, \tag{2.12}$$

with

$$c_n, c_{n+1}, \cdots, c_p > 0. \tag{2.13}$$

In general, F may not be a polynomial but a series with infinite terms. The previous argument which leads to Eq. (2.12) still holds. And now we have infinite number of parameters $c_n, c_{n+1}, \cdots$ that need to satisfy the inequality Eq. (2.13). However, it is somehow impracticable to apply those infinite many conditions on the thermodynamic variables. The problem can be circumvented by considering only very small value of ϕ because we are studying continuous phase transitions. As long as $c_n > 0$, the higher-order terms $c_{n+1}, c_{n+2}, \cdots$ can be neglected without changing the behavior of F in a sufficiently small neighborhood around $\phi = 0$. Therefore, we can say the n^{th}-order critical condition for a free energy F taking the form in Eq. (2.10) is given by Eq. (2.12) together with

$$c_n > 0. \tag{2.14}$$

Eq. (2.12) indicates that an n^{th}-order critical manifold has the dimension $\mathcal{D}-n+1$ where $\mathcal{D}$ is the dimension of the phase diagram.

Before we end this section, last but not least, let us discuss the scaling behaviors of the multicritical points within the mean-field theory. The multicritical conditions automatically generate multiple principal directions of scaling in the phase diagram. At an n^{th}-order critical point, $(n-1)$ coefficients in Eq. (2.12) vanish. In the phase diagram, when we move a little away from the multicritical point, some of the coefficients may become non-zero. Suppose we pick a special direction in the phase space such that only the value of c_k, $1 \leq k < n$, changes. If c_k becomes positive, then the global minimum of the free energy is located at $\phi = 0$ such that the system is in the normal phase. If c_k becomes negative, the position of the global minimum will be

$$\phi = \pm \left(-\frac{k c_k}{n c_n} \right)^{\frac{1}{2(n-k)}} . \tag{2.15}$$

Thus, $n-1$ different scaling directions can be identified. In general, a small change in an experimentally accessible thermodynamic variable x from its multicritical value x_0 will result in the change of multiple c_k's, determined by the non-zero component in the gradient vector $\partial_x \mathbf{c} := \left(\frac{\partial c_1}{\partial x}, \frac{\partial c_2}{\partial x}, \ldots, \frac{\partial c_{n-1}}{\partial x} \right)$, where the derivatives are taken at the multicritical point x_0. Because now c_k's are much smaller than c_n, the positions of the minimums have to be much smaller than 1. In this case, the dominant term in the power series of F would be the one with the smallest exponent. Suppose $k_{\min}(x)$ is the smallest k that $\left| \frac{\partial c_k}{\partial x} \right|$ has the same order of magnitude as $\frac{|\partial_x \mathbf{c}|}{\sqrt{n-1}}$, then we can approximate the position of the global minimum by

$$\phi \approx \begin{cases} 0, \text{ when } \frac{\partial c_{k_{\min}(x)}}{\partial x}(x - x_0) > 0 \\ \pm \left(-\frac{k_{\min}(x) \frac{\partial c_{k_{\min}(x)}}{\partial x}(x-x_0)}{n c_n} \right)^{\frac{1}{2(n-k_{\min}(x))}}, \text{ when } \frac{\partial c_{k_{\min}(x)}}{\partial x}(x - x_0) < 0 \end{cases} , \tag{2.16}$$

which characterizes the scaling behavior of the order parameter near the n^{th}-order

critical point.

2.4 Generalized Dicke models in the mean-field theory

After a general discussion of the multicriticality within the framework of Landau theory of phase transition, we now turn to study a generalized Dicke model which supports multicritical superradiance phase transitions.

2.4.1 The Dicke model with multi-level atoms

We have seen that a critical point occurs at the phase boundary of the superradiant phase transition in the Dicke model that describes atoms by the two-level approximation. However, real atoms possess complicated level structures. Even if we restrict ourselves to the ground state manifold, a typical atom often features more than two levels. This motivates us to investigate an important generalization of the Dicke model where the two-level atoms are replaced by multi-level atoms, and hopefully the additional degrees of freedom in the multi-level generalization of the Dicke model can bring about multicriticality.

Our multicritical Dicke model describes N l-level atoms coupled with a single photonic mode of frequency ω. The Hamiltonian can be written as:

$$H = \omega a^\dagger a + \frac{g\left(a + a^\dagger\right)}{2\sqrt{N}} \sum_{k=1}^{N} d^{(k)} + \epsilon \sum_{k=1}^{N} h^{(k)}, \tag{2.17}$$

where a is the photon annihilation operator, dimension-less single-atom Hamiltonian h and dipole operator d act on the l inner states of the atoms, g and ϵ set the energy scales of the atom-photon interaction and the internal energy of the atoms, respectively. Conventional Dicke model in Eq. (2.1) is recovered if we take $l = 2$, and d and h are replaced by the two-level Pauli operators σ_x and σ_z, respectively.

In order for the generalized Dicke model to support the superradiant quantum phase transition, we require the Hamiltonian to be invariant under the action: $a \to -a$, $d \to -d$, $h \to h$. The Z_2 symmetry will put some constraints on the dipole operator and the single-atom Hamiltonian, as we will show later.

2.4.2 The mean-field Hamiltonian and the stability of the mean-field ground state

First, we will analyse the phase transition of the generalized Dicke model through the mean-field approach.

To obtain the mean-field Hamiltonian, we perform the same replacement, $a \to \sqrt{N}\phi\epsilon/g$ as we did for the original Dicke model which results:

$$h_{\mathrm{MF}} := \epsilon\left(\kappa\phi^2 + \phi d + h\right). \tag{2.18}$$

We denote the l eigenvalues of h_{MF} as ϵ_k's, with $k = 1, 2, 3, \ldots, l$, corresponding to eigenstates $|k\rangle$. We assume that the mean-field ground state is non-degenerate with energy ϵ_1. The mean-field theory requires minimizing ϵ_1 in terms of ϕ. We assume ϵ_1 is a analytical function of ϕ, then the local minimums of ϵ_1 satisfies

$$\frac{\partial\epsilon_1}{\partial\phi} = 0, \tag{2.19}$$

$$\frac{\partial^2\epsilon_1}{\partial\phi^2} \geq 0. \tag{2.20}$$

We cast the above two formulas into another forms for future use.

First, let us prepare an arbitrary basis of the Hilbert space. For example, we can choose the eigenvectors of h as the basis vectors. Under this basis, the single-atom Hamiltonian h is represented by an diagonal matrix. Suppose in this basis, h_{MF} is diagonalized by a unitary matrix U:

$$h_{\mathrm{MF}} = UEU^\dagger, \tag{2.21}$$

where E is a diagonal matrix whose k^{th} diagonal element E_{kk} is ϵ_k, with $k = 1, 2, 3, \ldots, l$. In general, U and E are both functions of ϕ. Now we differentiate h_{MF} in Eq. (2.18) with respect to ϕ:

$$\frac{\partial h_{\text{MF}}}{\partial \phi} = \epsilon D, \tag{2.22}$$

where D is the shifted dipole operator:

$$D := 2\kappa\phi + d. \tag{2.23}$$

Alternatively, we differentiate h_{MF} in Eq. (2.21):

$$\frac{\partial h_{\text{MF}}}{\partial \phi} = \frac{\partial U}{\partial \phi} E U^\dagger + U \frac{\partial E}{\partial \phi} U^\dagger + U E \frac{\partial U^\dagger}{\partial \phi}. \tag{2.24}$$

Equating the right hand side of Eq. (2.22) and Eq. (2.24), we can obtain the matrix representation of the shifted dipole operator D in the basis consisting of the eigenvectors of h_{MF}

$$\begin{aligned} U^\dagger \epsilon D U &= U^\dagger \left(\frac{\partial U}{\partial \phi} E U^\dagger + U \frac{\partial E}{\partial \phi} U^\dagger + U E \frac{\partial U^\dagger}{\partial \phi} \right) U \\ &= U^\dagger \frac{\partial U}{\partial \phi} E + \frac{\partial E}{\partial \phi} + E \frac{\partial U^\dagger}{\partial \phi} U \\ &= U^\dagger \frac{\partial U}{\partial \phi} E + \frac{\partial E}{\partial \phi} + E \frac{\partial \left(U^\dagger U \right)}{\partial \phi} - E U^\dagger \frac{\partial U}{\partial \phi} \\ &= \left[U^\dagger \frac{\partial U}{\partial \phi}, E \right] + \frac{\partial E}{\partial \phi}, \end{aligned}$$

where we have used $\frac{\partial \left(U^\dagger U \right)}{\partial \phi} \equiv 0$. Because the diagonal elements of the commutator between a diagonal matrix and another matrix is always zero, the diagonal elements of $U^\dagger D U$ equal those of $\frac{\partial E}{\partial \phi}$. Therefore, the expectation value of the shifted dipole operator D with respect to the mean-field ground state is zero as the result of Eq. (2.19), i.e.,

$$\left(U^\dagger D U \right)_{11} = 0. \tag{2.25}$$

Next, let us consider Eq. (2.20). The second derivative of h_{MF} is $2\epsilon\kappa$ according to Eq. (2.22) and Eq. (2.23), and from Eq. (2.21) we have

$$\begin{aligned}\frac{\partial^2 h_{\mathrm{MF}}}{\partial\phi^2} =& \frac{\partial^2 U}{\partial\phi^2}EU^\dagger + U\frac{\partial^2 E}{\partial\phi^2}U^\dagger + UE\frac{\partial^2 U^\dagger}{\partial\phi^2} \\ &+ 2\frac{\partial U}{\partial\phi}\frac{\partial E}{\partial\phi}U^\dagger + 2U\frac{\partial E}{\partial\phi}\frac{\partial U^\dagger}{\partial\phi} + 2\frac{\partial U}{\partial\phi}E\frac{\partial U^\dagger}{\partial\phi}.\end{aligned}$$

By applying another basis transformation with the matrix U, we arrive at the equation:

$$\begin{aligned}& U^\dagger\frac{\partial^2 h_{\mathrm{MF}}}{\partial\phi^2}U \\ =& U^\dagger\frac{\partial^2 U}{\partial\phi^2}E + \frac{\partial^2 E}{\partial\phi^2} + E\frac{\partial^2 U^\dagger}{\partial\phi^2}U \\ &+ 2U^\dagger\frac{\partial U}{\partial\phi}\frac{\partial E}{\partial\phi} + 2\frac{\partial E}{\partial\phi}\frac{\partial U^\dagger}{\partial\phi}U + 2U^\dagger\frac{\partial U}{\partial\phi}E\frac{\partial U^\dagger}{\partial\phi}U \\ =& 2\epsilon\kappa\end{aligned}$$

Consider the $(1,1)$ element of the matrix above:

$$\begin{aligned}
2\epsilon\kappa =&\epsilon_1 \sum_{k=1}^{l} U_{k1}^* \frac{\partial^2 U_{k1}}{\partial\phi^2} + \frac{\partial^2\epsilon_1}{\partial\phi^2} + \epsilon_1 \sum_{k=1}^{l} \frac{\partial^2 U_{k1}^*}{\partial\phi^2} U_{k1} \\
&+ 2\frac{\partial\epsilon_1}{\partial\phi} \sum_{k=1}^{l} U_{k1}^* \frac{\partial U_{k1}}{\partial\phi} + 2\frac{\partial\epsilon_1}{\partial\phi} \sum_{k=1}^{l} \frac{\partial U_{k1}^*}{\partial\phi} U_{k1} \\
&+ 2 \sum_{k_1,k_2,k_3=1}^{l} U_{k_1 1}^* \frac{\partial U_{k_1 k_2}}{\partial\phi} \epsilon_{k_2} \frac{\partial U_{k_3 k_2}^*}{\partial\phi} U_{k_3 1} \\
=&\epsilon_1 \left(\sum_{k=1}^{l} U_{k1}^* \frac{\partial^2 U_{k1}}{\partial\phi^2} + \sum_{k=1}^{l} \frac{\partial^2 U_{k1}^*}{\partial\phi^2} U_{k1} + 2 \sum_{k_1,k_2,k_3=1}^{l} U_{k_1 1}^* \frac{\partial U_{k_1 k_2}}{\partial\phi^2} \frac{\partial U_{k_3 k_2}^*}{\partial\phi^2} U_{k_3 1} \right) \\
&+ 2 \sum_{k_1,k_2,k_3=1}^{l} U_{k_1 1}^* \frac{\partial U_{k_1 k_2}}{\partial\phi} \left(\epsilon_{k_2} - \epsilon_1\right) \frac{\partial U_{k_3 k_2}^*}{\partial\phi} U_{k_3 1} + \frac{\partial^2\epsilon_1}{\partial\phi^2} \\
=&\epsilon_1 \left(U^\dagger \frac{\partial^2 \left(UU^\dagger\right)}{\partial\phi^2} U \right)_{11} + \frac{\partial^2\epsilon_1}{\partial\phi^2} \\
&+ 2 \sum_{k_1,k_2,k_3=1}^{l} U_{k_1 1}^* \frac{\partial U_{k_1 k_2}}{\partial\phi} \left(\epsilon_{k_2} - \epsilon_1\right) \frac{\partial U_{k_3 k_2}^*}{\partial\phi} U_{k_3 1} \\
=&2 \sum_{k_1,k_2,k_3=1}^{l} U_{k_1 1}^* \frac{\partial U_{k_1 k_2}}{\partial\phi} \left(\epsilon_{k_2} - \epsilon_1\right) \frac{\partial U_{k_3 k_2}^*}{\partial\phi} U_{k_3 1} + \frac{\partial^2\epsilon_1}{\partial\phi^2},
\end{aligned} \tag{2.26}$$

where we have used $\frac{\partial\epsilon_1}{\partial\phi} = 0$ and $\frac{\partial^2\left(UU^\dagger\right)}{\partial\phi^2} = 0$. In the mean time, the following expression can be evaluated:

$$\begin{aligned}
&\epsilon^2 \sum_{k=2}^{l} \frac{\left|\left(U^\dagger DU\right)_{1k}\right|^2}{\epsilon_k - \epsilon_1} \\
=&\sum_{k=2}^{l} \sum_{k_1,k_2=1}^{l} \frac{\left(U_{k_1 1}^* \frac{\partial U_{k_1 k}}{\partial\phi}\epsilon_k + \epsilon_1 \frac{\partial U_{k_1 1}^*}{\partial\phi} U_{k_1 k}\right)\left(U_{k_2 k}^* \frac{\partial U_{k_2 1}}{\partial\phi}\epsilon_1 + \epsilon_k \frac{\partial U_{k_2 k}^*}{\partial\phi} U_{k_2 1}\right)}{\epsilon_k - \epsilon_1} \\
=&\sum_{k=2}^{l} \sum_{k_1,k_2=1}^{l} \frac{\left(U_{k_1 1}^* \frac{\partial U_{k_1 k}}{\partial\phi}\epsilon_k - \epsilon_1 U_{k_1 1}^* \frac{\partial U_{k_1 k}}{\partial\phi}\right)\left(-\frac{\partial U_{k_2 k}^*}{\partial\phi} U_{k_2 1}\epsilon_1 + \epsilon_k \frac{\partial U_{k_2 k}^*}{\partial\phi} U_{k_2 1}\right)}{\epsilon_k - \epsilon_1} \\
=&\sum_{k=2}^{l} \sum_{k_1,k_2=1}^{l} U_{k_1 1}^* \frac{\partial U_{k_1 k}}{\partial\phi} \left(\epsilon_k - \epsilon_1\right) \frac{\partial U_{k_2 k}^*}{\partial\phi} U_{k_2 1}.
\end{aligned} \tag{2.27}$$

Comparing Eq. (2.26) with Eq. (2.27), and using Eq. (2.20) we get

$$\epsilon \sum_{k=2}^{l} \frac{\left|\left(U^{\dagger} D U\right)_{1k}\right|^2}{\epsilon_k - \epsilon_1} \leq \kappa \tag{2.28}$$

Especially, when we are on the manifold specified by $\phi = 0$, which includes the critical manifold located on the phase boundary, we obtain

$$\sum_{k=2}^{l} \frac{|d_{1k}|^2}{h_{kk} - h_{11}} \leq \kappa, \tag{2.29}$$

where the matrix elements of d and h are taken with respect to the eigenvectors of h, which are now also the eigenvectors of h_{MF} because $\phi = 0$. The inequality takes the equal sign when we are on the critical manifold, as we will see later.

2.4.3 Counting the dimension of the phase diagrams

Next, let us discuss the geometry of the critical and multicritical manifolds within the mean-field theory. In the previous section, we have discussed the single-parameter Landau theory of phase transition with Z_2 symmetry. Now, within the mean-field description, the free energy in the current case is the mean-field ground state energy ϵ_1, which can be written as a Taylor series in ϕ:

$$\epsilon_1 = \sum_{k=0}^{\infty} c_k \phi^{2k}, \tag{2.30}$$

where c_k's are some real parameters as functions of κ and the matrix elements of d and h. Eq. (2.12) tells us that an n^{th}-order critical point put $(n-1)$ constraints on the parameters in the Hamiltonian, so there must exist at least $(n-1)$ freely tunable parameters to achieve an n^{th}-order critical point.

Therefore, we will count the number of freely tunable parameters in the generalized Dicke model. Because of the presence of the Z_2 symmetry, the number of independent variables in matrix d and h are less than the number of independent variables in a

general hermitian matrix. The Z_2 symmetry requires the existence of a parity operator P, which makes

$$PdP = -d, \tag{2.31}$$

and

$$PhP = h. \tag{2.32}$$

Such a parity operator can only take 1 and -1 as its eigenvalues. Because the total number of eigenvalues of P is l, we denote the number of ± 1 in the eigenvalues of P as $\frac{l \pm m}{2}$. m has to be smaller than l because it is not applicable when all of the eigenvalues of P are 1 or -1, in which case the equation $PdP = -d$ will never hold. Because P commutes with h as shown by Eq. (2.32), we can find a set of common eigenvectors of P and h. Using this set of vectors as a basis, and properly ordering the basis vectors, P takes the form

$$P = \mathrm{diag}\left(-1, -1, \ldots, -1, 1, 1, \ldots 1\right), \tag{2.33}$$

where the number of ± 1 are $\frac{l \pm m}{2}$, respectively. Then, we can evaluate the matrix elements of PdP:

$$PdP = \begin{pmatrix} d_{11} & \cdots & d_{1\frac{l-m}{2}} & -d_{1\frac{l-m+2}{2}} & \cdots & -d_{1l} \\ \cdots & \cdots & \cdots & \cdots & \cdots & \cdots \\ d_{\frac{l-m}{2}1} & \cdots & d_{\frac{l-m}{2}\frac{l-m}{2}} & -d_{\frac{l-m}{2}\frac{l-m+2}{2}} & \cdots & -d_{\frac{l-m}{2}l} \\ -d_{\frac{l-m+2}{2}1} & \cdots & -d_{\frac{l-m+2}{2}\frac{l-m}{2}} & d_{\frac{l-m+2}{2}\frac{l-m+2}{2}} & \cdots & d_{\frac{l-m+2}{2}l} \\ \cdots & \cdots & \cdots & \cdots & \cdots & \cdots \\ -d_{l1} & \cdots & -d_{l\frac{l-m}{2}} & d_{l\frac{l-m+2}{2}} & \cdots & d_{ll} \end{pmatrix}.$$

To make Eq. (2.31) hold, d has to take the form

$$d = \begin{pmatrix} 0 & M \\ M^\dagger & 0 \end{pmatrix}, \tag{2.34}$$

where M is a $\frac{l-m}{2} \times \frac{l+m}{2}$ matrix. So d contains $\frac{l^2-m^2}{2}$ variables (real), and h contains l free parameters because h is diagonal in the basis. Together with κ, there are in total $\frac{l^2-m^2}{2} + l + 1$ variables in the mean-field Hamiltonian h_{MF}, whereas ϵ is an irrelevant scaling factor. However, not all of these variables can affect the phase diagram. For example, if we shift the overall energy by adding an arbitrary real number to h_{MF}, the Hamiltonian changes but the Z_2 symmetry as well as the phase diagram is unaffected. We will then count the number of such irrelevant variables. Besides changing the overall energy, we can apply a unitary transformation that changes the relative phase between two eigenvectors of h chosen as the basis. Under this transformation, h is invariant, and d remain in the form given by Eq. (2.34) although the M matrix may change. There are in total $(l-1)$ relative phases that can be changed. In addition, we can rescale κ and ϵ by multiplying real factors r_1, r_2, and now h_{MF} changes into

$$h_{\mathrm{MF}} = \epsilon \left(\kappa r_1 r_2 \phi^2 + r_1 \phi d + r_1 h \right).$$

If we further absorb a factor $\pm\sqrt{r_1 r_2}$ into ϕ, we get

$$h_{\mathrm{MF}} = \epsilon \left(\kappa \phi^2 \pm \sqrt{\frac{r_1}{r_2}} \phi d + r_1 h \right).$$

Therefore, d and h can be changed by multiplying two arbitrary real factors, respectively, without changing the physics. In conclusion, the total number of freely tunable parameters which could change the phase diagram is

$$\mathcal{D} = \frac{l^2 - m^2}{2} + l + 1 - (l-1) - 3 = \frac{l^2 - m^2}{2} - 1.$$

For example, when we are dealing with two-level atoms with $l = 2$, m can only be ± 1, otherwise P reduces to an identity operator, and now $\mathcal{D} = \frac{2^2-1^2}{2} - 1 = 1$, which means all of the two-level Dicke models are equivalent to the original Dicke model in the sense of mean-field phase diagram. Here the only relevant variable is

κ, and the critical point is at most second order. To have higher order criticality, we have to consider atoms with more than two levels. When $l = 3$, m can only be ± 1, and $\mathcal{D} = \frac{3^2-1^2}{2} - 1 = 3$, so in principle, fourth-order criticality may be realized in a three-level Dicke system. In the experimental work reported in [20], a tricritical point is identified in a spin-1 Bose gas subjected to spin-orbit coupling. This system can be recast into the form of the generalized Dicke model with $l = 3$ in the classical oscillator limit. In our work [17] (see also [19]), by introducing a staggered magnetic field to the two-level atoms, we show that this modified Dicke model exhibits tricriticality. This model can be regarded as a special case of the multicritical Dicke model under current consideration with $l = 4$.

2.4.4 The multicritical conditions in terms of d and h

Next, we are going to derive explicit equations that the matrix elements of d and h satisfy when the system is critical or multicritical. To transform Eq. (2.12) into equations on the matrix elements of d and h, we need to express the coefficients c_k's in Eq. (2.30) as functions of the matrix elements. Because $\phi = 0$ on the critical manifolds, ϕ is small near the critical manifolds and it is applicable to use the perturbation theory, treating the ϕd term in Eq. (2.18) as a perturbation to the unperturbed part h, to derive the Taylor expansion in Eq. (2.30).

We apply the perturbation theory introduced in Appendix A to the mean-field Hamiltonian in Eq. (2.2) to obtain the coefficients c_k's in Eq. (2.30). The basis vectors are chosen as the eigenstates of h, with the first matrix element h_{11} being the non-degenerate smallest eigenvalue of h, and we shift the overall energy of the

mean-field Hamiltonian such that $h_{11} = 0$. Using Eq. (A.1) with $\rho = 1$, we get

$$\epsilon_1/\epsilon - h_{11} - \kappa\phi^2 = \sum_{k=1}^{\infty} \phi^k \mathrm{Tr} \left[\sum_{\sum_{i=1}^{k+1} k_i = k-1} S_{k_1} dS_{k_2} d \cdots dS_{k_{k+1}} \right],$$

where

$$S_k = \begin{cases} \mathcal{P}_1, \text{ when } k = 0, \\ -\sum_{n=2}^{l} \frac{\mathcal{P}_n}{h_{nn}^k}, \text{ when } k > 0, \end{cases}$$

and $\mathcal{P}_n$ is the projector corresponding to the n^{th} eigenstate of h. Because of the Z_2 symmetry, the power series must contain only even powers of ϕ. Because $d_{kk} = 0$, as required by Eq. (2.34), two adjacent S_k's, for example, S_{k_1} and S_{k_2}, cannot be S_0 simultaneously.

The coefficient c_1 is calculated by the second-order perturbation theory:

$$\begin{aligned} c_1 &= \mathrm{Tr} \left[\sum_{\sum_{i=1}^{3} k_i = 1} S_{k_1} dS_{k_2} dS_{k_3} \right] + \kappa \\ &= \mathrm{Tr} \left[\mathcal{P}_1 dS_1 d\mathcal{P}_1 \right] + \kappa \\ &= -\sum_{k \neq 1} \frac{d_{1k} d_{k1}}{h_{kk}} + \kappa \end{aligned}$$

Therefore, the critical condition $c_1 = 0$ is given by

$$\sum_{k \neq 1} \frac{|d_{1k}|^2}{h_{kk}} = \kappa, \tag{2.35}$$

which is consistent with the stability condition derived in Eq. (2.29).

The coefficient c_2 involves fourth-order perturbation theory:

$$\begin{aligned}
c_2 =& \mathrm{Tr}\left[\sum_{\sum_{i=1}^{5} k_i=3} S_{k_1} dS_{k_2} dS_{k_3} dS_{k_4} dS_{k_5}\right] \\
=& \mathrm{Tr}\left[\mathcal{P}_1 dS_1 dS_1 dS_1 d\mathcal{P}_1\right] + \mathrm{Tr}\left[S_1 d\mathcal{P}_1 dS_1 d\mathcal{P}_1 dS_1\right] \\
&+ \mathrm{Tr}\left[\mathcal{P}_1 dS_2 d\mathcal{P}_1 dS_1 d\mathcal{P}_1 + h.c.\right] \\
=& \sum_{k\neq 1} -\frac{d_{1k_1} d_{k_1k_2} d_{k_2k_3} d_{k_31}}{h_{k_1k_1} h_{k_2k_2} h_{k_3k_3}} - \frac{d_{k_11} d_{1k_2} d_{k_21} d_{1k_1}}{h^2_{k_1k_1} h_{k_2k_2}} + 2\frac{d_{1k_1} d_{k_11} d_{1k_2} d_{k_21}}{h^2_{k_1k_1} h_{k_2k_2}} \\
=& \sum_{k\neq 1} -\frac{d_{1k_1} d_{k_1k_2} d_{k_2k_3} d_{k_31}}{h_{k_1k_1} h_{k_2k_2} h_{k_3k_3}} + \frac{|d_{1k_1}|^2 |d_{1k_2}|^2}{h^2_{k_1k_1} h_{k_2k_2}},
\end{aligned}$$

Given $c_1 = 0$ in Eq. (2.35), the tricritical condition $c_2 = 0$ can be cast into

$$\sum_{k\neq 1} \frac{d_{1k_1} d_{k_1k_2} d_{k_2k_3} d_{k_31}}{h_{k_1k_1} h_{k_2k_2} h_{k_3k_3}} = \kappa \sum_{k\neq 1} \frac{|d_{1k_1}|^2}{h^2_{k_1k_1}}. \tag{2.36}$$

Given Eqs. (2.35)(2.36), the fourth-order critical condition $c_3 = c_2 = c_1 = 0$ is obtained through sixth order perturbation theory:

$$\begin{aligned}
0 =& \sum_{k\neq 1} -\frac{d_{1k_1} d_{k_1k_2} d_{k_2k_3} d_{k_3k_4} d_{k_4k_5} d_{k_51}}{h_{k_1k_1} h_{k_2k_2} h_{k_3k_3} h_{k_4k_4} h_{k_5k_5}} + 2\frac{d_{1k_1} d_{k_1k_2} d_{k_21}}{h^2_{k_1k_1} h_{k_2k_2}} \frac{d_{1k_3} d_{k_3k_4} d_{k_41}}{h_{k_3k_3} h_{k_4k_4}} \\
&+ \kappa \frac{d_{1k_2} d_{k_2k_3} d_{k_3k_4} d_{k_41}}{h_{k_2k_2} h^2_{k_3k_3} h_{k_4k_4}} + 2\kappa \frac{d_{1k_2} d_{k_2k_3} d_{k_3k_4} d_{k_41}}{h^2_{k_2k_2} h_{k_3k_3} h_{k_4k_4}} - \kappa^2 \frac{|d_{1k_1}|^2}{h^3_{k_1k_1}}.
\end{aligned} \tag{2.37}$$

In general, for any order of criticality, the multicritical condition can be obtained using the perturbation theory. However, as we have seen, the perturbation expansion becomes more and more complicated when the order of criticality increases, and it is impossible to solve the equation analytically to obtain the multicritical manifolds in the phase diagram. Therefore, we want to make some further restrictions on the d and h matrices such that the multicritical conditions can be greatly simplified. To this end, we notice that Eq. (2.36) can be written in a form similar to Eq. (2.35) if we require that the only non-zero matrix elements of d are the first diagonals, that

is, $d_{ij} = 0$ if $|i-j| \neq 1$. Such a restriction on d makes the mean-field Hamiltonian tridiagonal. So we call such a class of generalized Dicke models as tridiagonal Dicke models. Now

$$\begin{aligned}
&\sum_{k\neq 1} \frac{d_{1k_1} d_{k_1k_2} d_{k_2k_3} d_{k_31}}{h_{k_1k_1} h_{k_2k_2} h_{k_3k_3}} - \kappa \sum_{k\neq 1} \frac{|d_{1k_1}|^2}{h_{k_1k_1}^2} \\
=&\frac{|d_{12}|^2 |d_{23}|^2}{h_{22}^2 h_{33}} - \kappa \frac{|d_{12}|^2}{h_{22}^2} \\
=&\frac{\kappa}{h_{22}} \left(\frac{|d_{23}|^2}{h_{33}} - \kappa \right),
\end{aligned}$$

so the equation $c_2 = 0$ becomes

$$\frac{|d_{23}|^2}{h_{33}} = \kappa. \tag{2.38}$$

Under the same condition, Eq. (2.37) becomes

$$\begin{aligned}
&- \frac{d_{1k_1} d_{k_1k_2} d_{k_2k_3} d_{k_3k_4} d_{k_4k_5} d_{k_51}}{h_{k_1k_1} h_{k_2k_2} h_{k_3k_3} h_{k_4k_4} h_{k_5k_5}} + 2 \frac{d_{1k_1} d_{k_1k_2} d_{k_21}}{h_{k_1k_1}^2 h_{k_2k_2}} \frac{d_{1k_3} d_{k_3k_4} d_{k_41}}{h_{k_3k_3} h_{k_4k_4}} \\
&+ \kappa \frac{d_{1k_2} d_{k_2k_3} d_{k_3k_4} d_{k_41}}{h_{k_2k_2} h_{k_3k_3}^2 h_{k_4k_4}} + 2\kappa \frac{d_{1k_2} d_{k_2k_3} d_{k_3k_4} d_{k_41}}{h_{k_2k_2}^2 h_{k_3k_3} h_{k_4k_4}} - \kappa^2 \frac{|d_{1k_1}|^2}{h_{k_1k_1}^3} \\
=&- \left(\frac{|d_{12}|^2 |d_{23}|^2 |d_{34}|^2}{h_{22}^2 h_{33}^2 h_{44}} + \frac{|d_{12}|^2 |d_{23}|^4}{h_{22}^3 h_{33}^2} \right) \\
&+ \kappa \frac{|d_{12}|^2 |d_{23}|^2}{h_{22}^2 h_{33}^2} + 2\kappa \frac{|d_{12}|^2 |d_{23}|^2}{h_{22}^3 h_{33}} - \kappa^2 \frac{|d_{12}|^2}{h_{22}^3} \\
=&\frac{\kappa^2}{h_{22} h_{33}} \left(\kappa - \frac{|d_{34}|^2}{h_{44}} \right),
\end{aligned}$$

so the equation $c_3 = 0$ becomes

$$\frac{|d_{34}|^2}{h_{44}} = \kappa. \tag{2.39}$$

Eq. (2.38) and Eq. (2.39) suggest that there exists a general formula for arbitrary order of criticality. So we claim:

- For tridiagonal Dicke models, the n^{th} order critical condition is given by

$$|d_{k-1,k}|^2 = \kappa h_{kk}, \tag{2.40}$$

for all the k's satisfying $2 \leq k \leq n$.

Let us now prove this claim. First, we need to transform the general multicritical condition in Eq. (2.12) into another form. We have assumed that the ground state of the mean-field Hamiltonian h_{MF} is non-degenerate. Therefore, given Eq. (2.12), the eigenvalues of h_{MF} have the following asymptotic behavior for small ϕ:

$$\epsilon_1 = c_n \phi^{2n} + O\left(\phi^{2n+2}\right)$$
$$\epsilon_k = h_{kk} + O\left(\phi^2\right), \; k = 2, 3, \ldots, l$$

The determinant of h_{MF}, denoted as ζ_l, is the product of the eigenvalues, so it has the asymptotic behavior

$$\zeta_l = O\left(\phi^{2n}\right),$$

which can replace Eq. (2.12) to be the multicritical condition. We are going to prove that this equation holds as long as Eq. (2.40) is satisfied. To this end, we denote the determinant of the $k \times k$ upper-left submatrix of h_{MF} as ζ_k, then ζ's have the following recurrence relation:

$$\zeta_k = \left(h_{kk} + \kappa\phi^2\right)\zeta_{k-1} - \phi^2 \left|d_{k-1,k}\right|^2 \zeta_{k-2}$$

with the initial condition

$$\zeta_1 = \kappa\phi^2$$
$$\zeta_2 = \det \begin{pmatrix} \kappa\phi^2 & \phi d_{12} \\ \phi d_{21} & \kappa\phi^2 + h_{22} \end{pmatrix} = \left(\kappa h_{22} - \left|d_{12}\right|^2\right)\phi^2 + \kappa^2\phi^4.$$

When the 2$^{\mathrm{nd}}$-order critical condition is satisfied, $\kappa h_{22} - \left|d_{12}\right|^2 = 0$, $\zeta_2 = \kappa^2\phi^4$. Assume when Eq. (2.40) is satisfied, $\zeta_k = \kappa^k\phi^{2k}$ for $k = 1, 2, \ldots, k' - 1$, where $k' \leq n$. Then

the recurrence relation gives

$$\begin{aligned}\zeta_{k'} &= \left(h_{k'k'} + \kappa\phi^2\right)\zeta_{k'-1} - \phi^2\left|d_{k'-1,k'}\right|^2\zeta_{k'-2} \\ &= \left(h_{k'k'} + \kappa\phi^2\right)\kappa^{k'-1}\phi^{2k'-2} - \phi^2\left|d_{k'-1,k'}\right|^2\kappa^{k'-2}\phi^{2k'-4} \\ &= \kappa^{k'-2}\phi^{2k'-2}\left(\kappa h_{k'k'} - \left|d_{k'-1,k'}\right|^2\right) + \kappa^{k'}\phi^{2k'} \\ &= \kappa^{k'}\phi^{2k'}.\end{aligned}$$

By deduction, it is proved that

$$\zeta_k = \kappa^k\phi^{2k} \text{ for } k = 1, 2, \ldots, n.$$

If $n = l$, then the proof is complete. If $n < l$,

$$\zeta_l = \zeta_n\zeta^n - \phi^2\left|d_{n,n+1}\right|^2\zeta_{n-1}\zeta^{n+1} = \kappa^{n-1}\phi^{2n}\left(\kappa\zeta^n - \left|d_{n,n+1}\right|^2\zeta^{n+1}\right)$$

where ζ^k, $k = 1, 2, \ldots, n-1$, is defined as the determinant of the $(l-k)\times(l-k)$ lower-right submatrix of h_{MF}. Because ζ^k's are polynomials of ϕ^2, so $\zeta_l = O\left(\phi^{2n}\right)$. We have finished the proof.

As we will see in section 2.7, the tridiagonal Dicke Hamiltonian can be realized in experiments.

2.5 Quantum fluctuation in the generalized Dicke model in the thermodynamic limit

Quantum fluctuation plays an important role in quantum phase transitions. Usually, the change of the quantum fluctuation during a quantum phase transition can be represented by the varying correlation length. The correlation length grows when the critical points are approached and finally diverges at the critical points. The scaling relations between the correlation length and other control parameters in the system

are characterized by critical exponents which can be computed using various methods. However, in our case, the generalized Dicke model is a dimensionless model without a properly defined length scale. So the quantum fluctuation cannot be depicted by the correlation length. Instead, we will study the entanglement entropy between the atoms and the photons to tackle the quantum fluctuation in the generalized Dicke model.

To this end, we shift the bosonic operator a in Eq. (2.17) by the amount of the mean-field order parameter

$$b_1 := a - \epsilon\sqrt{N}\phi/g,$$

which turn the generalized Dicke Hamiltonian into the form

$$H = \omega b_1^\dagger b_1 + \frac{g\left(b_1 + b_1^\dagger\right)}{2\sqrt{N}} \sum_{k=1}^{N} D^{(k)} + \sum_{k=1}^{N} h_{\mathrm{MF}}^{(k)}, \tag{2.41}$$

where $D^{(k)}$ and $h_{\mathrm{MF}}^{(k)}$ are the shifted dipole operator and the mean-field Hamiltonian defined in Eq. (2.23) and Eq. (2.18), respectively, and the upper indices mark different atoms. As we will see, the new form of H enable us to carry out an asymptotic expansion of the Hamiltonian in terms of N in the thermodynamic limit, and the leading terms of the asymptotic series effectively describe the low-energy spectrum of H when the system is not critical. The ground state of the low-energy effective Hamiltonian can be readily obtained and offers the entanglement information we want.

To obtain the effective low-energy Hamiltonian, we need first restrict ourselves to an invariant subspace of the Hamiltonian. Like what is done in Eq. (2.4), where the dipole operator and the single-atom Hamiltonian represented by Pauli matrices are replaced by collective spin operators, and then the discussion is restricted in the subspace where the states possess the largest spin number, we now restrict

ourselves in the invariant subspace which contains the state where each atom is in the mean-field ground state. Such a subspace can have totally symmetrized Fock states $\left\{|n_1, n_2, n_3, \ldots, n_l\rangle \mid \sum_{k=1}^{l} n_k = N\right\}$ as its basis vectors, where n_k represents the number of atoms occupying the k^{th} eigenstate of the mean-field Hamiltonian. In particular, n_1 is the number of atoms in the mean-field ground state. We will evaluate the matrix elements of H with respect to this basis. Because every atom is in an eigenstate of h_{MF}, the summation $\sum_{k=1}^{N} h_{\text{MF}}^{(k)}$ must be a diagonal matrix under this basis, and the eigenvalues are given by

$$\sum_{k=1}^{N} h_{\text{MF}}^{(k)} |n_1, n_2, n_3, \ldots, n_l\rangle = \sum_{k=1}^{l} n_k \epsilon_k \; |n_1, n_2, n_3, \ldots, n_l\rangle \,. \tag{2.42}$$

where ϵ_k's are the eigenvalues of h_{MF}. For the same reason, the diagonal elements of $\sum_{k=1}^{N} D^{(k)}$ are given by

$$\langle n_1, n_2, n_3, \ldots, n_l| \sum_{k=1}^{N} D^{(k)} |n_1, n_2, n_3, \ldots, n_l\rangle = \sum_{i=2}^{l} n_i D_{i,i}, \tag{2.43}$$

where the matrix elements of D are evaluated with respect to the eigenstates of h_{MF}. The summation on the right hand side of the equation above starts from $i = 2$ because of the previous result $D_{11} = 0$ in Eq. (2.25), which is the consequence of the stability of the mean-field ground state. Note that Eq. (2.25) takes a different form because the matrix elements of D in Eq. (2.25) are written with respect to an arbitrary basis specified by the unitary matrix U. The off-diagonal elements of $\sum_{k=1}^{N} D^{(k)}$ annihilate an atom in certain mean-field eigenstate and create an atom in another mean-field eigenstate. So, the non-zero off-diagonal matrix elements of $\sum_{k=1}^{N} D^{(k)}$ are given by

$$\langle \ldots, n_i + 1, \ldots, n_j - 1, \ldots| \sum_{k=1}^{N} D^{(k)} |\ldots, n_i, \ldots, n_j, \ldots\rangle = \sqrt{(n_i + 1)\, n_j} D_{i,j}. \tag{2.44}$$

where i, j can take the values $1, 2, \ldots, l$, $i < j$ or $i > j$. Because we are only interested in the low-energy states of the Hamiltonian, it is reasonable to assume that most atoms

occupy the mean-field ground state, that is, $n_1 \sim N$ and $n_i \ll N$ for $i = 2, 3, \ldots, l$ in the thermodynamic limit, which can be verified self-consistently after we solve the low-energy effective Hamiltonian. Under this assumption, the matrix elements in Eq. (2.44) can be expanded as a power series in N^{-1}:

$$\begin{aligned}
&\langle \ldots, n_i + 1, \ldots, n_j - 1, \ldots | \sum_{k=1}^{N} D^{(k)} | \ldots, n_i, \ldots, n_j, \ldots \rangle \\
&= \begin{cases} D_{1,j}\sqrt{N n_j} + o\left(\sqrt{N}\right) & \text{, when } i = 1 \\ D_{i,1}\sqrt{N\left(n_i + 1\right)} + o\left(\sqrt{N}\right) & \text{, when } j = 1 \\ o\left(\sqrt{N}\right) & \text{, when } i, j > 1 \end{cases} .
\end{aligned} \tag{2.45}$$

Keeping the lowest order terms in the asymptotic expansion of the matrix elements of $\sum_{k=1}^{N} D^{(k)}$, the Hamiltonian in Eq. (2.41) can be greatly simplified. To do this, define bosonic operators b_i's, $i = 2, 3, \ldots, l$, by

$$b_i \left| n_1 \ldots, n_i, \ldots \right\rangle := \sqrt{n_i} \left| n_1 + 1 \ldots, n_i - 1, \ldots \right\rangle .$$

which satisfy $\left[b_i, b_j^\dagger\right] = \delta_{i,j}$ and similarly $[b_i, b_j] = 0$. Then

$$\sum_{k=1}^{N} D^{(k)} = \sqrt{N}\left[|D_{1,i}| \sum_{i=2}^{l} \left(b_i + b_i^\dagger \right) + o\left(1\right) \right], \tag{2.46}$$

where we have properly chosen the relative phases of the basis vectors such that the matrix element $D_{1,i}$ is real and positive. And we also have

$$\sum_{k=1}^{N} h_{\mathrm{MF}}^{(k)} = N\epsilon_1 + \sum_{i=2}^{l} \left(\epsilon_i - \epsilon_1\right) b_i^\dagger b_i. \tag{2.47}$$

So, the Hamiltonian in Eq. (2.41) can be expanded as an asymptotic series in terms of N^{-1} and the leading terms are quadratic in the bosonic operators b_i's:

$$H = N\epsilon_1 + H_{\mathrm{eff}} + o\left(1\right) \tag{2.48}$$

$$H_{\text{eff}} := \sum_{i=1}^{l} \omega_i b_i^\dagger b_i + \frac{g}{2}\left(b_1 + b_1^\dagger\right) \sum_{i=2}^{l} |D_{1,i}| \left(b_i + b_i^\dagger\right), \tag{2.49}$$

where

$$\omega_i := \begin{cases} \omega, \text{ when } i = 1 \\ \epsilon_i - \epsilon_1, \text{ when } i = 2, 3, \ldots, l \end{cases}. \tag{2.50}$$

From Eq. (2.44) we know that the validity of the asymptotic expansion in Eq. (2.48) is guaranteed if $\sum_{i=2}^{l} \left\langle b_i^\dagger b_i \right\rangle \ll N$. In other words, if we solve the effective Hamiltonian H_{eff} and find that the low-energy states of H_{eff} satisfy this condition, then H_{eff} correctly describes the low-energy states, otherwise the asymptotic expansion in Eq. (2.48) is invalid. Assuming Eq. (2.48) is valid, we notice that the leading term $N\epsilon_1$ is just the mean-field energy, which means that the mean-field approach, although neglects the quantum fluctuation encoded in H_{eff}, gives the exact ground-state energy up to a residue $o(N)$ which is negligibly small in the thermodynamic limit. Therefore, the mean-field phase diagram is the exact phase diagram in the thermodynamic limit as long as the asymptotic expansion in Eq. (2.48) is valid. In other words, the quantum fluctuation will not modify the multicritical manifolds predicted by the mean-field theory, which will facilitate experimental study on multicriticality.

The effective Hamiltonian H_{eff} in Eq. (2.49) is quadratic in the bosonic operators, so it can be solved analytically. We solve H_{eff} by transforming it into a Hamiltonian describing an l-dimensional harmonic oscillator. Define position and momentum operators by

$$X_i := \frac{1}{\sqrt{2\omega_i}}\left(b_i + b_i^\dagger\right),$$
$$P_i := i\sqrt{\frac{\omega_i}{2}}\left(b_i^\dagger - b_i\right).$$

Note that the operators with a lower index 1 represent the photonic degrees of freedom, while the ones with a lower index other than 1 represent the atomic degrees of

freedom. Now the effective Hamiltonian H_{eff} turns into:

$$H_{\text{eff}} = \frac{1}{2}\left(\sum_{j,k=1}^{l} P_j \delta_{jk} P_k + X_j \Omega_{jk}^2 X_k\right) - \frac{1}{2}\sum_{k=1}^{l} \omega_k \ , \tag{2.51}$$

where Ω^2 is an $l \times l$ matrix whose diagonal elements are given by

$$\Omega_{kk}^2 = \omega_k^2,\ k = 1, 2, \ldots, l,$$

and the non-zero off-diagonal elements are

$$\Omega_{1k}^2 = g\,|D_{1,k}|\,\sqrt{\omega\omega_k},$$
$$\Omega_{k1}^2 = \Omega_{1k}^2,$$

where $k = 2, 3, \ldots, l$. The spectrum of H_{eff} is solely determined by Ω^2. By diagonalizing Ω^2, H_{eff} can be represented as a sum of l independent one-dimensional harmonic oscillators, whose eigenfrequencies are equal to the eigenvalues λ_i's of Ω, $i = 1, 2, \ldots, l$. As such, the eigenvalues E_{eff} of H_{eff} are given by

$$E_{\text{eff}}\left(\chi_1, \chi_2, \ldots, \chi_l\right) = \sum_{i=1}^{l} \chi_i \lambda_i + \frac{1}{2}\left(\lambda_i - \omega_i\right),$$

where the non-negative integers χ_i's are the excitation number for each of the l independent one-dimensional harmonic oscillators. And the ground-state wave function of H_{eff} is given by

$$\Phi\left(\mathbf{X}\right) = \left(\frac{\det\Omega}{\pi^l}\right)^{1/4} \exp\left(-\frac{\sum_{i,j=1}^{l} \Omega_{ij} X_i X_j}{2}\right), \tag{2.52}$$

which is the product of the ground-state wave function of the l independent one-dimensional harmonic oscillators.

Information on the eigenvalues λ_i^2's of the matrix Ω^2 can be obtained by writing down the characteristic polynomial $p\left(\lambda^2\right) := \det\left(\Omega^2 - \lambda^2\right)$ of Ω^2. Denote the determinant of the upper-left $k \times k$ submatrix of $\Omega^2 - \lambda^2$ as p_k, then p_k's have the recurrence

relation

$$
\begin{aligned}
p_k &= \alpha_k p_{k-1} - \beta_k, \\
\alpha_k &:= \left(\Omega_{kk}^2 - \lambda^2\right) \\
\beta_k &:= \Omega_{1k}^2 \Omega_{k1}^2 \prod_{i=2}^{k-1} \left(\Omega_{ii}^2 - \lambda^2\right)
\end{aligned}
$$

which has the solution

$$
\begin{aligned}
p_k &= \prod_{i=2}^{k} \alpha_i p_1 - \sum_{i=2}^{k} \left(\beta_i \prod_{j=i+1}^{k} \alpha_j \right) \\
&= \prod_{i=1}^{k} \left(\Omega_{ii}^2 - \lambda^2\right) - \sum_{i=2}^{k} \Omega_{1i}^2 \Omega_{i1}^2 \left[\prod_{j=2}^{i-1} \left(\Omega_{jj}^2 - \lambda^2\right) \right] \left[\prod_{j=i+1}^{k} \left(\Omega_{jj}^2 - \lambda^2\right) \right] \\
&= \left(\prod_{i=1}^{k} \left(\Omega_{ii}^2 - \lambda^2\right) \right) \left(1 - \sum_{j=2}^{k} \frac{\Omega_{1j}^2 \Omega_{j1}^2}{\left(\Omega_{11}^2 - \lambda^2\right)\left(\Omega_{jj}^2 - \lambda^2\right)} \right) \\
&= \left(\prod_{i=1}^{k} \left(\omega_i^2 - \lambda^2\right) \right) \left(1 - g^2 \sum_{j=2}^{k} \frac{|D_{1,j}|^2 \, \omega \omega_j}{\left(\omega^2 - \lambda^2\right)\left(\omega_j^2 - \lambda^2\right)} \right).
\end{aligned}
$$

Especially,

$$
p\left(\lambda^2\right) \equiv p_l = \left(\prod_{i=1}^{l} \left(\omega_i^2 - \lambda^2\right) \right) \left(1 - g^2 \sum_{j=2}^{l} \frac{|D_{1,j}|^2 \, \omega \omega_j}{\left(\omega^2 - \lambda^2\right)\left(\omega_j^2 - \lambda^2\right)} \right). \tag{2.53}
$$

The eigenvalues λ_i^2 are the roots of the equation $p\left(\lambda^2\right) = 0$. First, consider the case where some of the mean-field eigenenergies are $(m+1)$-fold degenerate, for example, $\omega_k = \omega_{k+1} = \cdots = \omega_{k+m}$, then $\lambda^2 = \omega_k^2$ is a root of $p\left(\lambda^2\right)$ with multiplicity m, because now the first factor of $p\left(\lambda^2\right)$, $\prod_{i=1}^{l}\left(\omega_i^2 - \lambda^2\right)$, contains $\left(\omega_k^2 - \lambda\right)^{m+1}$ and $\left(\omega_k^2 - \lambda\right)\left(1 - g^2 \sum_{j=2}^{l} \frac{|D_{1,j}|^2 \omega \omega_j}{\left(\omega^2 - \lambda^2\right)\left(\omega_j^2 - \lambda^2\right)}\right)$ is analytic at $\lambda^2 = \omega_k^2$. The components v_i's of an eigenvector $\mathbf{v} \equiv (v_1, v_2, \ldots, v_l)$ of Ω^2 corresponding to this root is determined by the following equations

$$
v_i = 0, \text{ if } i < k \text{ or } i > k + m,
$$

and

$$\sum_{i=k}^{k+m} |D_{1,i}|\, v_i = 0.$$

The m solutions of the equations above involves only atomic degrees of freedom because $v_1 = 0$. They are therefore 'dark states' not interacting with the photons. The only atomic state $\mathbf{v}'$ with mean-field energy ϵ_k that interacts with the photons has the vector components

$$v_i' = \begin{cases} 0, \text{ if } i < k \text{ or } i > k+f \\ \frac{|D_{1,i}|}{\sqrt{\sum_{i=k}^{k+f} |D_{1,i}|^2}}, \text{ if } k \le i \le k+f \end{cases}.$$

And the coupling strength between this state and the photons is $g\sqrt{\omega\omega_k \sum_{i=k}^{k+f} |D_{1,i}|^2}$. Therefore, when we encounter dark states that we are not interested in, we can always reduce the dimension of Ω^2 to a smaller l by removing degenerate mean-field states and renormalizing the atom-photon coupling strength such that the resulting Ω^2 does not possess eigenvalues equal to certain ω_k^2. In this case, the characteristic equation $p(\lambda^2) = 0$ is equivalent to

$$q\left(\lambda^2\right) := \omega^2 - \lambda^2 - g^2 \sum_{j=2}^{l} \frac{|D_{1,j}|^2 \omega\omega_j}{\omega_j^2 - \lambda^2} = 0. \tag{2.54}$$

The function $q(\lambda^2)$ has simple poles at $\lambda^2 = \omega_j^2$, $j = 2, 3, \ldots, l$ and $q\left(\omega_j^2 \pm 0\right) \to \pm\infty$. Also, $q(\pm\infty) \to \mp\infty$. $q(\lambda^2)$ is monotonically decreasing within each interval $(-\infty, \omega_2^2), (\omega_2^2, \omega_3^2), \cdots, \left(\omega_{l-1}^2, \omega_l^2\right), (\omega_l^2, +\infty)$, supposing $\omega_2^2 < \omega_3^2 < \cdots < \omega_l^2$. Therefore we have $\lambda_1^2 \in (-\infty, \omega_2^2)$, $\lambda_2^2 \in (\omega_2^2, \omega_3^2)$, $\ldots$, $\lambda_{l-1}^2 \in \left(\omega_{l-1}^2, \omega_l^2\right)$, $\lambda_l^2 \in (\omega_l^2, +\infty)$. Note that if $\omega < \omega_2$, $q(\omega^2) = -g^2 \sum_{j=2}^{l} \frac{|D_{1,j}|^2 \omega\omega_j}{\omega_j^2 - \omega^2} < 0$, so $\lambda_1^2 \in (-\infty, \min(\omega^2, \omega_2^2))$.

Because it is meaningless if H_{eff} has imaginary eigenvalues, it is required that $\lambda_1^2 \ge 0$, equivalently $q(0) \ge 0$, that is,

$$g^2 \sum_{j=2}^{l} \frac{|D_{1,j}|^2}{\omega_j} \le \omega, \tag{2.55}$$

so we again encounter the stability condition in Eq. (2.28) derived by the mean-field theory. Thus, the mean-field theory that determines the classical energy landscape which has the same order of magnitude as the number of atom N, is consistent with the quantum theory that determines the quantum fluctuation whose energy scale has the order of magnitude 1. The critical condition is met when the inequality above takes the equal sign, which makes λ_1^2 vanish. When $\lambda_1^2 = 0$, the gap closes, and H_{eff} has a continuous spectrum. As for the trapping potential of the l-dimensional harmonic oscillator, along one direction specified by the eigenvector of Ω^2 corresponding to λ_1, the potential is flattened. Thus, the expectation values $\langle X_i^2 \rangle$ can be arbitrarily large for the low-energy states so that the condition $\sum_{i=2}^{l} \left\langle b_i^\dagger b_i \right\rangle \ll N$ for the validity of the asymptotic expansion of the Hamiltonian cannot hold. When λ_1^2 is small but positive, the expectation values $\langle X_i^2 \rangle$ over the ground-state wave function in Eq. (2.52) has the order of magnitude λ_1^{-1}, so the low-energy effective Hamiltonian H_{eff} is valid only when

$$\lambda_1 N \gg 1, \tag{2.56}$$

In other words, the system should be sufficiently away from the critical points to make H_{eff} valid, though the region of validity can be enlarged by increasing the number of atoms.

Next, we will calculate the von Neumann entanglement entropy between the atoms and photons in the ground state $\Phi(\mathbf{X})$ in Eq. (2.52) to understand the quantum fluctuation. To this purpose, first we calculate the reduced density matrix for the

photons:

$$\begin{aligned}\rho\left(x_1, x_1'\right) &:= \int dx_2 \cdots dx_l \, \Phi\left(x_1, x_2, \cdots, x_l\right) \Phi^*\left(x_1', x_2, \cdots, x_l\right) \\ &= \left(\frac{\det \Omega}{\pi^l}\right)^{1/2} \int dx_2 \cdots dx_l \\ &\quad e^{-\sum_{j,k=2}^{l} \Omega_{jk} x_j x_k - \frac{x_1 + x_1'}{2} \sum_{j=2}^{l} (\Omega_{j1} + \Omega_{1j}) x_j - \frac{\Omega_{11}\left(x_1^2 + x_1'^2\right)}{2}} \\ &= \left(\frac{\det \Omega}{\pi \det \Omega'}\right)^{1/2} e^{\frac{1}{4}\left(x_1 + x_1'\right)^2 \sum_{j,k=2}^{l} \Omega_{1j} \Omega'^{-1}_{j-1,k-1} \Omega_{k1} - \frac{\Omega_{11}\left(x_1^2 + x_1'^2\right)}{2}}, \end{aligned} \tag{2.57}$$

where Ω' is the $(l-1) \times (l-1)$ lower-right submatrix of Ω. Note that

$$\begin{aligned}\det \Omega &= \sum_{j=1}^{l} (-1)^{1+j} \, \Omega_{1j} M_{1j} \\ &= \Omega_{11} \det \Omega' + \sum_{j,k=2}^{l} (-1)^{1+j} \, \Omega_{1j} \Omega_{k1} \, (-1)^{1+k-1} \, M'_{k-1,j-1} \\ &= \Omega_{11} \det \Omega' - \sum_{j,k=2}^{l} \Omega_{1j} \Omega_{k1} C'_{k-1,j-1} \\ &= \det \Omega' \left(\Omega_{11} - \sum_{j,k=2}^{l} \Omega_{1j} \Omega'^{-1}_{j-1,k-1} \Omega_{k1}\right), \end{aligned} \tag{2.58}$$

where M_{ij} is the (i,j)-minor of Ω, the determinant of the submatrix of Ω that is obtained by removing the i^{th} row and the j^{th} column from Ω, M'_{ij} is the (i,j)-minor of Ω', and $C'_{ij} \equiv (-1)^{i+j} \, M'_{ij}$ is the (i,j)-cofactor of Ω'. We have used the fact that the inverse of Ω' can be expressed through its cofactor:

$$\Omega'^{-1}_{ij} = C'_{ji} / \det \Omega'.$$

Then using Eq. (2.58), the reduced density matrix can be written as

$$\begin{aligned}\rho\left(x_1, x_1'\right) &= \left(\frac{\det \Omega}{\pi \det \Omega'}\right)^{1/2} e^{\frac{1}{4}\left(x_1 + x_1'\right)^2 \left(\Omega_{11} - \frac{\det \Omega}{\det \Omega'}\right) - \frac{\Omega_{11}\left(x_1^2 + x_1'^2\right)}{2}} \\ &= \left(\frac{\det \Omega}{\pi \det \Omega'}\right)^{1/2} e^{-\frac{1}{2} A^+ \left(x_1^2 + x_1'^2\right) + A^- x_1 x_1'}, \end{aligned} \tag{2.59}$$

where

$$A^{\pm} := \frac{1}{2}\left(\Omega_{11} \pm \frac{\det\Omega}{\det\Omega'}\right).$$

The von Neumann entropy S is defined as

$$S = -\mathrm{Tr}\left(\rho \ln \rho\right)$$

To calculate the entanglement entropy, we need to know the eigenvalues of ρ. To this purpose, comparing ρ with the propagator of a one-dimensional harmonic oscillator

$$\langle x_1 |\, e^{-\frac{P_1^2+\gamma^2 X_1^2}{2}}\, |x_1'\rangle = \sqrt{\frac{\gamma}{2\pi\sinh\gamma}} e^{\frac{\gamma\left(-\cosh\gamma\left(x_1^2+x_1'^2\right)+2x_1x_1'\right)}{2\sinh\gamma}},$$

we can identify

$$\cosh\gamma \equiv \frac{A^+}{A^-} \tag{2.60}$$

such that the eigenvalues of ρ is given by $2\sinh\left(\frac{\gamma}{2}\right)\exp\left(-\gamma\left(k+\frac{1}{2}\right)\right)$, $k = 0, 1, 2, 3, \ldots$

Now the atom-photon entanglement entropy can be calculated as follows

$$\begin{aligned} S &= -\sum_{k=0}^{\infty}\left(-\gamma\left(k+\frac{1}{2}\right)+\ln\left(2\sinh\left(\frac{\gamma}{2}\right)\right)\right)2\sinh\left(\frac{\gamma}{2}\right)e^{-\gamma\left(k+\frac{1}{2}\right)} \\ &= -2\sinh\left(\frac{\gamma}{2}\right)\gamma\partial_\gamma\frac{1}{2\sinh\left(\frac{\gamma}{2}\right)} - \ln\left(2\sinh\left(\frac{\gamma}{2}\right)\right) \\ &= \frac{\gamma}{e^\gamma-1} - \ln\left(1-e^{-\gamma}\right). \end{aligned} \tag{2.61}$$

Therefore the entanglement entropy is determined by a single parameter γ. Quite remarkably, the parameter γ can be extracted from the photon correlation functions. To see this, we note that

$$\begin{aligned} \left\langle X_1^2\right\rangle &= \int x^2\rho\left(x,x\right)dx \\ &= \left(\frac{\det\Omega}{\pi\det\Omega'}\right)^{1/2}\int x^2 e^{-\frac{\det\Omega}{\det\Omega'}x^2}dx \\ &= \frac{\det\Omega'}{2\det\Omega}, \end{aligned} \tag{2.62}$$

and

$$\begin{aligned}\left\langle P_1^2\right\rangle &= -\int \left.\frac{\partial^2 \rho\left(x,x'\right)}{\partial x^2}\right|_{x'=x} dx \\ &= -\int \left[\left(\frac{\det\Omega}{\det\Omega'}\right)^2 x^2 - A^+\right]\rho\left(x,x\right)dx \\ &= A^+ - \frac{\det\Omega}{2\det\Omega'} \\ &= \frac{\Omega_{11}}{2}. \end{aligned} \tag{2.63}$$

We also have

$$\left\langle X_1^2\right\rangle = \frac{\left\langle\left(b_1+b_1^\dagger\right)^2\right\rangle}{2\omega},$$

and

$$\left\langle P_1^2\right\rangle = -\frac{\omega}{2}\left\langle\left(b_1^\dagger - b_1\right)^2\right\rangle.$$

So

$$\gamma = \cosh^{-1}\left(\frac{\zeta+1}{\zeta-1}\right),$$

$$\zeta := \frac{\Omega_{11}\det\Omega'}{\det\Omega} = -\left\langle\left(b_1^\dagger + b_1\right)^2\right\rangle\left\langle\left(b_1 - b_1^\dagger\right)^2\right\rangle.$$

The atom-photon entanglement entropy, away from the critical points, can be expressed as a function of the expectation values of squared quadrature operators $b_1+b_1^\dagger$ and $b_1-b_1^\dagger$, which can be measured in experiments.

2.6 Critical entanglement entropy in the generalized Dicke model with finite number of atoms

In the last section, we have seen that the atom-photon entanglement entropy diverges at the critical point. However, if the number of atoms is finite, then the entanglement

entropy will have an upper bound $N \ln l$. We want to study how the critical entanglement entropy scales with the number of atoms. Before presenting our results, we make two remarks:

1. It is not applicable to solve the Hamiltonian containing a few higher-order terms in the asymptotic series to characterize the finite-size effect at the critical point.

2. We need to artificially define criticality and multicriticality for finite-size systems.

The first remark is readily seen if we notice the symmetry of the higher-order terms in the asymptotic series. The full expansion of D is given by

$$\begin{aligned}
&\langle \ldots, n_i+1, \ldots, n_j-1, \ldots | \sum_{k=1}^{N} D^{(k)} | \ldots, n_i, \ldots, n_j, \ldots \rangle \\
=&\begin{cases}
D_{1,j}\sqrt{N n_j}\left(\sum_{k=0}^{\infty}\frac{\Gamma\left(\frac{3}{2}\right)}{\Gamma(1+k)\Gamma\left(\frac{3}{2}-k\right)}\left(-\frac{1+\sum_{r=2}^{l} n_r}{N}\right)^k\right) & \text{, when } i=1 \\
D_{i,1}\sqrt{N\left(n_i+1\right)}\left(\sum_{k=0}^{\infty}\frac{\Gamma\left(\frac{3}{2}\right)}{\Gamma(1+k)\Gamma\left(\frac{3}{2}-k\right)}\left(-\frac{\sum_{r=2}^{l} n_r}{N}\right)^k\right) & \text{, when } j=1 \\
D_{i,j}\sqrt{n_j\left(n_i+1\right)} & \text{, when } i,j>1
\end{cases},
\end{aligned}$$

which, together with Eq. (2.43), gives following asymptotic series of the Hamiltonian

$$\begin{aligned}
H =& N\epsilon_1 + H_{\text{eff}} + \frac{g\left(b_1+b_1^{\dagger}\right)\Xi}{2} \\
\Xi :=& \frac{1}{\sqrt{N}}\sum_{i,j=2}^{l} D_{ij} b_i^{\dagger} b_j \\
&+ \sum_{i=2}^{l} |D_{1,i}| \left(s\left(\frac{\sum_{j=2}^{l} b_j^{\dagger} b_j}{N}\right) b_i + b_i^{\dagger} s\left(\frac{\sum_{j=2}^{l} b_j^{\dagger} b_j}{N}\right)\right) \\
s\left(x\right) :=& \sum_{k=1}^{\infty} \frac{\Gamma\left(\frac{3}{2}\right)}{\Gamma\left(1+k\right)\Gamma\left(\frac{3}{2}-k\right)} \left(-x\right)^k .
\end{aligned}$$

We notice that Ξ does not contain b_1, so if there exist a state vector $|\Psi\rangle$ such that

$$\langle\Psi| \frac{g\left(b_1+b_1^{\dagger}\right)\Xi}{2} |\Psi\rangle = C_{\Psi}, \tag{2.64}$$

then there exists another state vector $|\Psi'\rangle = \exp\left(i\pi b_1^\dagger b_1\right)|\Psi\rangle$ such that

$$\langle\Psi'|\frac{g\left(b_1+b_1^\dagger\right)\Xi}{2}|\Psi'\rangle = -C_{\Psi'}.$$

So the Hamiltonian containing the first few terms in the asymptotic expansion does not have a lower bound unless we restrict the Hilbert space by $\sum_{j=2}^{l} b_j^\dagger b_j \leq N$. Therefore, the higher-order terms in the asymptotic series can only be understood perturbatively, provided that $|C_\Psi|$ is small comparing to the energy spacings in H_{eff}. However, the energy spacings in H_{eff} is infinitesimal at critical point.

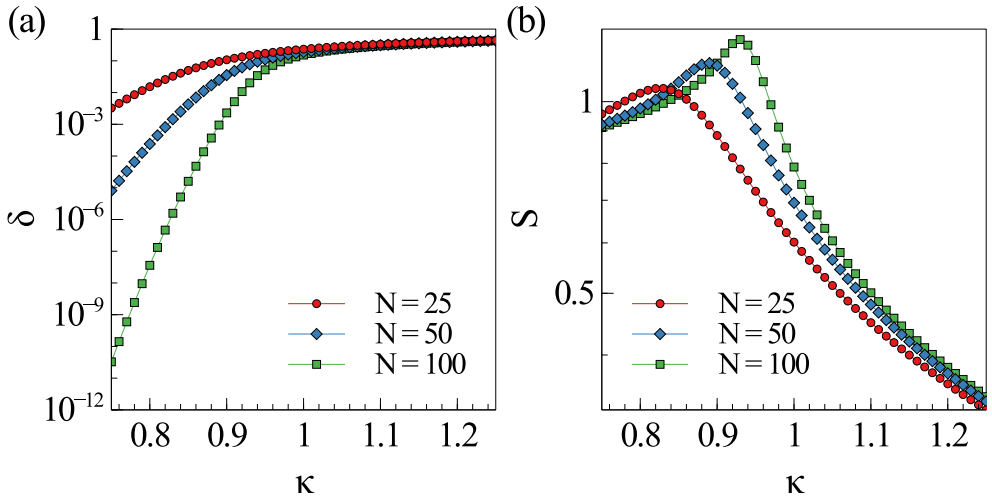

Figure 2.3 : (a) The gap δ between the ground state and the first excited state, and (b) the ground state atom-photon entanglement entropy S, of the original Dicke model for different atom number N. δ exponentially decreases when κ moves deep into the superradiant phase.

The second remark is because the singularities that mark the phase boundaries only occur in the limit $Ng^2/\omega^2 \to \infty$. When the number of atoms is finite, the gap does not close abruptly and the local maximums of the entanglement entropy are not located at the critical points predicted in the thermodynamic limit, which is illustrated in Fig. 2.3. We numerically diagonalize the original Dicke Hamiltonian

in Eq. (2.1), and in Fig. 2.3 we plot the lowest excitation energy δ and the ground state atom-photon entanglement entropy S as a function of κ. The number of atoms is chosen as $N = 25$, 50, or 100. We also limit the maximum number of photons to make the dimension of the Hilbert space finite. First we look at the panel (a). When κ is large, the system is in the normal phase, there is little difference between the gaps of different atom numbers, and the order of magnitude of the lowest excitation energy does not change. When κ is small, the system is in the superradiant phase, but the gap δ is not zero, unlike the case of the thermodynamic limit. Instead, δ drops exponentially as κ moves towards the superradiant phase. The transition between the two behaviors of δ happens in a region where κ is smaller than the mean-field phase boundary. We cannot identify a distinct boundary between the two phases from the graph. When N is larger, the gap drops faster and the transition region moves towards the mean-field phase boundary. Next let us take a look at panel (b). The atom-photon entanglement entropy has a maximum near the mean-field phase boundary. The more atoms the system has, the larger the maximum entropy of the system can reach, and the location of the maximum is closer to the mean-field boundary. The entropy drops faster when the system moves towards the normal phase than when the system moves towards the superradiant phase. This is because the ground state in the superradiant phase has additional trivial entanglement. In the thermodynamic limit, the ground states in the superradiant phase are doubly degenerate. In the last section, we calculate the entanglement entropy for the two ground states that break the Z_2 symmetry. The two states are not very much different from $\left|\pm\sqrt{N}\phi\epsilon/g\right\rangle\otimes|\pm\rangle$, where $\left|\pm\sqrt{N}\phi\epsilon/g\right\rangle$ are the photonic coherent states, and $|\pm\rangle$ are atom states where all the atoms occupy the mean-field ground state corresponding to $\pm\phi$. However, when there are finite number of atoms, the ground state is non-degenerate and the

Z_2 symmetry is not broken. Now, the single ground state resembles one of the states $\left|\sqrt{N}\phi\epsilon/g\right\rangle \otimes |+\rangle \pm \left|\sqrt{N}\phi\epsilon/g\right\rangle \otimes |-\rangle$. In the thermodynamic limit, the atom-photon entanglement entropy of such states is $\ln 2$ plus the result in Eq. (2.61), where $\ln 2$ arises from the superposition of the two symmetry breaking ground states. When the trivial factor $\ln 2$ occurs in the numerical calculation, it raises the left side of Fig. 2.3 (b) , shifting the location of the maximum entropy to the left and flattening the peak. Because we are interested in the critical entropy, it is reasonable to define the maximums of S in Fig. 2.3 (b) as the critical entropy and define the location of the maximum as the critical point for the finite-N system.

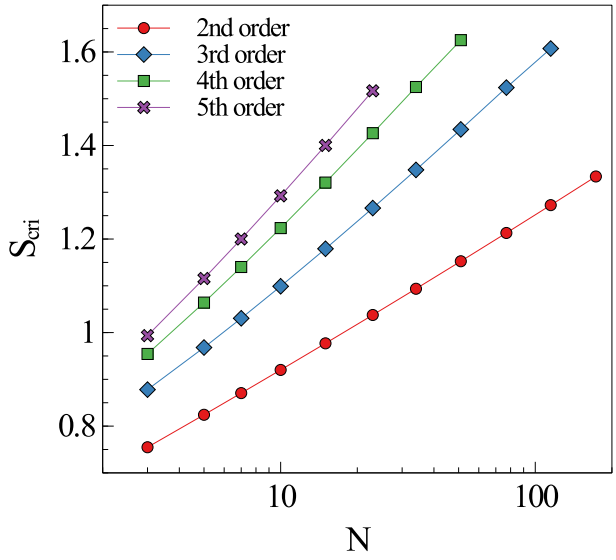

Figure 2.4 : Critical atom-photon entanglement entropy S_{cri} plotted against the atom number N for tridiagonal Dicke models with different orders of criticality.

We now numerically compare the critical entropy for different order of criticality. We consider a five-level tridiagonal Dicke model, where κ is set as 1, and the non-zero matrix elements of the dipole operator d are given by $(d_{12}, d_{23}, d_{34}, d_{45}) = \left(\sqrt{2}, \sqrt{3}, \sqrt{3}, \sqrt{2}\right)$ in a basis consisting of eigenvectors of h, and the diagonal elements

of h are tuned around the 5^{th} order critical point $(h_{11}, h_{22}, h_{33}, h_{44}, h_{55}) = (0, 2, 3, 3, 2)$ according to the multicritical conditions in Eq. (2.40). The reason we choose such a d matrix is that it is easy to realize in experiment as we will see in the next section. If we tune h_{55} to a sufficiently large value, then the 5^{th} eigenstate of h effectively decouples from the rest of the states. As a result, we arrive at a tetracritical (4^{th} order critical) 4-level tridiagonal Dicke model. And if we further tune h_{44} to be sufficiently large, we can reach an effective 3-level tricritical model. And finally if we tune h_{33} large, we obtain the original Dicke model.

As mentioned earlier, we need to define the critical and multicritical manifolds because of the finite atom numbers. Unlike the original Dicke model where a single parameter κ determines the phase diagram, now the critical manifold is not a single isolated point so it cannot be determined by the global maximum of the entropy. In Eq. (2.40), we see that each equation contains variables that independent from other equations. Especially, the equation for the ordinary criticality involves only κ, d_{12} and h_{22}. With κ and d_{12} fixed, we can define the ordinary critical manifold by maximizing the entropy with respect to h_{22}.

As for the multicritical manifolds, we define them by the mean-field values of (h_{33}, h_{44}, h_{55}). For example, the 5^{th} order critical point locates at the point maximizing the entropy with respect to h_{22} with fixed $(h_{33}, h_{44}, h_{55}) = (3, 3, 2)$. We plot the critical entropy S_{cri} against the number of atoms for different order of criticality in Fig. 2.4. We notice that the relation between S_{cri} and $\ln N$ has quite good linearity:

$$S_{\text{cri}} \approx s_0 + s_1 \ln N. \tag{2.65}$$

We extract the values of s_0 and s_1 from the graph and collect them in Table. 2.1 We see that both s_0 and s_1 increases when the order of criticality increases. Thus

Table 2.1 : Asymptotic behavior of the critical entropy $S_{\rm cri} \sim s_0 + s_1 \ln N$.

Order of Criticality	2	3	4	5
s_0	0.593(2)	0.642(7)	0.682(7)	0.704(8)
s_1	0.1428(7)	0.207(2)	0.238(3)	0.257(3)

we conclude that higher-order of criticality is associated with larger degrees of atom-photon entanglement entropy.

2.7 Realizing the tridiagonal Dicke models in experiments

In this section, we introduce the experimental proposal to realize high-order criticality in tridiagonal Dicke models. The proposal is based on the one reported in [50] and realized in experiment in [51]. The parameters in the experiment of [51] were not tuned to realize high-order criticality. Nevertheless, we show that all the parameters in the tridiagonal Dicke model can be tuned in state-of-the-art experiments in principle.

The proposal utilizes cavity-assisted Raman transitions between hyperfine states of the atom. The cavity-assisted Raman transitions were first discussed in [52] to realize the original Dicke model. Though originally Dicke considered the electric dipole coupling induced by photons between an electronically ground and an electronically excited atomic states, the dipole interaction is not strong enough to reach the threshold of the superradiant phase transition. Furthermore, there were some debates over the no-go theorem [53–57], which put some doubt on whether the Dicke model oversimplifies the reality and whether the superradiant phase transition can truly happen. However, it has been verified that the superradiant phase transition can occur in sys-

tems that take the Dicke model as an effective description [51, 58]. In the very first proposal [52], the atom states are coupled through cavity-assisted Raman transition, a two-photon process in which an atom, by absorbing (emitting) a cavity photon and emitting (absorbing) a photon to (from) classical laser fields, transfer from one hyperfine ground state to another. Unlike the one-photon electric dipole transition in which the atomic level spacing and the photon frequency are typically orders of magnitude larger than the coupling strength, in the two-photon Raman process, the coupling strength can be made to be comparable with the other energy scales such that the superradiant phase transition can be induced. Later, [50] generalizes the proposal to systems containing multiple atomic levels. This proposal realizes a tridiagonal Dicke model where the relative strength between the matrix elements of the dipole operator d is fixed. We modify the proposal in [50] to make the d matrix tunable.

Consider an atom whose relevant internal levels are denoted $|i, j\rangle$'s with energy $\varepsilon_{i,j}$, where $i = 0, 1, 2, \ldots, q$ denotes some hyperfine manifolds and j distinguishes the hyperfine states. Suppose when $i = 0$, $j = -F, -F+1, \ldots, F-1, F$. The hyperfine manifold with $i = 0$ has the lowest energy and is coupled with other hyperfine manifolds with $i > 0$ through optical transitions. Suppose the optical frequency is much larger than all the other energy scales in the system. The system is subject to two driving laser beams with opposite circular polarization. The driving beams have frequencies ω_+ and ω_-, and they mediate the atom transitions through the two Hamiltonians:

$$H_\pm = \sum_{i=1}^{q} \sum_{j=-F}^{F} g^i_{j\pm1,j} e^{-i\omega_\pm t} |i, j \pm 1\rangle \langle 0, j| + h.c., \tag{2.66}$$

where t is the time and $g^i_{j\pm1,j}$ is the coupling strength. The atom is placed in a cavity with a single linearly π-polarized mode and we denote the cavity frequency as ω_c.

The Hamiltonian for the cavity photons and the atoms without interaction is:

$$H_0 = \omega_c a^\dagger a + \sum_{i=1}^{q} \sum_{j=-F}^{F} \varepsilon_{i,j} \left|i,j\right\rangle \left\langle i,j\right| . \tag{2.67}$$

The basis vectors for the whole Hilbert space are denoted as $|n,i,j\rangle$ where n is the photon number and i,j marks the atom state. The cavity mode can also mediate optical transitions of the atoms through:

$$H_c = \sum_{i=1}^{q} \sum_{j=-F}^{F} g_j^i a \left|i,j\right\rangle \left\langle 0,j\right| + h.c., \tag{2.68}$$

where g_j^i's are the coupling strengths. The total Hamiltonian of this system is the sum of the previous fours. A schematic level diagram for the system is illustrated in Fig. 2.5. We will show that the Hamiltonian may effectively reduce to a time-independent one through adiabatic elimination.

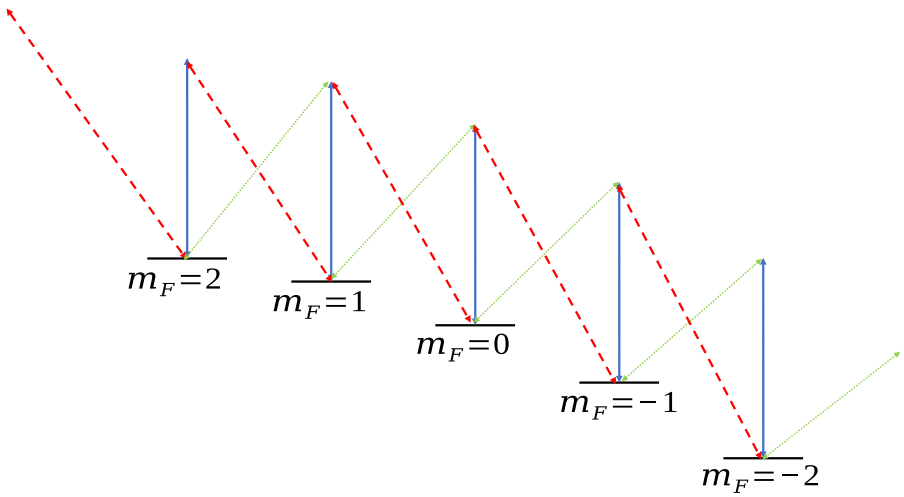

Figure 2.5 : An experimental scheme for realizing a tridiagonal Dicke model. Using a pair of Raman beams with opposite circular polarization, as marked by the dashed and the dotted lines, respectively, and a linearly π-polarized cavity mode, as marked by the solid line, it is possible to couple adjacent hyperfine states of ^{85}Rb (or other) atoms through Raman coupling.

The adiabatic elimination puts some constraints on the order of magnitudes of

the parameters in the system. We list the order of magnitudes of the parameters as follows ($i > 0$):

$$\omega_c \sim \omega_- \sim \omega_+ \sim \varepsilon_{i,j} - \varepsilon_{0,j},$$

$$\omega_c \gg \omega_c - (\varepsilon_{i,j} - \varepsilon_{0,j}) \sim \omega_- - (\varepsilon_{i,j-1} - \varepsilon_{0,j}) \sim \omega_+ - (\varepsilon_{i,j+1} - \varepsilon_{0,j}) \sim \Delta,$$

$$\Delta \gg |\varepsilon_{i,j} - \varepsilon_{i+1,j}|,$$

$$\Delta \gg |\varepsilon_{0,j} - \varepsilon_{0,j+1}|,$$

$$\Delta \gg g_j^i \sim g_{j-1,j}^i \sim g_{j+1,j}^i.$$

In the second line above, we have used Δ to denote the single-photon detuning. Because the coupling strengths are small compared to Δ, we can approximate the time evolution operator $U(t, t')$ through time-dependent perturbation theory, treating H_0 as the unperturbed Hamiltonian. We will neglect the transition amplitudes much smaller than 1.

To perform the perturbation, first we transform the Hamiltonian into the interaction picture:

$$H_c' = \sum_{i=1}^{q} \sum_{j=-F}^{F} g_j^i a e^{i(\varepsilon_{i,j} - \varepsilon_{0,j} - \omega_c)t} |i, j\rangle \langle 0, j| + h.c.,$$

$$H_\pm' = \sum_{i=1}^{q} \sum_{j=-F}^{F} g_{j\pm1,j}^i e^{i(\varepsilon_{i,j\pm1} - \varepsilon_{0,j} - \omega_\pm)t} |i, j \pm 1\rangle \langle 0, j| + h.c..$$

The first-order perturbation gives the transition amplitudes between atomic states with $i = 0$ and $i > 0$, and the amplitudes take the following form

$$\left\langle U^{(1)}(t, 0) \right\rangle \sim \frac{g\left(e^{i\Delta t} - 1\right)}{\Delta}.$$

Because $g/\Delta \ll 1$, we ignore the states with $i > 1$ in the effective Hamiltonian.

The second-order perturbation gives the transition amplitudes between atomic

states within the $i = 0$ manifold. The diagonal elements of $U^{(2)}(t,0)$ are

$$\langle n,0,j|\, U^{(2)}(t,0)\, |n,0,j\rangle = \frac{-it}{\Delta}\left(\sum_{i=1}^{q} n\left(g_j^i\right)^2 + \left(g_{j+1,j}^i\right)^2 + \left(g_{j-1,j}^i\right)^2\right),$$

which cannot be neglected when t is large. And the off-diagonal elements of $U^{(2)}(t,0)$ are

$$\langle n+1,0,j\pm 1|\, U^{(2)}(t,0)\, |n,0,j\rangle = \frac{\sqrt{n+1}\sum_{i=1}^{q} g_{j\pm1}^i g_{j\pm1,j}^i e^{-it(\varepsilon_{0,j}-\varepsilon_{0,j\pm1}+\omega_\pm-\omega_c)} - 1}{\Delta\left(\varepsilon_{0,j}-\varepsilon_{0,j\pm1}+\omega_\pm-\omega_c\right)},$$
$$\langle n,0,j+2|\, U^{(2)}(t,0)\, |n,0,j\rangle = \frac{\sum_{i=1}^{q} g_{j+1,j+2}^i g_{j+1,j}^i e^{-it(\varepsilon_{0,j}-\varepsilon_{0,j+2}+\omega_+-\omega_-)} - 1}{\Delta\left(\varepsilon_{0,j}-\varepsilon_{0,j+2}+\omega_+-\omega_-\right)},$$

and their conjugates. These amplitudes cannot be neglected when the coefficients, for example, $\frac{\sum_{i=1}^{q} g_{j+1}^i g_{j+1,j}^i}{\Delta(\varepsilon_{0,j}-\varepsilon_{0,j+1}+\omega_{j+1,j}-\omega_c)}$, are of order 1. Therefore, by tuning the atomic bare energies $\varepsilon_{0,j}$'s, we can decide how many hyperfine states are coupled through this single beam. We consider two cases:

- Case 1: All hyperfine states are coupled;
- Case 2: Only a pair of hyperfine states are coupled.

First we discuss the Case 1. The transition amplitudes, though obtained via second-order perturbation on the original Hamiltonian, can be regarded as the first-order perturbation result from an effective Hamiltonian H'_{eff}, whose matrix elements are given by

$$\langle n,0,j|\, H'_{\text{eff}}\, |n,0,j\rangle = \frac{\sum_{i=1}^{q} n\left(g_j^i\right)^2 + \left(g_{j+1,j}^i\right)^2 + \left(g_{j-1,j}^i\right)^2}{\Delta}, \tag{2.69}$$

$$\langle n+1,0,j\pm1|\, H'_{\text{eff}}\, |n,0,j\rangle = \frac{\sqrt{n+1}\sum_{i=1}^{q} g_{j\pm1}^i g_{j\pm1,j}^i}{\Delta} e^{-it(\varepsilon_{0,j}-\varepsilon_{0,j\pm1}+\omega_\pm-\omega_c)}, \tag{2.70}$$

$$\langle n,0,j+2|\, H'_{\text{eff}}\, |n,0,j\rangle = \frac{\sum_{i=1}^{q} g_{j+1,j+2}^i g_{j+1,j}^i}{\Delta} e^{-it(\varepsilon_{0,j}-\varepsilon_{0,j+2}+\omega_+-\omega_-)}, \tag{2.71}$$

and the Hermitian conjugates of the last three lines.

Table 2.2 : The relative strengths between the summations of g-squares for Rb^{87}

j	-1	0	1
$\sum_{i=1}^{q}\left(g_j^i\right)^2$	$\frac{1}{3}$	$\frac{1}{3}$	$\frac{1}{3}$
$\sum_{i=1}^{q}\left(g_{j+1,j}^i\right)^2$	$\frac{1}{6}$	$\frac{1}{3}$	$\frac{1}{2}$
$\sum_{i=1}^{q}\left(g_{j-1,j}^i\right)^2$	$\frac{1}{2}$	$\frac{1}{3}$	$\frac{1}{6}$
$\sum_{i=1}^{q} g_{j+1}^i g_{j+1,j}^i$	$-\frac{1}{6}$	$-\frac{1}{6}$	0
$\sum_{i=1}^{q} g_{j-1}^i g_{j-1,j}^i$	0	$-\frac{1}{6}$	$-\frac{1}{6}$

In order to transform H'_{eff} into a time-independent Hamiltonian, some conditions need to be satisfied. First, the matrix elements $\langle n,0,j+2|\, H'_{\text{eff}}\, |n,0,j\rangle$ need to vanish, which also guarantees that H'_{eff} is tridiagonal in terms of atomic states. This requirement leads to:

$$\sum_{i=1}^{q} g_{j+1,j+2}^i g_{j+1,j}^i = 0. \tag{2.72}$$

In the case that $|i=0,j\rangle$'s are $F=1$ ground states of ^{87}Rb atoms or $F=2$ ground states of ^{85}Rb atoms, and the laser beams drive the D_1 transitions, the equation above holds. And the relative strengths between the other summations of g-squares encountered in the matrix elements of H'_{eff} are listed in Table. 2.2 and 2.3, evaluated by Clebsch-Gordan coefficients.

To make H'_{eff} time-independent, a second requirement is that the phase accumulated in the following series of transition process,

$$|n,j\rangle \to |n+1,j+1\rangle \to |n+2,j\rangle \to |n+1,j-1\rangle \to |n,j\rangle\,, \tag{2.73}$$

is zero, where we have omitted the $i=0$ index in the notation for simplicity. This

Table 2.3 : The relative strengths between the summations of g-squares for Rb^{85}

j	-2	-1	0	1	2
$\sum_{i=1}^{q}\left(g_j^i\right)^2$	$\frac{1}{3}$	$\frac{1}{3}$	$\frac{1}{3}$	$\frac{1}{3}$	$\frac{1}{3}$
$\sum_{i=1}^{q}\left(g_{j+1,j}^i\right)^2$	$\frac{1}{9}$	$\frac{2}{9}$	$\frac{3}{9}$	$\frac{4}{9}$	$\frac{5}{9}$
$\sum_{i=1}^{q}\left(g_{j-1,j}^i\right)^2$	$\frac{5}{9}$	$\frac{4}{9}$	$\frac{3}{9}$	$\frac{2}{9}$	$\frac{1}{9}$
$\sum_{i=1}^{q} g_{j+1}^i g_{j+1,j}^i$	$-\frac{\sqrt{2}}{9}$	$-\frac{\sqrt{3}}{9}$	$-\frac{\sqrt{3}}{9}$	$-\frac{\sqrt{2}}{9}$	0
$\sum_{i=1}^{q} g_{j-1}^i g_{j-1,j}^i$	0	$-\frac{\sqrt{2}}{9}$	$-\frac{\sqrt{3}}{9}$	$-\frac{\sqrt{3}}{9}$	$-\frac{\sqrt{2}}{9}$

leads to

$$\begin{aligned} 0 = &\left(\varepsilon_{0,j} - \varepsilon_{0,j+1} + \omega_+ - \omega_c\right) + \left(\varepsilon_{0,j+1} - \varepsilon_{0,j} + \omega_- - \omega_c\right) \\ &- \left(\varepsilon_{0,j-1} - \varepsilon_{0,j} + \omega_+ - \omega_c\right) - \left(\varepsilon_{0,j} - \varepsilon_{0,j-1} + \omega_- - \omega_c\right), \end{aligned}$$

which always holds. We denote

$$2\omega_0 := \omega_+ + \omega_-.$$

So, with the vanish of $\langle n, 0, j+2| H'_{\text{eff}} |n, 0, j\rangle$, we can hereby transform H'_{eff} through

$$H'_0 := \left(\omega_0 - \omega_c\right) a^\dagger a + \sum_{j=-F}^{F} \sum_{k=-F}^{j} \left(\varepsilon_{0,k} - \varepsilon_{0,k+1} + \frac{\omega_+ - \omega_-}{2}\right) |0, j+1\rangle \langle 0, j+1|$$

to

$$\begin{aligned} H_{\text{eff}} =& \exp\left(iH'_0 t\right) H'_{\text{eff}} \exp\left(-iH'_0 t\right) - H'_0 \\ =& \left(\omega_c - \omega_0\right) a^\dagger a + \sum_{j=-F}^{F} \varepsilon_j |0, j\rangle \langle 0, j| \\ &+ \sum_{j=-F}^{F-1} \frac{\sum_{i=1}^{q} a^\dagger g_{j+1}^i g_{j+1,j}^i + a g_j^i g_{j,j+1}^i}{\Delta} |0, j+1\rangle \langle 0, j| + h.c. \end{aligned}$$

with

$$\varepsilon_j := \sum_{k=-F}^{j} \varepsilon_{0,k+1} - \varepsilon_{0,k} - \frac{\omega_+ - \omega_-}{2} + \frac{\sum_{i=1}^{q} \left(g_{j+1,j}^i\right)^2 + \left(g_{j-1,j}^i\right)^2}{\Delta} + \frac{\sum_{i=1}^{q} \left(g_j^i\right)^2}{\Delta} a^\dagger a$$

According to Table. 2.2 and 2.3, by setting $\sum_{i=1}^{q} \left(g_j^i\right)^2 := \frac{g_c^2}{3}$ and $\sum_{i=1}^{q} \left(g_{-1,0}^i\right)^2 = \sum_{i=1}^{q} \left(g_{1,0}^i\right)^2 := \frac{g_{\mathrm{drv}}^2}{3}$, we obtain

$$H_{\mathrm{eff}} = \left(\omega_c - \omega_0 + \frac{g_c^2}{3}\right) a^\dagger a + \sum_{j=-F}^{F} \sum_{k=-F}^{j} \left(\varepsilon_{0,k+1} - \varepsilon_{0,k} - \frac{\omega_+ - \omega_-}{2}\right) |0,j\rangle \langle 0,j| \tag{2.74}$$

$$+ g_{\mathrm{drv}} g_c \left(a + a^\dagger\right) \sum_j C_j |0,j+1\rangle \langle 0,j| + h.c. \tag{2.75}$$

where C_j's are read from the Table. 2.2 and 2.3, and we omit an unimportant constant. We notice that the term $\sum_j C_j |0,j+1\rangle \langle 0,j| + h.c$ is proportional to the angular momentum operator F_x of the hyperfine manifold. So we end up with a tridiagonal Dicke model where the relative strengths between the matrix elements of the dipole operator d are fixed, and the eigenvalues of single-atom Hamiltonian h can be altered by changing the bare atomic energies $\varepsilon_{0,j}$'s. Experimentally, adjusting $\varepsilon_{0,j}$'s can be achieved using external magnetic fields via the Zeeman shift or using external microwave fields via the AC-Stark shift [59–65].

In order to tune the dipole operator d, it is necessary to use multiple pairs of laser beams, each pair of lasers couple only one pair of hyperfine states, as in Case 2 described above Eq. (2.69). Suppose the pair of driving beams coupling $|0,j\rangle$ and

$|0, j+1\rangle$ have frequencies $\omega_{\pm}^{j,j+1}$ and coupling strength $g_{\text{drv}}^{j,j+1}$. Now Eq. (2.73) yields

$$\begin{aligned} 0 &= \left(\varepsilon_{0,j} - \varepsilon_{0,j+1} + \omega_{+}^{j,j+1} - \omega_c\right) + \left(\varepsilon_{0,j+1} - \varepsilon_{0,j} + \omega_{-}^{j,j+1} - \omega_c\right) \\ &\quad - \left(\varepsilon_{0,j-1} - \varepsilon_{0,j} + \omega_{+}^{j-1,j} - \omega_c\right) - \left(\varepsilon_{0,j} - \varepsilon_{0,j-1} + \omega_{-}^{j-1,j} - \omega_c\right) \\ &= \omega_{+}^{j,j+1} + \omega_{-}^{j,j+1} - \omega_{+}^{j-1,j} - \omega_{-}^{j-1,j}. \end{aligned}$$

Therefore, to make H_{eff} time-independent, the following equation must hold

$$\omega_{+}^{j,j+1} + \omega_{-}^{j,j+1} \equiv 2\omega_0. \tag{2.76}$$

Now, for ^{85}Rb and ^{87}Rb,

$$\begin{aligned} H_{\text{eff}} = &\left(\omega_c - \omega_0 + \frac{g_c^2}{3}\right) a^\dagger a \\ &+ \sum_{j=-F}^{F} \sum_{k=-F}^{j} \left(\varepsilon_{0,k+1} - \varepsilon_{0,k} - \frac{\omega_{+}^{k,k+1} - \omega_{-}^{k,k+1}}{2}\right) |0,j\rangle \langle 0,j| \\ &+ g_c \left(a + a^\dagger\right) \sum_j C_j g_{\text{drv}}^{j,j+1} |0, j+1\rangle \langle 0,j| + h.c. \end{aligned} \tag{2.77}$$

In this tridiagonal Dicke Hamiltonian, arbitrary d matrix can be achieved by tuning the intensities of the driving lasers, to which $g_{\text{drv}}^{j,j+1}$ is proportional.

2.8 Quantum fluctuation of the generalized Dicke model in the classical oscillator limit

In Section 2.2, we introduce the superradiant phase transition of the original Dicke model in the classical oscillator limit, $\frac{\omega}{\epsilon} \sim \frac{g^2}{\epsilon^2} \ll 1$. The phase transition in the classical oscillator limit share the same mean-field theory with that in the thermodynamic limit. Nevertheless, the quantum fluctuation behaves dramatically different in the two limits. In this section, we will investigate the quantum fluctuation of the generalized Dicke model in the classical oscillator limit.

Here we take $N = 1$. As long as N is finite, we can always make $N = 1$ by redefining d and h. Now, Eq. (2.41) reads

$$H = \omega b^\dagger b + \frac{g\left(b + b^\dagger\right) D}{2} + h_{\mathrm{MF}}, \tag{2.78}$$

where we have omitted the subscript of b_1. Because ω and g are small compared to the energy spacings in h_{MF} in the classical oscillator limit, we treat the first two terms as perturbation to the mean-field Hamiltonian, using Eq. (A.1) with $\rho = 1$ to project H onto its lowest-energy manifold and obtain an effective Hamiltonian as follows:

$$\begin{aligned}
H_{\mathrm{eff}} =& \left(H - \epsilon_1\right) P_1^{(\lambda)} \\
=& S_0 \left(\omega b^\dagger b\right) S_0 + S_0 \frac{g\left(b + b^\dagger\right) D}{2} S_1 \frac{g\left(b + b^\dagger\right) D}{2} S_0 \\
&+ \left[S_0 \left(\omega b^\dagger b\right) S_0 \frac{g\left(b + b^\dagger\right) D}{2} S_1 + h.c. \right] \\
&+ S_0 \frac{g\left(b + b^\dagger\right) D}{2} S_1 \frac{g\left(b + b^\dagger\right) D}{2} S_1 \frac{g\left(b + b^\dagger\right) D}{2} S_0 \\
&+ \left[S_0 \frac{g\left(b + b^\dagger\right) D}{2} S_1 \frac{g\left(b + b^\dagger\right) D}{2} S_0 \frac{g\left(b + b^\dagger\right) D}{2} S_1 + h.c. \right] + O\left(\frac{\omega^2}{\epsilon^2}\right) \\
=& \left|1\right\rangle \left(\omega b^\dagger b - \alpha_0 \left[\frac{g\left(b + b^\dagger\right)}{2}\right]^2 + \alpha_1 \left[\frac{g\left(b + b^\dagger\right)}{2}\right]^3 \right) \left\langle 1\right| \\
&+ \left[\left|1\right\rangle \left(-\omega b^\dagger b + \alpha_0 \left[\frac{g\left(b + b^\dagger\right)}{2}\right]^2 \right) \frac{g\left(b + b^\dagger\right)}{2} \sum_{k_1=2}^{l} \alpha_{k_1} \left\langle k_1\right| + h.c. \right] \\
&+ O\left(\frac{\omega^2}{\epsilon^2}\right),
\end{aligned} \tag{2.79}$$

with

$$\alpha_k := \begin{cases} \sum_{k_1=2}^{l} \frac{\left|D_{1k_1}\right|^2}{\epsilon_{k_1} - \epsilon_1}, & k = 0 \\ \sum_{k_1,k_2=2}^{l} \frac{D_{1k_2} D_{k_2 k_1} D_{k_1 1}}{\left(\epsilon_{k_2} - \epsilon_1\right)\left(\epsilon_{k_1} - \epsilon_1\right)}, & k = 1 \\ \frac{D_{1k}}{\epsilon_k - \epsilon_1}, & k > 1 \end{cases},$$

where $\left|k\right\rangle$'s are the mean-field eigenstates. Because the third-order terms with the order of magnitude $\left(\frac{g}{\epsilon}\right)^3$ are cubic in b and $b^\dagger$, they do not have a lower bound, thus

can only be understood perturbatively, assuming $\langle b^\dagger b\rangle \sim 1$. To the lowest (second) order, we have

$$H_{\text{eff}} = |1\rangle \left(\omega b^\dagger b - \alpha_0 \left[\frac{g\left(b + b^\dagger\right)}{2} \right]^2 \right) \langle 1| + o\left(\frac{\omega}{\epsilon}\right), \tag{2.80}$$

which takes the same form as the one appears in the original Dicke model in Eq. (2.9). We denote the eigenvectors of H_{eff} in Eq. (2.80) as $|1,k\rangle$, where 1 represents the atomic state and k the photon state, and the corresponding eigenvalues are

$$\left(k+\frac{1}{2}\right)\omega_{\text{CO}} := \left(k+\frac{1}{2}\right)\sqrt{\omega\left(\omega-\alpha_0 g^2\right)}, \quad k = 0,1,2,\ldots$$

It is required that $\omega \geq \alpha_0 g^2$, which is consistent with the stability condition of the mean-field solution in Eq. (2.28). The effective Hamiltonian (2.80) does not produce entanglement between atoms and photons.

When ω_{CO} is not vanishingly small, we can treat the third-order terms in Eq. (2.79) as perturbation to Eq. (2.80). This will lead to atom-photon entanglement. The ground state under this situation is given by:

$$\begin{aligned} |\text{CO}\rangle = &|1,0\rangle - \frac{\alpha_1 g^3 \omega^{3/2}}{8\omega_{\text{CO}}^{5/2}}\left(3\,|1,1\rangle + \frac{\sqrt{6}}{3}\,|1,3\rangle\right) \\ &+ \sum_{k_1=2}^{l} \frac{\alpha_{k_1} g\sqrt{\omega\omega_{\text{CO}}}}{4\left(\epsilon_1 - \epsilon_{k_1}\right)}\,|k_1,1\rangle + o\left(\left(\frac{g}{\epsilon}\right)^3\right) \end{aligned} \tag{2.81}$$

Using the method in Appendix B, we can calculate the atom-photon entanglement entropy of $|\text{CO}\rangle$:

$$\begin{aligned} S = &-\left(\frac{1}{2}+\sqrt{\frac{1}{4}-\mu}\right)\ln\left(\frac{1}{2}+\sqrt{\frac{1}{4}-\mu}\right) \\ &-\left(\frac{1}{2}-\sqrt{\frac{1}{4}-\mu}\right)\ln\left(\frac{1}{2}-\sqrt{\frac{1}{4}-\mu}\right) \\ \approx &-\mu\ln\mu, \end{aligned} \tag{2.82}$$

where μ has the same order of magnitude as $\frac{\omega^2}{\epsilon^2}$:

$$\mu = \frac{g^2\omega\omega_{\mathrm{CO}}}{16}\sum_{k_1=2}^{l}\frac{|D_{1k_1}|^2}{(\epsilon_1-\epsilon_{k_1})^4} + o\left(\frac{\omega^2}{g^2}\right). \tag{2.83}$$

We see that the entanglement entropy is vanishingly small, which is qualitatively different from that in the thermodynamic limit.

2.9 Realizing generalized Dicke model in the classical oscillator limit

An experiment realizing a tricritical point in a spin-one Dicke model in the classical oscillator limit has been reported in [20]. The experimental scheme can be generalized to incorporate more atomic levels, as we show in this section.

The experiment is also based on Raman transitions between hyperfine levels of atoms, however, no cavity but a one-dimensional harmonic trap is used, and the motion of the atom within this trap is treated as a relevant degree of freedom. Like what is done in Section 2.7, we denote the internal levels of the atom as $|i,j\rangle$, $i = 0,1,2\ldots,$ $j = -F, -F+1, \ldots, F-1, F$. Without the driving lasers, a single atom subject to the Hamiltonian

$$H_{\mathrm{atom}} = \frac{P^2}{2} + \frac{1}{2}\omega_{\mathrm{trap}}^2 X^2 + \sum_{i,j}\varepsilon_{i,j}\,|i,j\rangle\langle i,j| \tag{2.84}$$

A linearly π-polarized laser replaces the cavity field, and drives the transition between $|0,j\rangle$ and $|i,j\rangle$ for $i>0$:

$$H_\pi = \sum_{i,j} g_j^i \exp\left(i\left(k_{\mathrm{R}}X - \omega_\pi t\right)\right)|i,j\rangle\langle 0,j| + h.c. \tag{2.85}$$

where k_{R} is the recoil momentum. The pair of circularly polarized lasers remain the

same:

$$H_{\pm} = \sum_{i=1}^{q} \sum_{j=-F}^{F} g^{i}_{j\pm1,j} \exp\left(-i\left(k_{\mathrm{R}}X + \omega_{\pm}t\right)\right) |i, j\pm1\rangle \langle 0, j| + h.c. \tag{2.86}$$

We make the laser with frequency ω_{-} detuned to some degree such that it does not couple adjacent states. After adiabatic elimination, we arrive at the following effective Hamiltonian:

$$\begin{aligned} H_{\mathrm{eff}} =& \frac{P^2}{2} + \frac{1}{2}\omega^2_{\mathrm{trap}}X^2 + \sum_{j=-F}^{F} \varepsilon_j |0, j\rangle \langle 0, j| \\ &+ \sum_{j=-F}^{F} \frac{\sum_{i=1}^{q} e^{2ik_{\mathrm{R}}X} g^{i}_{j+1} g^{i}_{j+1,j}}{\Delta} |0, j+1\rangle \langle 0, j| + h.c., \end{aligned} \tag{2.87}$$

with

$$\begin{aligned} \varepsilon_j :=& \sum_{k=-F}^{j} \left(\varepsilon_{0,k+1} - \varepsilon_{0,k} + \omega_{+} - \omega_{\pi}\right) \\ &+ \frac{\sum_{i=1}^{q} \left(g^{i}_{j+1,j}\right)^2 + \left(g^{i}_{j-1,j}\right)^2 + \left(g^{i}_{j}\right)^2}{\Delta} \end{aligned}$$

Performing a unitary transformation $|0, j\rangle \rightarrow \exp\left(2ijk_{\mathrm{R}}X\right)|0, j\rangle$, we can transform H_{eff} into the form:

$$H_{\mathrm{eff}} = \frac{\left(P + 2k_{\mathrm{R}}F_z\right)^2}{2} + \frac{1}{2}\omega^2_{\mathrm{trap}}X^2 + H_{\mathrm{internal}} \tag{2.88}$$

$$\begin{aligned} H_{\mathrm{internal}} :=& \sum_{j=-F}^{F} \varepsilon_j |0, j\rangle \langle 0, j| \\ &+ \sum_{j=-F}^{F} \frac{\sum_{i=1}^{q} g^{i}_{j+1} g^{i}_{j+1,j}}{\Delta} |0, j+1\rangle \langle 0, j| + h.c. \end{aligned} \tag{2.89}$$

If we represent X and P in terms of bosonic operators a and $a^{\dagger}$,

$$\begin{aligned} X &= \frac{i}{\sqrt{2\omega_{\mathrm{trap}}}}\left(a - a^{\dagger}\right), \\ P &= \sqrt{\frac{\omega_{\mathrm{trap}}}{2}}\left(a^{\dagger} + a\right), \end{aligned}$$

then

$$H_{\text{eff}} = \omega_{\text{trap}} \left(a^\dagger a + \frac{1}{2} \right) + 2k_{\text{R}} \sqrt{\frac{\omega_{\text{trap}}}{2}} F_z \left(a^\dagger + a \right) + 2k_{\text{R}}^2 F_z^2 + H_{\text{internal}} \tag{2.90}$$

which takes the form of the generalized Dicke Hamiltonian with $d \propto F_z$ and $h = \frac{2k_{\text{R}}^2}{m} F_z^2 + H_{\text{internal}}$.

Chapter 3

Building flat-band lattice models from Gram matrices

In this chapter, we introduce the Gram matrix method for building flat-band Hamiltonians. We first introduce the basic properties about tight-binding models, especially the ones whose translational symmetry has a projective representation in the Hilbert space, which happens, for example, when a magnetic field is presented. Next, based on the knowledge about tight-binding models, we introduce our Gram matrix-based protocol of building any lattice model whose lowest few bands are flat. As explicit examples, we provide some finite-range models with ordinary translational symmetry built from the protocol. Finally, we reproduce the Kapit-Mueller model with magnetic translational symmetry and topological flat band, whose Hamiltonian can be understood as the Gram matrix built from certain subset of coherent states, and can be generalized to infinite many other flat-band models with magnetic translational symmetry.

3.1 Tight-binding lattice models and flat bands

In this section, we make an introduction on tight-binding lattice models in which flat bands may appear.

A lattice can be regarded as infinite replica of unit cells, which models the periodic arrangement of atoms in a real crystal. We can associate each unit cell with a lattice

vector denoted as $\mathbf{R}$:

$$\mathbf{R} = \sum_{i=1}^{d} x_i \mathbf{e}_i,\ x_i \in \mathbb{Z} \tag{3.1}$$

where d and $\mathbf{e}_i$'s are the spatial dimension and the primitive vectors of the lattice, respectively. In a real crystal, a cell contains infinite number of states that can be occupied by particles of interest. However, it is often the case that only finite number of them are relevant. For example, in an optical lattice, the cold atoms may only occupy the lowest energy state in a cell because of the ultra-low temperature. Neglecting the unimportant high-energy states is called tight-binding approach. Without interactions, a single-particle tight-binding model possesses a Hilbert space which is spanned by the basis vectors $|\mathbf{R}; i\rangle$ with $i = 1, 2, \ldots, n_s$, where n_s is the total number of states within a cell. Realistically, these states can be electronic orbitals around an atom, spin degrees of freedom, atomic states in an optical lattice, etc. In general, the Hamiltonian for a single-particle tight-binding model can be written as

$$H = \sum_{\mathbf{R},\mathbf{R}'} \sum_{i,i'} h^{i,i'}_{\mathbf{R},\mathbf{R}'} \left|\mathbf{R}; i\right\rangle \left\langle \mathbf{R}'; i'\right|, \tag{3.2}$$

where the hopping amplitudes $h^{i,i'}_{\mathbf{R},\mathbf{R}'}$ form a hermitian matrix:

$$h^{i,i'}_{\mathbf{R},\mathbf{R}'} = \left(h^{i',i}_{\mathbf{R}',\mathbf{R}}\right)^*. \tag{3.3}$$

The most important feature of a lattice is its translational symmetry. If we translate the system by one of its lattice vector $\mathbf{R}$, the physics should not change. The translational symmetry group can be represented by unitary matrices $U_{\mathbf{R}}$'s defined with a phase factor $\phi\left(\mathbf{R}, \mathbf{R}', i\right)$:

$$U_{\mathbf{R}} \left|\mathbf{R}'; i\right\rangle = e^{i\phi(\mathbf{R},\mathbf{R}',i)} \left|\mathbf{R} + \mathbf{R}'; i\right\rangle,\ \forall\, \mathbf{R}, \mathbf{R}'. \tag{3.4}$$

such that the Hamiltonian is invariant under the following unitary transformation:

$$U_{\mathbf{R}} H U^{\dagger}_{\mathbf{R}} = H,\ \forall\, \mathbf{R}. \tag{3.5}$$

Usually, the phase factor $\phi(\mathbf{R}, \mathbf{R}', i)$ is trivial such that

$$U_{\mathbf{R}} |\mathbf{R}'; i\rangle = |\mathbf{R}' + \mathbf{R}; i\rangle , \forall \mathbf{R}, \mathbf{R}'.$$

In this case, the translational symmetry group has an linear representation, meaning

$$U_{\mathbf{R}} U_{\mathbf{R}'} = U_{\mathbf{R}'+\mathbf{R}},$$

and the hopping amplitude $h^{i,i'}_{\mathbf{R},\mathbf{R}'}$ satisfies

$$h^{i,i'}_{\mathbf{R}+\mathbf{R}'',\mathbf{R}'+\mathbf{R}''} = h^{i,i'}_{\mathbf{R},\mathbf{R}'}.$$

However, we can encounter the cases in which $\phi(\mathbf{R}, \mathbf{R}', i)$ is non-trivial and $U_{\mathbf{R}}$'s form a projective representation of the translational symmetry group.

In Appendix C, we show that, by properly choosing the gauge, first, the function $\phi(\mathbf{R}, \mathbf{R}', i)$ is independent from the index i, so abbreviated as $\phi(\mathbf{R}, \mathbf{R}')$, and second, $\phi(\mathbf{R}, \mathbf{R}')$ satisfies the following identities:

$$\phi(\mathbf{0}, \mathbf{R}) \equiv \phi(\mathbf{R}, \mathbf{0}) \equiv \phi(\mathbf{R}, \mathbf{R}) \equiv \phi(\mathbf{R}, -\mathbf{R}) \equiv 0. \tag{3.6}$$

As a result, the hopping amplitude $h^{i,i'}_{\mathbf{R},\mathbf{R}'}$ satisfies

$$h^{i,i'}_{\mathbf{R}+\mathbf{R}'',\mathbf{R}'+\mathbf{R}''} = h^{i,i'}_{\mathbf{R},\mathbf{R}'} e^{i(\phi(\mathbf{R}'',\mathbf{R}) - \phi(\mathbf{R}'',\mathbf{R}'))}. \tag{3.7}$$

And $U_{\mathbf{R}}$'s satisfy

$$U_{\mathbf{R}'} U_{\mathbf{R}} = e^{i\phi(\mathbf{R}',\mathbf{R})} U_{\mathbf{R}'+\mathbf{R}}, \tag{3.8}$$

and $U_{-\mathbf{R}}$ is the inverse of $U_{\mathbf{R}}$:

$$U_{\mathbf{R}} U_{-\mathbf{R}} = 1. \tag{3.9}$$

Now, let us discuss the eigenstates of the H. When $U_{\mathbf{R}}$'s form a linear representation of the translational group, all $U_{\mathbf{R}}$'s commute with each other as well as the

Hamiltonian, so the eigenstates of the Hamiltonian can be marked by pseudo momenta which correspond to the eigenvalues of $U_{\mathbf{R}}$'s. This is just the content of the well-known Bloch theorem of periodic systems. In general, according to Eq. (3.8), $U_{\mathbf{R}}$ and $U_{\mathbf{R}'}$ commute only when

$$\phi(\mathbf{R}, \mathbf{R}') = \phi(\mathbf{R}', \mathbf{R}). \tag{3.10}$$

To mark the eigenstates of H, we want to find the largest subset of $U_{\mathbf{R}}$'s whose elements commute with each other. We mark the corresponding lattice vectors as ρ's. We can make use of the Bloch theorem if U_ρ's form a representation of a subgroup of the translational group, in other words, ρ's also form a lattice. To this end, we require that $\phi(\mathbf{R}, \mathbf{R}')$ is a bilinear function of $\mathbf{R}$ and $\mathbf{R}'$

$$\phi(\mathbf{R}, \mathbf{R}') = \sum_{i,i'=1}^{d} \phi(\mathbf{e}_i, \mathbf{e}_{i'}) x_i x'_{i'} \tag{3.11}$$

Now, if

$$\phi(\rho, \rho') = \phi(\rho', \rho) \tag{3.12}$$

then any linear combination of ρ and ρ' commute with ρ and ρ', so ρ's form a linear vector space, or a lattice. Especially, we let $(2\pi)^{-1}\phi(\mathbf{e}_i, \mathbf{e}_{i'})$ be rational number such that the lattice is d-dimensional. In the rest of this chapter, we will only discuss bilinear and rational $\phi(\mathbf{R}, \mathbf{R}')$. We denote the primitive vectors of this lattice as τ_i's, which coincide with $\mathbf{e}_i$ when all the $U_{\mathbf{R}}$'s commute with each other. We call the cells of the lattice ρ as the enlarged cells, each of which corresponds to a lattice vector ρ, and each enlarged cell contains q cells. The bilinearity of $\phi(\mathbf{R}, \mathbf{R}')$ together with $\phi(\mathbf{R}, \mathbf{R}) \equiv \mathbf{0}$ implies that $\phi(\mathbf{R}, \mathbf{R}')$ is asymmetric

$$\phi(\mathbf{R}, \mathbf{R}') = -\phi(\mathbf{R}', \mathbf{R}). \tag{3.13}$$

So a non-trivial bilinear $\phi(\mathbf{R}, \mathbf{R}')$ represents a magnetic field. For example, a magnetic field perpendicular to a two-dimensional lattice is represented by

$$\phi(\mathbf{e}_1, \mathbf{e}_2) \propto (\mathbf{e}_1 \times \mathbf{e}_2) \cdot \mathbf{e}_3.$$

Therefore, we call a translational symmetry with a linear representation as an ordinary translational symmetry, and a translational symmetry with a projective representation with bilinear $\phi(\mathbf{R}, \mathbf{R}')$ as a magnetic translational symmetry.

Now we can find the common eigenstates of H and U_ρ's, the Bloch waves $|\psi_{\mathbf{k},i}\rangle$. Here we only give the major properties of the Bloch waves, leaving the calculation details to Appendix D. $|\psi_{\mathbf{k},i}\rangle$ satisfies

$$H|\psi_{\mathbf{k},i}\rangle = \epsilon_{\mathbf{k},i}|\psi_{\mathbf{k},i}\rangle, \tag{3.14}$$

$$U_\rho|\psi_{\mathbf{k},i}\rangle = e^{-i\rho\cdot\mathbf{k}+i\rho^2}|\psi_{\mathbf{k},i}\rangle, \tag{3.15}$$

with

$$\rho^2 := \sum_{i=1}^{d}\sum_{i'=i+1}^{d} y_i y_{i'} \phi(\tau_i, \tau_{i'}). \tag{3.16}$$

for $\rho = \sum_{i=1}^{d} y_i \tau_i$. The pseudo momentum

$$\mathbf{k} = \sum_{i=1}^{d} k_i \tau^i, \tag{3.17}$$

is defined on the Brillouin zone $k_i \in [0, 2\pi)$, and τ^i's are the primitive vectors of the reciprocal lattice of the lattice ρ:

$$\tau_i \cdot \tau^j = \delta_{i,j}. \tag{3.18}$$

The index i in the energy $\epsilon_{\mathbf{k},i}$ marks the bands, $i = 1, 2, \ldots, qn_s$. $|\psi_{\mathbf{k},i}\rangle$ resides in the momentum space spanned by momentum states $|\mathbf{k}, \mathbf{r}; i\rangle$ defined by

$$|\mathbf{k}, \mathbf{r}; i\rangle := \sum_{\rho} e^{i\mathbf{k}\cdot(\rho+\mathbf{r})-i\rho^2} U_\rho |\mathbf{r}; i\rangle, \tag{3.19}$$

where $\mathbf{r}$ is any $\mathbf{R}$ modulo ρ, the position of cells in a single enlarged cell. Thus, we can project the Hamiltonian into the momentum space:

$$H = \int \frac{d^d\mathbf{k}}{(2\pi)^d} H_{\mathbf{k}} \tag{3.20}$$

with

$$H_{\mathbf{k}} := \sum_{\mathbf{r},\mathbf{r}'} \sum_{i,i'} h^{i,i'}_{\mathbf{r},\mathbf{r}'}(\mathbf{k}) \left|\mathbf{k},\mathbf{r};i\right\rangle \left\langle\mathbf{k},\mathbf{r}';i'\right|, \tag{3.21}$$

$$h^{i,i'}_{\mathbf{r},\mathbf{r}'}(\mathbf{k}) := \sum_{\rho'} h^{i,i'}_{\mathbf{r},\mathbf{r}'+\rho'} e^{-i\mathbf{k}\cdot(\rho'+\mathbf{r}'-\mathbf{r})+i\phi(\rho',\mathbf{r}')-i\rho'^2}, \tag{3.22}$$

and the integral is over the Brillouin zone

$$\int \frac{d^d\mathbf{k}}{(2\pi)^d} := \prod_{i=1}^{d} \left(\int_0^{2\pi} \frac{dk_i}{2\pi} \right).$$

We can express $|\psi_{\mathbf{k},i}\rangle$ in the basis of $|\mathbf{k},\mathbf{r};i\rangle$'s

$$|\psi_{\mathbf{k},i}\rangle = \sum_{\mathbf{r},i'} u^{i',i}_{\mathbf{k},\mathbf{r}} \left|\mathbf{k},\mathbf{r};i'\right\rangle, \tag{3.23}$$

where $u^{i',i}_{\mathbf{k},\mathbf{r}}$ represents the eigenvectors of $h^{i,i'}_{\mathbf{r},\mathbf{r}'}(\mathbf{k})$:

$$h^{i,i'}_{\mathbf{r},\mathbf{r}'}(\mathbf{k}) = \sum_{i''} u^{i,i''}_{\mathbf{k},\mathbf{r}} \epsilon_{\mathbf{k},i''} \left(u^{i',i''}_{\mathbf{k},\mathbf{r}'} \right)^*. \tag{3.24}$$

In addition, $h^{i,i'}_{\mathbf{r},\mathbf{r}'}(\mathbf{k})$ must fulfill the following equation as required by the translational symmetry:

$$h^{i,i'}_{\mathbf{r}+\mathbf{r}'',\mathbf{r}'+\mathbf{r}''}(\mathbf{k}) = h^{i,i'}_{\mathbf{r},\mathbf{r}'}(\mathbf{k}+\mathbf{k}(\mathbf{r}'')) e^{i\phi(\mathbf{r}'',\mathbf{r}'-\mathbf{r})}, \tag{3.25}$$

where

$$\mathbf{k}(\mathbf{r}) := \sum_{i=1}^{d} \left[\phi(\mathbf{r},\mathbf{e}_i) - \phi(\mathbf{e}_i,\mathbf{r})\right] \mathbf{e}^i, \tag{3.26}$$

given that $\mathbf{e}^i$ is the reciprocal lattice of lattice $\mathbf{R}$

$$\mathbf{e}_i \cdot \mathbf{e}^j = \delta_{i,j}. \tag{3.27}$$

Eq. (3.25) requires that $\epsilon_{\mathbf{k},i}$ is periodic in $\mathbf{k}\,(\mathbf{r})$

$$\epsilon_{\mathbf{k},i} = \epsilon_{\mathbf{k}+\mathbf{k}(\mathbf{r}),i},\ \forall\,\mathbf{r} \tag{3.28}$$

and

$$u^{i,i'}_{\mathbf{k},\mathbf{r}+\mathbf{r}'} = u^{i,i'}_{\mathbf{k}+\mathbf{k}(\mathbf{r}'),\mathbf{r}}\, e^{i\phi(\mathbf{r},\mathbf{r}')}, \tag{3.29}$$

up to a phase factor depending on $\mathbf{k}$ and i'.

Now let us discuss the flat bands. We say that the i^{th} band is flat when $\epsilon_{\mathbf{k},i}$ is a constant independent from the momentum $\mathbf{k}$. If $\epsilon_{\mathbf{k},i} \equiv \epsilon_i$ is a flat band, a direct consequence is that any linear combination of $|\psi_{\mathbf{k},i}\rangle$'s with different $\mathbf{k}$'s is an eigenstate of the Hamiltonian with the same eigenenergy ϵ_i. Thus there can be localized eigenstates of H with energy ϵ_i. For example, consider the Wannier states:

$$|W_{\rho,i}\rangle := \int \frac{d^d\mathbf{k}}{(2\pi)^d} e^{-i\rho\cdot\mathbf{k}}\,|\psi_{\mathbf{k},i}\rangle\,, \tag{3.30}$$

which form a complete basis of the band:

$$\sum_\rho |W_{\rho,i}\rangle\,\langle W_{\rho,i}|\psi_{\mathbf{k},i}\rangle = \sum_\rho e^{i\rho\cdot\mathbf{k}}\,|W_{\rho,i}\rangle = |\psi_{\mathbf{k},i}\rangle\,.$$

$|W_{\rho,i}\rangle$ is not generally an eigenstate of the Hamiltonian, but it is when the i^{th} band is flat.

Conversely, for any localized eigenstate $|\text{loc}\rangle$ of the Hamiltonian, $U_{\mathbf{R}}\,|\text{loc}\rangle$ must also be an eigenstate because

$$HU_{\mathbf{R}}\,|\text{loc}\rangle = U_{\mathbf{R}}H\,|\text{loc}\rangle = 0,$$

where we suppose $H\,|\text{loc}\rangle = 0$ without loss of generality. The following state must be a linear combination of some $|\psi_{\mathbf{k},i}\rangle$'s satisfying $H\,|\psi_{\mathbf{k},i}\rangle = 0$

$$|\mathbf{k};\mathbf{R}\rangle := \sum_\rho e^{i\mathbf{k}\cdot\rho - i\rho^2} U_\rho U_{\mathbf{R}}\,|\text{loc}\rangle\,. \tag{3.31}$$

which satisfies

$$\begin{aligned}
|\mathbf{k};\mathbf{r}+\rho'\rangle &= \sum_{\rho} e^{i\mathbf{k}\cdot\rho - i\rho^2} U_{\rho} U_{\mathbf{r}+\rho'} \,|\mathrm{loc}\rangle \\
&= e^{-i\phi(\rho',\mathbf{r}) - i\rho'^2} \sum_{\rho} e^{i\mathbf{k}\cdot\rho - i\rho^2} U_{\rho+\rho'} U_{\mathbf{r}} \,|\mathrm{loc}\rangle \\
&= e^{-i\mathbf{k}\cdot\rho - i\phi(\rho',\mathbf{r}) - i\rho'^2} \,|\mathbf{k};\mathbf{r}\rangle \,.
\end{aligned}$$

Now, consider generating a flat-band model in the momentum space. If the system has an ordinary translational symmetry, we can generate a flat-band model by the following procedures: First we write down $\epsilon_{\mathbf{k},i}$'s with some of them independent from $\mathbf{k}$, then we collect them as a diagonal matrix $\mathrm{diag}\,(\epsilon_{\mathbf{k},1},\ldots,\epsilon_{\mathbf{k},n_s})$ and apply an arbitrary unitary transformation associated with the matrix $u^{i',i}_{\mathbf{k},\mathbf{0}}$ to obtain $h^{i,i'}_{\mathbf{0},\mathbf{0}}(\mathbf{k})$, and finally we Fourier transform $h^{i,i'}_{\mathbf{0},\mathbf{0}}(\mathbf{k})$ to obtain the Hamiltonian in the position space. However, this approach is too general to be practical, because we want the Hamiltonian to have some special properties. For example, a realistic model may require finite-range or short-range hoppings, that is, $h^{i,i'}_{\mathbf{R},\mathbf{R}'}$ vanishes or decays fast when $|\mathbf{R}-\mathbf{R}'|$ is large. Also, we may want the model process some additional symmetries, for example, being invariant under certain point group. These properties are not easy to be implemented in the momentum space. Furthermore, when the system has a magnetic translational symmetry, it is difficult to generate a $h^{i,i'}_{\mathbf{r},\mathbf{r}'}(\mathbf{k})$ fulfilling the requirement in Eq. (3.25). Therefore, we turn our attention from the momentum space to the real position space, and propose the Gram matrix method to build flat-band models.

3.2 Building flat-band models from the Gram matrix - the protocol

To introduce the Gram matrix method for building flat-band models, let us first introduce some basic properties of Gram matrices. The definition of a Gram matrix is as follows: Given a set of vectors $|v_1'\rangle, |v_2'\rangle, |v_3'\rangle \ldots$, the Gram matrix G built upon these vectors is defined by its matrix elements:

$$G_{i,j} := \langle v_i' | v_j' \rangle . \tag{3.32}$$

The simple definition of the Gram matrix readily shows that G is hermitian:

$$G_{i,j} = G_{j,i}^*.$$

$\sum_{i,j} z_i^* G_{i,j} z_j \geq 0$ for any complex numbers z_i's, because the left side of the inequality is the norm of the vector $\sum_i z_i |v_i'\rangle$, which must be non-negative. So G is positive semi-definite, which means all of the eigenvalues of G are non-negative.

Conversely, given any positive semi-definite Hermitian matrix G, we can readily find a set of vectors upon which G as a Gram matrix is built: A positive semi-definite Hermitian matrix G can be written as $G = T^\dagger T$ and we can identify $|v_i'\rangle$ as the i^{th} column vector of the T matrix.

Furthermore, we can understand G as an operator in a Hilbert space V, and T a linear transformation from V to another Hilbert space V':

$$G_{i,j} := \langle v_i | G | v_j \rangle ,$$
$$T |v_i\rangle := |v_i'\rangle .$$

Therefore, G can be regarded as the pullback of the inner product of V' to V by T. The rank of G is the same as the rank of T. The number of zero eigenvalues

of G equals the dimension of the null space of T, and the latter is no less than $\dim V - \dim V'$. This property serves as the basic principle underlying our method for building flat-band models.

Given a Hamiltonian of an arbitrary physical system, we can shift the energy by an unimportant constant and make all eigenvalues of the Hamiltonian non-negative. Without loss of generality, we set the ground state energy zero. Thus, any Hamiltonian can be interpreted as a Gram matrix. Now, the Hamiltonian can be represented by a T matrix:

$$H = T^\dagger T, \tag{3.33}$$

and the T matrix has a non-trivial null space spanned by the ground state manifold of H. The dimension of the null space equals to the ground state degeneracy. We consider T as a linear transformation from the physical Hilbert space V to an auxiliary space V'. If we construct H from a T matrix, we can control the degeneracy of the ground states by properly choosing the auxiliary space, making $\dim V' < \dim V$ such that the degeneracy is at least $\dim V - \dim V'$. As a result, it is possible to make the ground state degeneracy equal the degeneracy of a flat band. However, the degeneracy itself does not guarantee that the ground state manifold forms a band. The key is to implement the translational symmetry in the auxiliary space. It is apparent that if the T matrix is invariant under translations then

$$U_{\mathbf{R}} T U_{\mathbf{R}}^\dagger = T, \, \forall \, \mathbf{R}, \tag{3.34}$$

H will also be translationally invariant. However, this equation is meaningful only after we define $U_{\mathbf{R}}$ in the auxiliary space.

Suppose the basis vectors of the auxiliary space are $|\mathbf{R}; i\rangle_{\text{aux}}$ with $i = 1, 2, ..., n_s^{\text{aux}}$. They are not necessarily orthonormal. Define $U_{\mathbf{R}}$'s in the auxiliary space by the same

formula as that in the physical Hilbert space in Eq. (3.4):

$$U_{\mathbf{R}'} \left|\mathbf{R}; i\right\rangle_{\text{aux}} = e^{i\phi(\mathbf{R}',\mathbf{R})} \left|\mathbf{R}+\mathbf{R}'; i\right\rangle_{\text{aux}}. \tag{3.35}$$

and define the Gram matrix in the auxiliary space:

$$G^{i,i'}_{\mathbf{R},\mathbf{R}'} = {}_{\text{aux}}\left\langle \mathbf{R}; i|\mathbf{R}'; i'\right\rangle_{\text{aux}}. \tag{3.36}$$

The translational symmetry puts restriction on the Gram matrix:

$$G^{i,i'}_{\mathbf{R}+\mathbf{R}'',\mathbf{R}'+\mathbf{R}''} = G^{i,i'}_{\mathbf{R},\mathbf{R}'} e^{i\phi(\mathbf{R}'',\mathbf{R}-\mathbf{R}')} \tag{3.37}$$

$G_{\mathbf{R},\mathbf{R}'}$ can be interpreted as a Hamiltonian with qn_s^{aux} bands, with $qn_s^{\text{aux}} - p$ of them having zero-energy, where p could be $0, 1, 2, \ldots, qn_s^{\text{aux}}$.

We denote the matrix elements of T as

$$T =: \sum_{\mathbf{R},\mathbf{R}'} \sum_{i,i'} T^{i,i'}_{\mathbf{R},\mathbf{R}'} \left|\mathbf{R}; i\right\rangle \left\langle \mathbf{R}'; i'\right|. \tag{3.38}$$

where we have omitted the subscript 'aux' for the auxiliary space when there is no ambiguity. Eq. 3.34 yields

$$T^{i,i'}_{\mathbf{R}+\mathbf{R}'',\mathbf{R}'+\mathbf{R}''} = T^{i,i'}_{\mathbf{R},\mathbf{R}'} e^{i\phi(\mathbf{R}'',\mathbf{R}-\mathbf{R}')} \tag{3.39}$$

In particular, we can construct a T matrix by assigning arbitrary values to $T^{i,i'}_{\mathbf{R},\mathbf{0}}$'s and generate the rest of matrix elements by

$$T^{i,i'}_{\mathbf{R}+\mathbf{R}',\mathbf{R}'} = T^{i,i'}_{\mathbf{R},\mathbf{0}} e^{i\phi(\mathbf{R}',\mathbf{R})}. \tag{3.40}$$

We now prove that a T matrix generated this way produce a lattice model with at least $n_s q - p$ zero-energy flat bands as long as $n_s^{\text{aux}} \leq n_s$:

First, the matrix elements of the Hamiltonian is given by

$$h^{i,i'}_{\mathbf{R},\mathbf{R}'} = \sum_{\mathbf{R}'',\mathbf{R}'''} \sum_{i''} \left(T^{i'',i}_{\mathbf{R}'',\mathbf{R}}\right)^* G^{i'',i'''}_{\mathbf{R}'',\mathbf{R}'''} T^{i''',i'}_{\mathbf{R}''',\mathbf{R}'},$$

so

$$h^{i,i'}_{\mathbf{r},\mathbf{r}'}(\mathbf{k}) = \sum_{\rho'} \sum_{\mathbf{R}'',\mathbf{R}'''} \sum_{i''} \left(T^{i'',i}_{\mathbf{R}'',\mathbf{R}}\right)^* G^{i'',i'''}_{\mathbf{R}'',\mathbf{R}'''} T^{i''',i'}_{\mathbf{R}''',\mathbf{R}'} e^{-i\mathbf{k}\cdot(\rho'+\mathbf{r}'-\mathbf{r})+i\phi(\rho',\mathbf{r}')-i\rho'^2}.$$

Define

$$G^{i,i'}_{\mathbf{r},\mathbf{r}'}(\mathbf{k}) := \sum_{\rho'} G^{i,i'}_{\mathbf{r},\mathbf{r}'+\rho'} e^{-i\mathbf{k}\cdot(\rho'+\mathbf{r}'-\mathbf{r})+i\phi(\rho',\mathbf{r}')-i\rho'^2},$$

$$T^{i,i'}_{\mathbf{r},\mathbf{r}'}(\mathbf{k}) := \sum_{\rho'} T^{i,i'}_{\mathbf{r},\mathbf{r}'+\rho'} e^{-i\mathbf{k}\cdot(\rho'+\mathbf{r}'-\mathbf{r})+i\phi(\rho',\mathbf{r}')-i\rho'^2},$$

then we have

$$h^{i,i'}_{\mathbf{r},\mathbf{r}'}(\mathbf{k}) = \sum^{*}_{\mathbf{r}'',\mathbf{r}'''} \sum^{*}_{i''} \left(T^{i'',i}_{\mathbf{r}'',\mathbf{r}}(\mathbf{k})\right)^* G^{i'',i'''}_{\mathbf{r}'',\mathbf{r}'''}(\mathbf{k})\, T^{i''',i'}_{\mathbf{r}''',\mathbf{r}'}(\mathbf{k}). \tag{3.41}$$

By counting the rank of $h^{i,i'}_{\mathbf{r},\mathbf{r}'}(\mathbf{k})$, we conclude that there are at least $n_s q - p$ zero eigenvalues of $h^{i,i'}_{\mathbf{r},\mathbf{r}'}(\mathbf{k})$, which completes the proof.

Conversely, we can prove that, given any Gram matrix $G^{i,i'}_{\mathbf{r},\mathbf{r}'}(\mathbf{k})$, any lattice model with $n_s q - p$ zero-energy lowest bands can be generated through certain T matrix:

First, diagonalize $G^{i,i'}_{\mathbf{r},\mathbf{r}'}(\mathbf{k})$ as:

$$G^{i,i'}_{\mathbf{r},\mathbf{r}'}(\mathbf{k}) = \sum_{i''=1}^{p} g^{i,i''}_{\mathbf{k},\mathbf{r}} \epsilon^{G}_{\mathbf{k},i''} \left(g^{i',i''}_{\mathbf{k},\mathbf{r}'}\right)^*,$$

where $\epsilon^{G}_{\mathbf{k},i''} > 0$ and $g^{i,i''}_{\mathbf{k},\mathbf{r}}$ are the eigenvalue and the normalized eigenvector of $G^{i,i'}_{\mathbf{r},\mathbf{r}'}$, respectively, satisfying

$$\epsilon^{G}_{\mathbf{k},i} = \epsilon^{G}_{\mathbf{k}+\mathbf{k}(\mathbf{r}),i},$$

$$g^{i,i'}_{\mathbf{k},\mathbf{r}+\mathbf{r}'} = g^{i,i'}_{\mathbf{k}+\mathbf{k}(\mathbf{r}'),\mathbf{r}} e^{i\phi(\mathbf{r},\mathbf{r}')}.$$

We know that $h^{i,i'}_{\mathbf{r},\mathbf{r}'}(\mathbf{k})$ can be decomposed into $u^{i,i''}_{\mathbf{k},\mathbf{r}}$ in Eq. (3.24), so the following T matrix:

$$T^{i,i'}_{\mathbf{r},\mathbf{r}'}(\mathbf{k}) = \sum_{i''=1}^{p} \sqrt{\frac{\epsilon_{\mathbf{k},i''}}{\epsilon^{G}_{\mathbf{k},i''}}} g^{i,i''}_{\mathbf{k},\mathbf{r}} \left(u^{i',i''}_{\mathbf{k},\mathbf{r}'}\right)^*,$$

makes Eq. (3.41) hold. Also, the symmetry requirement in Eq. (3.34) holds because

$$T^{i,i'}_{\mathbf{r}+\mathbf{r}'',\mathbf{r}'+\mathbf{r}''}\left(\mathbf{k}\right)=T^{i,i'}_{\mathbf{r},\mathbf{r}'}\left(\mathbf{k}+\mathbf{k}\left(\mathbf{r}''\right)\right)e^{i\phi\left(\mathbf{r}'',\mathbf{r}'-\mathbf{r}\right)}$$

which completes the proof.

For summary, we have proved that, given a Hilbert space spanned by $|\mathbf{R};i\rangle$, $i=1,2,\ldots,n_s$, and the translational symmetry represented by $U_{\mathbf{R}}$'s, associating with a bilinear and rational phase $\phi\left(\mathbf{R},\mathbf{R}'\right)$ such that the Hamiltonian invariant under translations has n_sq bands, we can use the following protocol to generate any lattice model with n_sq-p zero-energy lowest bands:

1. Construct an auxiliary space spanned by $|\mathbf{R};i=1,2,\ldots,n_s^{\text{aux}}\rangle_{\text{aux}}$, where $n_s^{\text{aux}}\leq n_s$, such that the Gram matrix $G^{i,i'}_{\mathbf{R},\mathbf{R}'}:={}_{\text{aux}}\langle\mathbf{R};i|\mathbf{R}';i'\rangle_{\text{aux}}$ is also invariant under $U_{\mathbf{R}}$'s and the number of zero-energy flat bands of $G^{i,i'}_{\mathbf{R},\mathbf{R}'}$ is $n_s^{\text{aux}}q-p$.

2. Construct a T mapping $T=\sum_{\mathbf{R},\mathbf{R}'}\sum_{i,i'}T^{i,i'}_{\mathbf{R},\mathbf{R}'}\left|\mathbf{R};i\right\rangle\left\langle\mathbf{R}';i'\right|$ from the physical Hilbert space to the auxiliary space by assign arbitrary values to $T^{i,i'}_{\mathbf{R},\mathbf{0}}$ and generating the rest of the matrix elements by $T^{i,i'}_{\mathbf{R}+\mathbf{R}',\mathbf{R}'}=T^{i,i'}_{\mathbf{R},\mathbf{0}}e^{i\phi\left(\mathbf{R}',\mathbf{R}\right)}$.

3. The Hamiltonian can the constructed as $H=T^{\dagger}T$. The lowest n_sq-p bands of H are guaranteed to be flat with energy 0.

To make the Hamiltonian possess some special properties, we need to put constraints on the T matrix. For example, the finite-rangeness of the Hamiltonian can be simply achieved by making $G^{i,i'}_{\mathbf{R},\mathbf{R}'}$ and $T^{i,i'}_{\mathbf{R},\mathbf{0}}$ finite-range.

The protocol can be simplified when the system has an ordinary translational symmetry. In this case, the protocol becomes:

1. Construct an auxiliary space spanned by orthonormal states $|\mathbf{R};i\rangle_{\text{aux}}$, $i=1,2,\ldots,n_s^{\text{aux}}$, where $n_s^{\text{aux}}<n_s$.

2. Construct an arbitrary T mapping $T = \sum_{\mathbf{R},\mathbf{R}'} \sum_{i,i'} T^{i,i'}_{\mathbf{R}-\mathbf{R}'} |\mathbf{R}; i\rangle \langle \mathbf{R}'; i'|$ from the physical Hilbert space to the auxiliary space.

3. The Hamiltonian can the constructed as $H = T^\dagger T$. The lowest $n_s - n_s^{\text{aux}}$ bands of H are guaranteed to be flat with energy 0.

In the rest of the chapter, we will show some examples of flat-band models built from these protocols.

3.3 Examples of flat-band models with ordinary translational symmetry and finite-range hoppings

In this section, we will show some examples of using the Gram matrix method to generate flat-band models with ordinary translational symmetry and finite-range hoppings.

First, we consider the simplest case, two-band models. The Hilbert space is spanned by $|\mathbf{R}; 1\rangle$ and $|\mathbf{R}; 2\rangle$ and the auxiliary space is spanned by $|\mathbf{R}\rangle_{\text{aux}}$. Note that if H is a two-band model with a flat lower band, then $-H$ has a flat higher band, so all the two-band models without band crossing can be obtained by the Gram matrix method. The simplest choice of the T matrix is the 'identity mapping' given by

$$T |\mathbf{R}; 1\rangle = A^{(1)} |\mathbf{R}\rangle_{\text{aux}} ,$$
$$T |\mathbf{R}; 2\rangle = A^{(2)} |\mathbf{R}\rangle_{\text{aux}} ,$$

where $A^{(1)}$ and $A^{(2)}$ are complex hopping amplitudes from the physical Hilbert space

to the auxiliary space. However, the Hamiltonian constructed is trivial:

$$H = \sum_{\mathbf{R}} \left|A^{(1)}\right|^2 |\mathbf{R};1\rangle \langle \mathbf{R};1| + \left|A^{(2)}\right|^2 |\mathbf{R};2\rangle \langle \mathbf{R};2| + \left(A^{(2)*}A^{(1)} |\mathbf{R};2\rangle \langle \mathbf{R};1| + h.c.\right),$$

in which a particle can only hop between states within a single cell. To make the model non-trivial, the T matrix has to map $|\mathbf{R};1\rangle$ or $|\mathbf{R};2\rangle$ to multiple cells in the auxiliary space. For example, if we choose the following T matrix:

$$T|\mathbf{R};1\rangle = A_0^{(1)} |\mathbf{R}\rangle_{\text{aux}} + A_1^{(1)} |\mathbf{R}-\mathbf{e}_1\rangle_{\text{aux}},$$
$$T|\mathbf{R};2\rangle = A^{(2)} |\mathbf{R}\rangle_{\text{aux}},$$

the Hamiltonian generated will be:

$$\begin{aligned} H = &\sum_{\mathbf{R}} \left(\left|A_0^{(1)}\right|^2 + \left|A_1^{(1)}\right|^2\right) |\mathbf{R};1\rangle \langle \mathbf{R};1| + \left|A^{(2)}\right|^2 |\mathbf{R};2\rangle \langle \mathbf{R};2| \\ &+ \left(A^{(2)*}A_0^{(1)} |\mathbf{R};2\rangle \langle \mathbf{R};1| + h.c.\right) + \left(A^{(2)*}A_1^{(1)} |\mathbf{R}-\mathbf{e}_1;2\rangle \langle \mathbf{R};1| + h.c.\right) \\ &+ \left(A_0^{(1)*}A_1^{(1)} |\mathbf{R}-\mathbf{e}_1;1\rangle \langle \mathbf{R};1| + h.c.\right), \end{aligned}$$

which describes a one-dimensional Tasaki's lattice. In general, a d-dimensional model could be obtained if we make the T matrix map $|\mathbf{R};1\rangle$ to $|\mathbf{R}\rangle_{\text{aux}}$ and $|\mathbf{R}\rangle_{\text{aux}}$'s nearest neighbors $|\mathbf{R}-\mathbf{e}_i\rangle_{\text{aux}}$, $i = 1, 2, \ldots, d$:

$$T|\mathbf{R};1\rangle = \sum_{i=0}^{d} A_i^{(1)} |\mathbf{R}-\mathbf{e}_i\rangle_{\text{aux}}, \tag{3.42}$$

$$T|\mathbf{R};2\rangle = A^{(2)} |\mathbf{R}\rangle_{\text{aux}}, \tag{3.43}$$

where we define $\mathbf{e}_0 = \mathbf{0}$ to simplify the notation. And the generated Hamiltonian is

$$\begin{aligned} H = &\sum_{\mathbf{R}} \sum_{i,j=0}^{d} A_j^{(1)*}A_i^{(1)} |\mathbf{R}+\mathbf{e}_j-\mathbf{e}_i;1\rangle \langle \mathbf{R};1| \\ &+ \sum_{i=0}^{d} \left(A^{(2)*}A_i^{(1)} |\mathbf{R}-\mathbf{e}_i;2\rangle \langle \mathbf{R};1| + h.c.\right) + \left|A^{(2)}\right|^2 |\mathbf{R};2\rangle \langle \mathbf{R};2|. \end{aligned}$$

The Hamiltonian in the momentum space is given by

$$H_{\mathbf{k}} = \left|A^{(1)}_{\mathbf{k}}\right|^2 |\mathbf{k};1\rangle \langle \mathbf{k};1| + \left(A^{(2)*}A^{(1)}_{\mathbf{k}} |\mathbf{k};2\rangle \langle \mathbf{k};1| + h.c.\right) + \left|A^{(2)}\right|^2 |\mathbf{k};2\rangle \langle \mathbf{k};2|,$$

where

$$A^{(1)}_{\mathbf{k}} := \sum_{i=0}^{d} A^{(1)}_i e^{i\mathbf{k}\cdot\mathbf{e}_i}$$

Apparently, $\det H_{\mathbf{k}} = 0$, which indicates the existence of the zero-energy flat band. Given the zero-energy lower band, the higher band is given by the trace of $H_{\mathbf{k}}$

$$\mathrm{tr}\,(H_{\mathbf{k}}) = \left|A^{(1)}_{\mathbf{k}}\right|^2 + |B|^2,$$

which indicates that the gap will never close, because if $B = 0$ the model is no-longer a two-band model.

In general, a T given by

$$T|\mathbf{R};1\rangle = \sum_{\mathbf{R}'} A^{(1)}_{\mathbf{R}'} |\mathbf{R}-\mathbf{R}'\rangle_{\mathrm{aux}}, \tag{3.44}$$

$$T|\mathbf{R};2\rangle = \sum_{\mathbf{R}'} A^{(2)}_{\mathbf{R}'} |\mathbf{R}-\mathbf{R}'\rangle_{\mathrm{aux}}, \tag{3.45}$$

generates the Hamiltonian

$$H = \sum_{\mathbf{R},\mathbf{R}'} \sum_{i,j=1}^{2} h^{i,j}_{\mathbf{R}'} |\mathbf{R}+\mathbf{R}';i\rangle \langle \mathbf{R};j|, \tag{3.46}$$

where $h^{i,j}_{\mathbf{R}}$ is given by the correlation functions of A's:

$$h^{i,j}_{\mathbf{R}} := \sum_{\mathbf{R}'} A^{(i)*}_{\mathbf{R}+\mathbf{R}'} A^{(j)}_{\mathbf{R}'}. \tag{3.47}$$

Eq. (3.46) can express all two-band lattice Hamiltonians whose lowest band is flat. For example, the model studied in [66] can be obtained by setting all coefficients zero except $A^{(1)}_{\mathbf{0}}$, $A^{(1)}_{\mathbf{e}_1}$, $A^{(1)}_{\mathbf{e}_2}$, $A^{(1)}_{\mathbf{e}_1+\mathbf{e}_2}$, and $A^{(2)}_{\mathbf{0}}$.

From Eq. (3.47) we notice that a d-dimensional two-band flat-band model must contain hopping terms that connect non-adjacent cells. By adjacent cells, we mean a cell marked by $\mathbf{R}$ and one of the cells marked by $\mathbf{R} \pm \mathbf{e}_i$, $i = 1, 2, \ldots, d$. If we want a flat-band model whose hopping terms only connect adjacent cells, we have to increase the number of bands, n_s. For example, the following T matrix:

$$T\left|\mathbf{R}; 1\right\rangle = \sum_{j=1}^{d} \left(a_j \left|\mathbf{R}; j\right\rangle_{\text{aux}} + b_j \left|\mathbf{R} - \mathbf{e}_j; j\right\rangle_{\text{aux}}\right), \tag{3.48}$$

$$T\left|\mathbf{R}; i+1\right\rangle = c_i \left|\mathbf{R}; i\right\rangle_{\text{aux}}, \; i = 1, \ldots, d, \tag{3.49}$$

generates

$$\begin{aligned} H = \sum_{\mathbf{R}} \Bigg[\sum_{i=1}^{d} \left(|a_i|^2 + \left|b_i^2\right|\right) \left|\mathbf{R}; 1\right\rangle\left\langle\mathbf{R}; 1\right| + \sum_{i=2}^{d+1} |c_{i-1}|^2 \left|\mathbf{R}; i\right\rangle\left\langle\mathbf{R}; i\right| \Bigg] \\ + \sum_{\mathbf{R}} \sum_{i=1}^{d} \Big[c_i^* a_i \left|\mathbf{R}; i+1\right\rangle \left\langle\mathbf{R}; 1\right| + c_i^* b_i \left|\mathbf{R} - \mathbf{e}_i; i+1\right\rangle \left\langle\mathbf{R}; 1\right| \\ + a_i^* b_i \left|\mathbf{R} + \mathbf{e}_i; 1\right\rangle \left\langle\mathbf{R}; 1\right| + h.c. \Big]. \end{aligned} \tag{3.50}$$

The underlying lattice is the d-dimensional Tasaki's lattice (examples in 1D and 2D are presented in Fig. 3.1(a) and (b), respectively), and the hopping amplitudes in the original Tasaki's Hamiltonian [67] represents a special case of Eq. (3.50) with $a_i = b_i = 1/\lambda$. This Hamiltonian has $n_s = d + 1$ bands. Since each unit cell in the auxiliary space has $n_s^{\text{aux}} = d$ states, H possesses $n_s - n_s^{\text{aux}} = 1$ zero-energy band.

The Hamiltonian in the momentum space is given by

$$\begin{aligned} H_{\mathbf{k}} = \sum_{\mathbf{k}} \sum_{i=1}^{d} \left|\alpha_{\mathbf{k}}^i\right|^2 \left|\mathbf{k}; 1\right\rangle\left\langle\mathbf{k}; 1\right| + |c_i|^2 \left|\mathbf{k}; i+1\right\rangle\left\langle\mathbf{k}; i+1\right| \\ + \left(c_i^* \alpha_{\mathbf{k}}^i \left|\mathbf{k}; i+1\right\rangle \left\langle\mathbf{k}; 1\right| + h.c.\right). \end{aligned}$$

where

$$\alpha_{\mathbf{k}}^i := a_i + b_i e^{i\mathbf{k}\cdot\mathbf{e}_i}$$

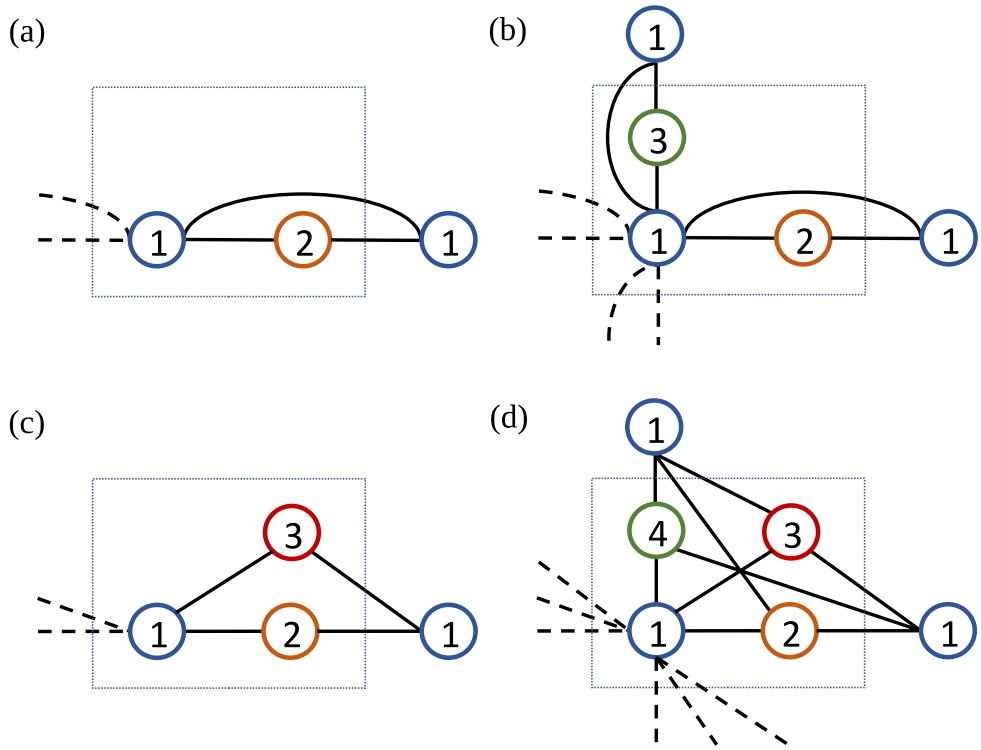

Figure 3.1 : Tasaki lattice in 1D (a) and 2D (b) governed by Hamiltonian (3.50). Bipartite lattice in 1D (c) and 2D (d) governed by Hamiltonian (3.58). Rectangular boxes represent cells, each containing several states labelled by circled numbers. Solid lines represent non-zero hoppings starting from a single cell. Duplicated hopping terms are marked by dashed lines.

$H_{\mathbf{k}}$ contains a zero-energy band, and the corresponding eigenvector is given by

$$\left|\psi^0_{\mathbf{k}}\right\rangle = |\mathbf{k};1\rangle - \sum_{i=1}^{d} \frac{\alpha^i_{\mathbf{k}}}{c_i} |\mathbf{k};i+1\rangle \,. \tag{3.51}$$

Because of degeneracy, the following localized state, which is a linear combination of $|\psi^0_{\mathbf{k}}\rangle$'s, is also an eigenvector of the Hamiltonian:

$$\left|\psi^0_{\mathbf{R}}\right\rangle = |\mathbf{R};1\rangle - \sum_{i=1}^{d} \left(\frac{a_i}{c_i} |\mathbf{R};i+1\rangle + \frac{b_i}{c_i} |\mathbf{R}-\mathbf{e}_i;i+1\rangle \right). \tag{3.52}$$

Nevertheless, we notice that there could be more flat bands other than the zero-energy one. If we group the states $|\mathbf{R};1\rangle$ as sublattice A and the remaining states

$|\mathbf{R}; i = 2, 3, ..., d+1\rangle$ as sublattice B, we find that a particle in B can only hop to A. If some of the $|c_i|^2$ are the same, for example, $|c_{i_0}|^2 = |c_{i_0+1}|^2$, then there exist a flat band with energy $|c_{i_0}|^2$. This is because $H - |c_{i_0}|^2$ maps the two-dimensional space spanned by $|\mathbf{k}; i_0\rangle$ and $|\mathbf{k}; i_0+1\rangle$ to the one-dimensional space spanned by $|\mathbf{k}; 1\rangle$ such that the kernel of the operator $H - |c_{i_0}|^2$ is non-zero. The corresponding eigenvector is given by

$$\left|\psi_{\mathbf{k}}^{i_0}\right\rangle = c_{i_0+1}\left(\alpha_{\mathbf{k}}^{i_0+1}\right)^* |\mathbf{k}; i_0\rangle - c_{i_0}\left(\alpha_{\mathbf{k}}^{i_0}\right)^* |\mathbf{k}; i_0+1\rangle . \tag{3.53}$$

And the localized eigenstate is

$$\begin{aligned}\left|\psi_{\mathbf{R}}^{0}\right\rangle =& c_{i_0+1}a_{i_0+1}^* |\mathbf{R}; i_0\rangle + c_{i_0+1}b_{i_0+1}^* |\mathbf{R}+\mathbf{e}_{i_0+1}; i_0\rangle \\ & - c_{i_0}a_{i_0}^* |\mathbf{R}; i+1\rangle - c_{i_0}b_{i_0}^* |\mathbf{R}+\mathbf{e}_{i_0}; i+1\rangle .\end{aligned} \tag{3.54}$$

The rest of the bands of $H_{\mathbf{k}}$ are dispersive.

In the case that all the $|c_i|$'s are the same, $|c_i| \equiv c$, there exists a single dispersive top band with energy $c^2 + \sum_{i=1}^{d} |\alpha_{\mathbf{k}}^i|^2$. The corresponding eigenstate is

$$\left|\psi_{\mathbf{k}}^{d}\right\rangle = \sum_{i=1}^{d} \left|\alpha_{\mathbf{k}}^i\right|^2 |\mathbf{k}; 1\rangle + \sum_{i=1}^{d} c_i^* \alpha_{\mathbf{k}}^i |\mathbf{k}; i+1\rangle . \tag{3.55}$$

The Tasaki's model contains at least one dispersive band. We can also use the Gram matrix method to construct models in which all of the bands are flat. The basic idea is rooted in the reflection symmetry of the upper and lower bands in a bipartite model. A bipartite lattice is a lattice consisting of two sublattices, and the hopping amplitudes between states within the same sublattice are zero. From [68] we know that the middle bands in a bipartite model are necessarily flat. As a result, if there is only one lower band (i.e., the ground band) whose flatness is guaranteed by the Gram matrix, then the only upper band must also be flat because of the reflection symmetry. So in order to build a model in which all bands are flat, we are going

to design a bipartite structure which guarantees $n_s - 2$ middle flat bands and, by choosing $n_s^{\text{aux}} = n_s - 1$, there is a zero-energy flat ground band. Such a T matrix can be chosen as follows:

$$T\left|\mathbf{R};1\right\rangle = c_{d+1}\left|\mathbf{R};d+1\right\rangle_{\text{aux}} + \sum_{j=1}^{d} c_j \left|\mathbf{R}-\mathbf{e}_j;j\right\rangle_{\text{aux}}, \tag{3.56}$$

$$T\left|\mathbf{R};i+1\right\rangle = \sum_{j=1}^{d+1} u_{i,j}\left|\mathbf{R};j\right\rangle_{\text{aux}},\ i=1,2,\ldots,d+1, \tag{3.57}$$

where $c_j \in \mathbb{C}$ and $u_{i,j}$ is an arbitrary unitary matrix. The unitary matrix guarantees the bipartite structure: Different rows of $u_{i,j}$ are orthogonal to each other, so the hopping amplitudes between states $\left|\mathbf{R};i=2,3,\ldots,d+2\right\rangle$ are zero, and the on-site energy of these states is uniform because each row of the unitary matrix has the same norm. The generated Hamiltonian is given by:

$$\begin{aligned} H =& \sum_{\mathbf{R}} \left(\sum_{i=1}^{d+1} \left|c_i\right|^2 \right) \left|\mathbf{R};1\right\rangle \left\langle \mathbf{R};1\right| + \sum_{\mathbf{R}} \sum_{i=2}^{d+2} \left|\mathbf{R};i\right\rangle \left\langle \mathbf{R};i\right| \\ &+ \sum_{\mathbf{R}} \sum_{i=1}^{d+1} \Bigg[u_{i,d+1}^{*} c_{d+1} \left|\mathbf{R};i+1\right\rangle \left\langle \mathbf{R};1\right| \\ &+ \sum_{j=1}^{d} u_{i,j}^{*} c_j \left|\mathbf{R}-\mathbf{e}_j;i+1\right\rangle \left\langle \mathbf{R};1\right| + h.c. \Bigg], \end{aligned} \tag{3.58}$$

The lattice connectivity in 1D and 2D are illustrated in Fig. 3.1(c) and (d), respectively. The bipartite nature can be easily seen if we group $\left|\mathbf{R};1\right\rangle$ as sublattice A with on-site energy $E_A = \sum_i^{d+1} \left|c_i\right|^2$, and $\left|\mathbf{R};i=2,..,d+2\right\rangle$ as sublattice B with on-site energy $E_B = 1$. This $(d+2)$-band model consists of a flat ground band with energy zero, d flat bands with energy $E_B = 1$, and a flat top band with energy $E_A + E_B = 1 + \sum_i^{d+1} \left|c_i\right|^2$, reflecting the reflection symmetry of bipartite lattices. The

Hamiltonian in the momentum space is given by

$$H_{\mathbf{k}} = \sum_{i=1}^{d+1} |c_i|^2 \, |\mathbf{k};1\rangle \langle \mathbf{k};1| + \sum_{i=2}^{d+2} |\mathbf{k};i\rangle \langle \mathbf{k};i| + \sum_{i=1}^{d+1} \left(u^*_{i,d+1} c_{d+1} + \sum_{j=1}^{d} u^*_{i,j} c_j e^{i\mathbf{k}\cdot\mathbf{e}_j} \right) |\mathbf{k};i+1\rangle \langle \mathbf{k};1|$$

The eigenvectors take the same form as those in Eqs. (3.51)(3.53)(3.55), in which c_i is replaced by 1 and $\alpha^i_{\mathbf{k}}$ is replaced by $u^*_{i,d+1} c_{d+1} + \sum_{j=1}^{d} u^*_{i,j} c_j e^{i\mathbf{k}\cdot\mathbf{e}_j}$.

Last but not least, we remark that it is not difficult to make the flat-band models to possess certain symmetries by putting constraints on the coefficients appearing in the constructed Hamiltonian.

3.4 Topological flat band in the Kapit-Mueller model

In this section, we use the Gram matrix method to reproduce the Kapit-Mueller model which contains a topologically nontrivial flat ground band, and investigate the properties of the model.

In Ref. [39], Kapit and Mueller, working in the real space, found such a topological flat band in a 2D square lattice, and attributed the massive degeneracies in the flat band to some unrevealed symmetries. It was realized that the degenerate ground states can be regarded as discrete lowest Landau levels (LLLs), and that the degeneracy of the LLLs give birth to the flatness [40]. Here we find an alternative way to understand the origin of this topological flat band by reproducing the model with Gram matrices. More specifically, we reproduce the Kapit-Mueller model by a Gram matrix built upon a subset of coherent states. From this construction, the massive degeneracy of the ground band can be straightforwardly understood as a result of the linear dependency of the coherent states. In addition, using the protocol

introduced in 3.2, we can find the generalizations of the model, which are beyond the LLL descriptions, can also share the ground band degeneracy.

In terms of topological flat bands, there is an important theorem [69] which states that the following three conditions concerning a band cannot be simultaneously satisfied: (1) Being flat; (2) Having a non-zero Chern number; (3) The Hamiltonian contains only finite-range hopping. In other words, models contain topological flat bands must have infinite-range hoppings. Therefore, in order to construct a lattice model with topological flat bands, it may be convenient to choose a basis of the auxiliary space such that each pair of basis vectors has a non-zero inner product. Also, a magnetic translational symmetry may be preferred because realistically the quantum Hall effect is induced by a magnetic field. The basis may be overcomplete such that the zero-energy states occur.

We find that certain subsets of the coherent states automatically satisfy the aforementioned requirements.

A coherent state $|z\rangle$ is an eigenstate of a bosonic annihilation operator with complex eigenvalue z. It is well known that the full set of coherent states form an overcomplete basis. Perelomov [70] studied the completeness of a countable subset of coherent states. Define

$$z_{x_1,x_2} := x_1\zeta_1 + x_2\zeta_2, \quad x_1, x_2 \in \mathbb{Z}, \quad \zeta_1, \zeta_2 \in \mathbb{C}.$$

z_{x_1,x_2}'s form a two-dimensional lattice on the complex plane whose unit cell area is $S := \mathrm{Im}\,\zeta_1^*\zeta_2$. We collect the set of coherent states $\{|z_{x_1,x_2}\rangle\}$. Perelomov found that: If $S \leq \pi$, the set represents an overcomplete basis; If $S > \pi$, the set is incomplete; If $S = \pi$, we can take away any one of the $|z_{x_1,x_2}\rangle$'s from the set, and the remaining states form a complete basis.

Following the basic procedures described in Section 3.2, and making the lattice of coherent states the basis vectors of the auxiliary space

$$|x_1\mathbf{e}_1 + x_2\mathbf{e}_2; 1\rangle_{\text{aux}} = |z_{x_1,x_2}\rangle\,, \tag{3.59}$$

we find the Kapit-Mueller model is generated by the linear transformation T that maps $|x_1, x_2\rangle := |x_1\mathbf{e}_1 + x_2\mathbf{e}_2; 1\rangle$, a state on a two-dimensional lattice, to $|z_{x_1,x_2}\rangle$'s:

$$T\,|x_1, x_2\rangle = |z_{x_1,x_2}\rangle\ . \tag{3.60}$$

The Hamiltonian $H^{\zeta_1,\zeta_2} := T^\dagger T$ is therefore the Gram matrix of coherent states:

$$\begin{aligned} H^{\zeta_1,\zeta_2}_{x_1,x_2;x_1',x_2'} &:= \langle x_1, x_2|\, H^{\zeta_1,\zeta_2}\, |x_1', x_2'\rangle \\ &= \left\langle z_{x_1,x_2} | z_{x_1',x_2'} \right\rangle \\ &= \exp\left(-\frac{\left| z_{x_1,x_2} - z_{x_1',x_2'} \right|^2}{2} + i\mathrm{Im}\, z^*_{x_1,x_2} z_{x_1',x_2'} \right) \\ &= \exp\left(-\frac{\left| z_{x_1,x_2} - z_{x_1',x_2'} \right|^2}{2} + iS\left(x_1 x_2' - x_2 x_1'\right) \right). \end{aligned} \tag{3.61}$$

Physically, this Hamiltonian describes a fully connected two-dimensional lattice under a magnetic field, and the flux per unit cell is $2S$. It reduces to the Kapit-Mueller model [39] when z_{x_1,x_2}'s form a square lattice, and to the Hofstadter model [71] by further taking the limit $S \to \infty$.

The Hamiltonian has a magnetic translational symmetry because

$$H^{\zeta_1,\zeta_2}_{x_1+x_1'',x_2+x_2'';x_1'+x_1'',x_2'+x_2''} = H^{\zeta_1,\zeta_2}_{x_1,x_2;x_1',x_2'} \exp\left(iS\left(x_1''\left(x_2' - x_2\right) - x_2''\left(x_1{}' - x_1\right)\right)\right), \tag{3.62}$$

and we have

$$\phi\left(\mathbf{e}_1, \mathbf{e}_2\right) = -S \tag{3.63}$$

From our construction, it immediately becomes clear that the emergence of the zero-energy ground states is guaranteed by the properties of the Gram matrix and the

(over-)completeness of the coherent states. When $S > \pi$, the set of coherent states on lattice are linearly independent, and the smallest eigenvalue of the resulting H^{ζ_1,ζ_2} must be positive. When $S = \pi$, the set becomes complete if we take away any one of the states, so H^{ζ_1,ζ_2} has a single zero eigenvalue. When $S < \pi$, we have $1/S$ states per unit area on the complex plane, while only $1/\pi$ states per unit area are needed to construct a complete basis, so a fraction of $1 - S/\pi$ eigenvalues of H^{ζ_1,ζ_2} must be zero. As a result, the massive degeneracy of the ground states of H^{ζ_1,ζ_2} follows a universal scaling behavior, in the sense that it only depends on S and is completely independent of the lattice geometry of the coherent states. As we will see, it is more convenient to interpret S, instead of as the unit cell area, as the averaged area on the complex plane occupied by each coherent state, because the relation between S and the completeness extends beyond the cases that Perelomov studied. The universal degeneracy is one of the most elegant features of this model.

We carry out numerical calculation to verify the universal scaling rule between the degeneracy and S. We choose N coherent states distributed in a square region on the complex plane, where N is large but finite (typically, $N \sim 3 \times 10^3$), and numerically diagonalize the corresponding Gram matrix H^{ζ_1,ζ_2} to find the density of states as a function of S and the energy E. In Fig. 3.2(a)-(c), we display the spectrum for several distinct lattice geometry (The lattice geometry refers to the geometry of the coherent states on the complex plane.): square lattice, triangular lattice, and honeycomb lattice. The positive-energy part of the spectrum forms a Hofstadter butterfly, whose specific pattern depends on the lattice geometry. The universal feature for these different lattices is, however, the massively degenerate ground states at zero energy when $S < \pi$. Remarkably, this massive degeneracy exists even when the coherent states has a random distribution over the whole region (we specify a

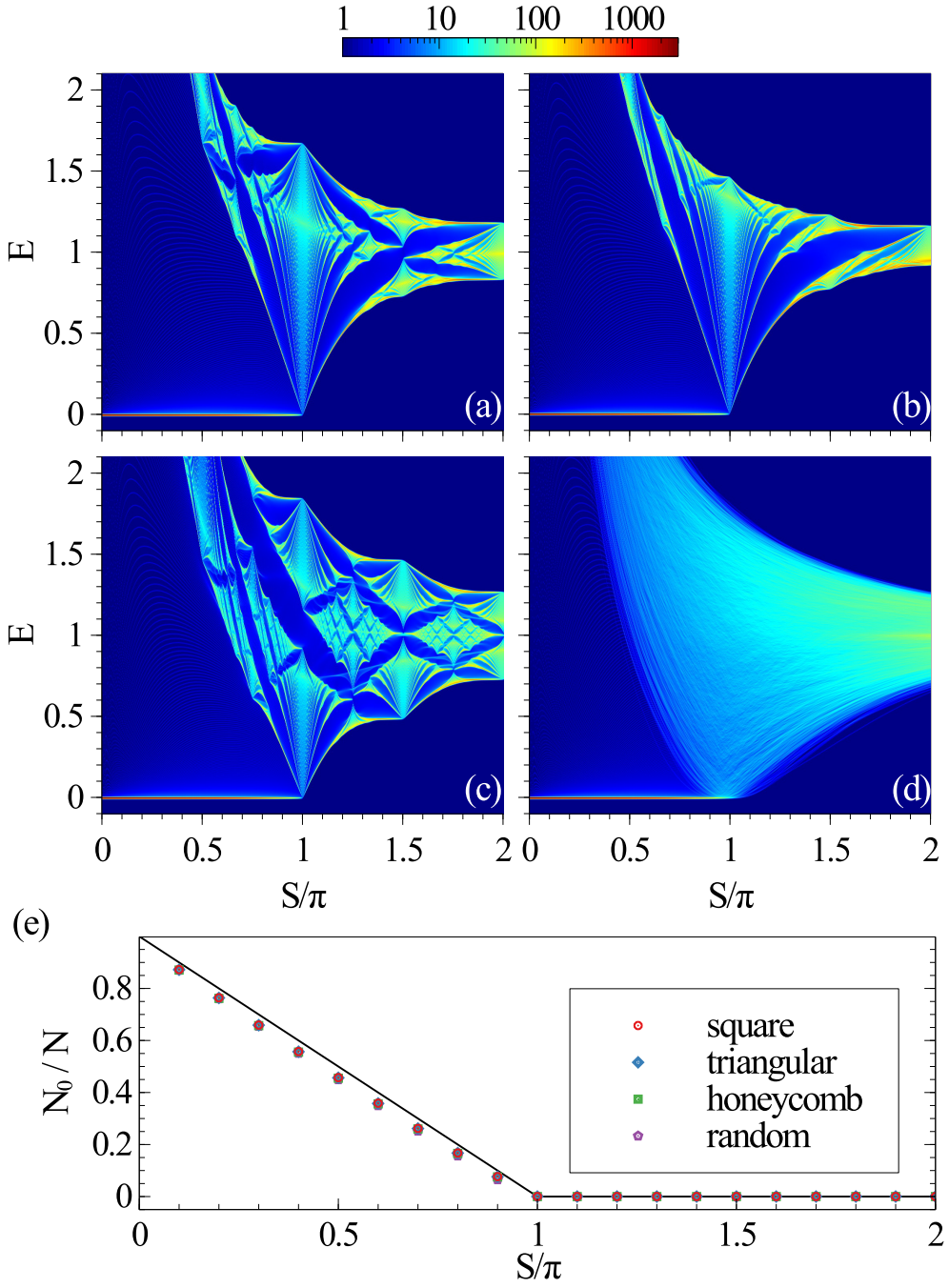

Figure 3.2 : (a)-(d) Spectrum of H^S for a Square lattice (a), Triangular lattice (b), Honeycomb lattice (c), and Random lattice (d). The color map represents $(D+1)$ where $D(E) = \sum_n \delta(E - E_n)$ is the density of states, with E_n being the n^{th} eigenvalue of H^S. In the calculation, the Dirac δ-function is replaced by a smooth narrow distribution function. S is the averaged area per state. (e) We count N_0, the number of eigenenergy that is less than 10^{-5}, and compare the ratio N_0/N with the theoretical value ρ marked by the line, where $\rho = \max(1 - S/\pi, 0)$.

lower bound on the distances between sites to ensure that no two sites are too close together in order to exclude trivial zero eigenvalues of the Gram matrix) as we show in Fig. 3.2(d). Although in this random lattice case, the positive-energy butterfly pattern no longer exists.

As mentioned earlier, the degeneracy of the ground band is given by $N_0 = (1 - S/\pi)N$, which should be a universal feature independent of the lattice geometry. In Fig. 3.2(e), we plot the numerically obtained fraction of zero-energy states as a function for S. Results from all four lattice geometries show excellent agreement with the theoretical prediction. The small discrepancies can be attributed to the finite-size effect. In Fig. 3.2(a)-(d), we see a gap between the zero-energy and the positive-energy states, which increases as S decreases and diverges when $S \to 0$. This can be easily understood as follows: Since $\mathrm{Tr}\left[H^{\zeta_1,\zeta_2}\right] = N$ which is the sum of the positive eigenenergies, the averaged energy of the excited states should be π/S when $S < \pi$ according to the degeneracy of the ground states.

Up to now, we have not yet proved that the fraction of $1 - S/\pi$ zero eigenvalues of H^{ζ_1,ζ_2} form a flat band. To do this, we use the following identity proved by Perelomov [70]:

$$\sum_{x_1,x_2} (-1)^{x_1+x_2+x_1x_2} \exp\left(-\frac{\pi \left|z_{x_1,x_2}\right|^2}{2S} + z_{x_1,x_2} z\right) \equiv 0 \tag{3.64}$$

where z is an arbitrary complex number. As a result,

$$\begin{aligned}
&\sum_{x_1',x_2'} (-1)^{x_1'-x_1''+x_2'-x_2''+x_1'x_2'-x_1''x_2''} H^{\zeta_1,\zeta_2}_{x_1,x_2;x_1',x_2'} H^{\sqrt{\pi/S-1}\zeta_1,\sqrt{\pi/S-1}\zeta_2}_{x_1'',x_2'';x_1',x_2'} \\
=&\sum_{x_1',x_2'} (-1)^{x_1'-x_1''+x_2'-x_2''+x_1'x_2'-x_1''x_2''} \exp\left(-\frac{\left|z_{x_1,x_2}-z_{x_1',x_2'}\right|^2}{2}+i\mathrm{Im}\, z^*_{x_1,x_2}z_{x_1',x_2'}\right) \\
&\times \exp\left(-\frac{(\pi/S-1)\left|z_{x_1',x_2'}-z_{x_1'',x_2''}\right|^2}{2}+i\,(\pi/S-1)\,\mathrm{Im}\, z^*_{x_1'',x_2''}z_{x_1',x_2'}\right) \\
\propto&\sum_{x_1',x_2'} (-1)^{x_1'+x_2'+x_1'x_2'} \exp\left(-\frac{\pi\left|z_{x_1',x_2'}\right|^2}{2S}+z_{x_1',x_2'}\left(z^*_{x_1,x_2}+(\pi/S-1)\,z^*_{x_1'',x_2''}\right)\right) \\
=&0.
\end{aligned}$$

Therefore, each row of the matrix $(-1)^{x_1'-x_1''+x_2'-x_2''+x_1'x_2'-x_1''x_2''} H^{\sqrt{\pi/S-1}\zeta_1,\sqrt{\pi/S-1}\zeta_2}_{x_1'',x_2'';x_1',x_2'}$ represents a localized eigenstate of $H^{\zeta_1,\zeta_2}_{x_1,x_2;x_1',x_2'}$ with zero energy:

$$H^{\zeta_1,\zeta_2}\left|\mathrm{loc}^{\zeta_1,\zeta_2}_{x_1,x_2}\right\rangle=0, \tag{3.65}$$

$$\left|\mathrm{loc}^{\zeta_1,\zeta_2}_{x_1,x_2}\right\rangle:=\sum_{x_1',x_2'}(-1)^{x_1'-x_1+x_2'-x_2+x_1'x_2'-x_1x_2}H^{\sqrt{\pi/S-1}\zeta_1,\sqrt{\pi/S-1}\zeta_2}_{x_1,x_2;x_1',x_2'}\left|x_1',x_2'\right\rangle. \tag{3.66}$$

The dimension of the space spanned by $\left|\mathrm{loc}^{\zeta_1,\zeta_2}_{x_1,x_2}\right\rangle$'s is the same as the rank of the matrix $H^{\sqrt{\pi/S-1}\zeta_1,\sqrt{\pi/S-1}\zeta_2}$, which has a fraction of S/π zero-energy states. Hence there is a fraction of $1-S/\pi$ states $\left|\mathrm{loc}^{\zeta_1,\zeta_2}_{x_1,x_2}\right\rangle$'s that are linearly independent. Because a fraction of $1-S/\pi$ eigenvalues of H^{ζ_1,ζ_2} are zero, $\left|\mathrm{loc}^{\zeta_1,\zeta_2}_{x_1,x_2}\right\rangle$'s span the null space of H^{ζ_1,ζ_2}. Thus, we can construct zero-energy band from the localized states using Eq. (3.31), which completes the proof.

Suppose $S=\pi p/q$ where p,q are coprime integers, there must be $q-p$ zero-energy bands out of q band. According to Eq. (3.22), the Hamiltonian in the momentum

space is given by

$$H^{\zeta_1,\zeta_2}_{x_2,x_2'}(\mathbf{k}) = \sum_{m,n} \exp\left(-\frac{1}{2}\left|z_{m,qn+x_2'-x_2}\right|^2 + i\pi pmn\right)$$
$$\times \exp\left(-i\left(k_1 + p\pi\left(x_2+x_2'\right)/q\right)m - ik_2\left(qn+x_2'-x_2\right)\right). \tag{3.67}$$

The trace of $H^{\zeta_1,\zeta_2}_{x_2,x_2'}(\mathbf{k})$ has a compact form

$$\mathrm{Tr}\left(H^{\zeta_1,\zeta_2}_{x_2,x_2'}(\mathbf{k})\right) = q\sum_{m,n}\exp\left(-\frac{1}{2}\left|z_{qm,qn}\right|^2 - iq\left(k_1 m + k_2 n - \pi pmn\right)\right), \tag{3.68}$$

and the average energy of the positive-energy bands is $\mathrm{Tr}\left(H^{\zeta_1,\zeta_2}_{x_2,x_2'}(\mathbf{k})\right)/p$.

To confirm the zero-energy band is indeed a topological band, we calculate the Chern number of it. Readers can find the definition of the Chern number and how it is related with the Hall conductivity in Appendix E. Because of the robustness of the topological invariant, the Chern number will not change when we change the model continuously without closing the gap. Therefore, we can calculate the Chern number in the simplest case $\zeta_1 = i\sqrt{\frac{\pi}{q}}$, $\zeta_2 = \sqrt{\frac{\pi}{q}}$ and the result applies to arbitrary ζ_1 and ζ_2 as long as $S < \pi$. Now the single eigenstate with positive energy is given by the columns of $H^{\zeta_1,\zeta_2}_{x_2,x_2'}(\mathbf{k})$

$$u^{\zeta_1,\zeta_2}_{\mathbf{k},x_2} = A\sum_{m,n}\exp\left(-\frac{\pi}{2q}\left(m^2 + (qn-x_2)^2\right) + i\pi mn\right) \tag{3.69}$$
$$\times \exp\left(-i\left(k_1 + \pi x_2/q\right)m - ik_2\left(n - x_2/q\right)\right), \tag{3.70}$$

where A is an unimportant normalization constant. So the absolute value of the Chern number of this positive energy band, which equals the absolute value of the Chern number of the flat bands, is 1:

$$|C| = \left|2\,\mathrm{Im}\int_0^{2\pi}\frac{dk_1 dk_2}{2\pi}\sum_{x_2=0}^{q-1}\left(\partial_{k_1}u^{\zeta_1,\zeta_2}_{\mathbf{k},x_2}\right)^*\partial_{k_2}u^{\zeta_1,\zeta_2}_{\mathbf{k},x_2}\right| = 1, \tag{3.71}$$

where the number is obtained using the method of discretization presented in [72].

Last but not least, we want to remark that the Kapit-Mueller model can also be constructed using a projection method [40] which is analogous to the inverse method by treating the LLLs as CLSs. However, using the Gram matrix method, infinite variations of the model, which cannot be regarded as the parent Hamiltonians of the LLLs, can be constructed by modifying the T matrix in Eq. (3.60) according to the protocol introduced in Section 3.2. For example, if we make

$$T\left|m,n\right\rangle = \left|z_{m,n}\right\rangle + e^{iSn}\left|z_{m+1,n}\right\rangle + e^{-iSm}\left|z_{m,n+1}\right\rangle, \tag{3.72}$$

then we will obtain a model with the same zero-energy degeneracy for $S < \pi$ as that of the Kapit-Mueller model, as shown in Fig. 3.3.

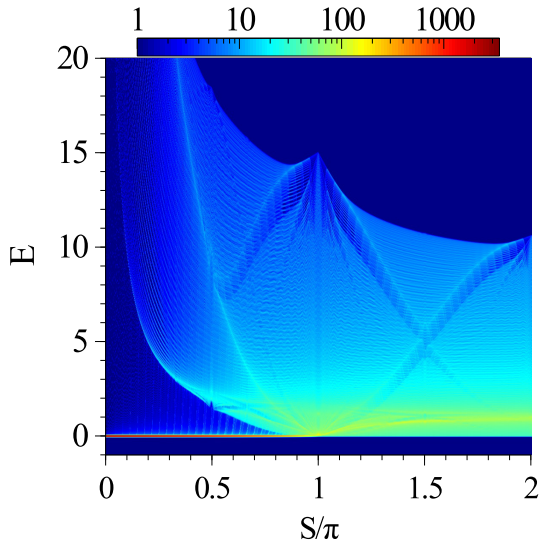

Figure 3.3 : The spectrum of a generalization of the Kapit-Mueller model given by the T matrix Eq. (3.72). The color map has the same meaning as that in Fig. 3.2 (a).

Chapter 4

Summary

The tunability and controllability of AMO systems provided great motivation for engineering Hamiltonians that give rise to novel physics. In this dissertation, we have focused on designing two types of novel Hamiltonians, which lead to generalized multicritical Dicke models and flat-band lattice models, respectively.

Quantum phase transition is an important topic in quantum many-body physics, and has been widely studied. However, most studies focus on second-order phase transition and the associated criticality. Higher-order phase transitions possess unique properties and are of interest of their own. Nevertheless, materials exhibiting multicriticality, not to mention tunable multicriticality, are very rare. Here we propose a simple generalization of the Dicke model where the generalized model supports critical points whose order can be tuned within some extent. Specifically, we replace the two-level atoms in the conventional Dicke model with l-level atoms and study the superradiance phase transition in the modified model. The increased number of tuning parameters for $l > 2$ leads to the emergence of multicriticality whose order can be controlled. The phase diagram and the multicritical conditions can be obtained from the mean-field theory. For a subclass of the multicritical Dicke models, which can be readily realized experimentally, we show that the multicritical conditions of arbitrary order can be expressed analytically in compact forms, which facilitates the realization of phase transition of desired orders. We show that the superradiant phase transition can occur in either the thermodynamic limit or the classical oscillator

limit. The two limits share the same mean-field description but differ significantly in quantum fluctuation. We calculate the atom-photon entanglement entropy to characterize the quantum fluctuation in the generalized Dicke models. In both limits, the non-critical entanglement entropy can be calculated analytically, through some low-energy effective Hamiltonian. In the classical oscillator limit, the entanglement between atoms and photons is vanishingly small away from the critical points. By contrast, in the thermodynamic limit, the non-critical entanglement entropy is finite and can be measured in experiments from cavity field quadrature fluctuations. In the classical oscillator limit, the critical entropy is bounded. In the thermodynamic limit, the entropy diverges logarithmically when approaching the critical point. We numerically calculate the scaling between the critical entropy and the number of atoms and find a logarithmic scaling, and find that higher-order criticality is associated with larger entanglement. The multicritical Dicke model provides deep insights into the physics of quantum phase transition and multicritical points, whose realization is typically very challenging in any other contexts.

Flat-band models often underlie interesting strongly correlated phenomena — due to quenched kinetic energy, weak interaction between particles can lead to dramatic effects. It is desirable to come up with a general protocol to build flat-band models systematically. Here we have proposed a powerful and elegant protocol based on the mathematical properties of Gram matrices. Any lattice model with flat lowest band can be constructed through the method. Our method does not require any elaborate calculations such as solving the inverse eigenvalue problems, works for arbitrary spatial dimensions, and guarantees to produce a flat ground band. We have presented a variety of examples, including both finite- and infinite-range hopping, both ordinary and magnetic translational symmetry, topologically trivial and nontrivial flat bands.

Specifically, we have constructed the d-dimensional Tasaki lattice, a d-dimensional bipartite lattice whose bands are all flat, and the generalized Kapit-Mueller lattice whose flat ground band features universal (i.e., geometry-independent) degeneracy. We study the generalized Kapit-Mueller in detail and, especially, conclude that the (over-)completeness of the coherent states is the origin of the universal degeneracy.

Appendix A

Time-independent perturbation theory

Here we introduce the time-independent perturbation theory derived by Green's functions following the approach in [73].

Consider a time-independent Hamiltonian $\mathcal{H}^{(\lambda)}$ parameterized by a real number λ:

$$\mathcal{H}^{(\lambda)} \equiv \mathcal{H}^{(0)} + \lambda V.$$

The spectrum of $\mathcal{H}^{(\lambda)}$ is expressed by

$$\mathcal{H}^{(\lambda)} = \sum_n \mathcal{E}_n^{(\lambda)} \mathcal{P}_n^{(\lambda)},$$

where $\mathcal{E}_n^{(\lambda)}$'s are the discrete eigenvalues of $\mathcal{H}^{(\lambda)}$ and $\mathcal{P}_n^{(\lambda)}$ is the projecting operator corresponding to the eigenspace of $\mathcal{H}^{(\lambda)}$ with energy $\mathcal{E}_n^{(\lambda)}$. It is assumed that $\mathcal{E}_n^{(\lambda)}$ and $\mathcal{P}_n^{(\lambda)}$ are continuous function of λ, which is true for Hilbert spaces with finite dimensions. We suppose $\mathcal{E}_n^{(\lambda)}$ and $\mathcal{P}_n^{(\lambda)}$ are unknown except for $\lambda = 0$.

The Green's function $\mathcal{G}^{(\lambda)}(z)$ of $\mathcal{H}^{(\lambda)}$ is defined by

$$\mathcal{G}^{(\lambda)}(z) = \frac{1}{z - \mathcal{H}^{(\lambda)}} \equiv \sum_n \frac{\mathcal{P}_n^{(\lambda)}}{z - \mathcal{E}_n^{(\lambda)}},$$

where z is a complex variable. Using the Green's function $\mathcal{G}^{(\lambda)}(z)$ and Cauchy's integral formula, we can express the projecting operator $\mathcal{P}_n^{(\lambda)}$ as

$$\mathcal{P}_n^{(\lambda)} = \int_{\mathcal{E}_n^{(\lambda)}+} \frac{dz}{2\pi i} \mathcal{G}^{(\lambda)}(z),$$

where $\int\limits_{\mathcal{E}_n^{(\lambda)}+} \frac{dz}{2\pi i}$ is integrated along a contour circling counterclockwise around the point $z = \mathcal{E}_n^{(\lambda)}$ on the complex z-plane, without enclosing any other eigenvalue of $\mathcal{H}^{(\lambda)}$.

The following equation holds, relating the inverse of the Green's function $\mathcal{G}^{(0)}$ with that of $\mathcal{G}^{(\lambda)}$:

$$\left(\mathcal{G}^{(\lambda)}\right)^{-1} = \left(\mathcal{G}^{(0)}\right)^{-1} - \lambda V.$$

Then, $\mathcal{G}^{(\lambda)}$ can be expressed formally as a series in λ:

$$\begin{aligned}\mathcal{G}^{(\lambda)} &= \mathcal{G}^{(0)} + \lambda \mathcal{G}^{(0)} V \mathcal{G} \\ &= \mathcal{G}^{(0)} \sum_{k=0}^{\infty} \left(\lambda V \mathcal{G}^{(0)}\right)^k\end{aligned}$$

Now $\mathcal{P}_n^{(\lambda)}$ can be evaluated by the known Green's function $\mathcal{G}^{(0)}$. Expand $\mathcal{G}^{(0)}$ around $z = \mathcal{E}_n^{(0)}$ as

$$\mathcal{G}^{(0)}(z) = \frac{\mathcal{P}_n^{(0)}}{z - \mathcal{E}_n^{(0)}} - \sum_{m \neq n} \frac{\mathcal{P}_m^{(0)}}{\mathcal{E}_m^{(0)} - \mathcal{E}_n^{(0)}} \sum_{l=0}^{\infty} \left(\frac{z - \mathcal{E}_n^{(0)}}{\mathcal{E}_m^{(0)} - \mathcal{E}_n^{(0)}}\right)^l.$$

Then, by exchanging the order of the integration and summation, and collecting all the terms proportional to $\left(z - \mathcal{E}_n^{(0)}\right)^{-1}$, the Cauchy's integral is evaluated as

$$\begin{aligned}\mathcal{P}_n^{(\lambda)} &= \sum_{k=0}^{\infty} \int\limits_{\mathcal{E}_n^{(\lambda)}+} \frac{dz}{2\pi i} \mathcal{G}^{(0)} \left(\lambda V \mathcal{G}^{(0)}\right)^k \\ &= \sum_{k=0}^{\infty} \lambda^k \sum_{\sum_{i=1}^{k+1} k_i = k} S_{k_1} V S_{k_2} V \cdots V S_{k_{k+1}},\end{aligned}$$

where the integral contour is supposed to enclosing $z = \mathcal{E}_n^{(0)}$ but any other pole of $\mathcal{G}^{(0)}(z)$ which can be done when λ is sufficiently small, and S_k is defined as

$$S_k = \begin{cases} \mathcal{P}_n^{(0)}, \text{ when } k = 0, \\ -\sum_{m \neq n} \frac{\mathcal{P}_m^{(0)}}{\left(\mathcal{E}_m^{(0)} - \mathcal{E}_n^{(0)}\right)^k}, \text{ when } k > 0. \end{cases}$$

By defining another projecting operator,

$$\mathcal{Q}_n^{(\lambda)} \equiv 1 - \mathcal{P}_n^{(\lambda)},$$

S_k can be expressed as

$$S_k = \begin{cases} \mathcal{P}_n^{(0)}, \text{ when } k = 0, \\ -\mathcal{Q}_n^{(0)} \left(-\mathcal{G}^{(0)}\left(\mathcal{E}_n^{(0)}\right)\right)_n^{k\mathcal{Q}(0)}, \text{ when } k > 0. \end{cases}$$

Now we obtain the series expansion of $\mathcal{P}_n^{(\lambda)}$ in terms of λ.

In general, we are able to express any analytical function of $\mathcal{H}^{(\lambda)}$ in terms of a power series in λ:

$$\begin{aligned} \left(\mathcal{H}^{(\lambda)} - \mathcal{E}_n^{(0)}\right)^\rho \mathcal{P}_n^{(\lambda)} &= \int\limits_{\mathcal{E}_n^{(\lambda)}+} \frac{dz}{2\pi i} \left(z - \mathcal{E}_n^{(0)}\right)^\rho \mathcal{G}^{(\lambda)}(z) \\ &= \sum_{k=0}^{\infty} \int\limits_{\mathcal{E}_n^{(\lambda)}+} \frac{dz}{2\pi i} \left(z - \mathcal{E}_n^{(0)}\right)^\rho \mathcal{G}^{(0)} \left(\lambda V \mathcal{G}^{(0)}\right)^k \\ &= \sum_{k=\rho}^{\infty} \lambda^k \sum_{\sum_{i=1}^{k+1} k_i = k-\rho} S_{k_1} V S_{k_2} V \cdots V S_{k_{k+1}} \end{aligned} \tag{A.1}$$

Appendix B

Bipartite entanglement entropy of a 2-by-2 density matrix

Given a normalized state $\rho_0 |0\rangle \otimes |0'\rangle + \rho_1 |1\rangle \otimes |1'\rangle$ in which $\langle 0|1\rangle = 0$. We are going to calculate the bipartite entanglement entropy of this state, given the Hilbert space is separated into the space spanned by $|0\rangle, |1\rangle$ and the space spanned by $|0'\rangle, |1'\rangle$.

We have the reduced density matrix $\rho = |\rho_0|^2 |0'\rangle \langle 0'| + |\rho_1|^2 |1'\rangle \langle 1'|$. Set $\rho_2 := \langle 0'|1'\rangle$. If $|1'\rangle = \rho_2 |0'\rangle + \sqrt{1 - |\rho_2|^2}\,|0' - 1'\rangle$, then ρ can be represented in the matrix form

$$\rho = \begin{pmatrix} |\rho_0|^2 + |\rho_1|^2 |\rho_2|^2 & |\rho_1|^2 \rho_2 \sqrt{1 - |\rho_2|^2} \\ |\rho_1|^2 \rho_2^* \sqrt{1 - |\rho_2|^2} & |\rho_1|^2 \left(1 - |\rho_2|^2\right) \end{pmatrix}$$

The eigenvalues of ρ are $\frac{1}{2} \pm \sqrt{\frac{1}{4} - \mu}$, $\mu := |\rho_0|^2 |\rho_1|^2 \left(1 - |\rho_2|^2\right)$. Then

$$\begin{aligned} S_E &= -\mathrm{Tr}\left(\rho \ln \rho\right) \\ &= -\left(\frac{1}{2} + \sqrt{\frac{1}{4} - \mu}\right) \ln \left(\frac{1}{2} + \sqrt{\frac{1}{4} - \mu}\right) \\ &\quad - \left(\frac{1}{2} - \sqrt{\frac{1}{4} - \mu}\right) \ln \left(\frac{1}{2} - \sqrt{\frac{1}{4} - \mu}\right) \\ &\approx -\mu \ln \mu, \text{ if } \mu \to +0 \end{aligned} \tag{B.1}$$

Appendix C

Properties of the phase factor in the projective representation of the translational group in a lattice model

According to Eq. (3.4), the matrices $U_{\mathbf{R}}$'s obey the following composition rule:

$$\begin{aligned} U_{\mathbf{R}}U_{\mathbf{R}'}\left|\mathbf{R}'';i\right\rangle &= e^{i(\phi(\mathbf{R}',\mathbf{R}'',i))}U_{\mathbf{R}}\left|\mathbf{R}'+\mathbf{R}'';i\right\rangle \\ &= e^{i(\phi(\mathbf{R}',\mathbf{R}'',i)+\phi(\mathbf{R},\mathbf{R}'+\mathbf{R}'',i))}\left|\mathbf{R}+\mathbf{R}'+\mathbf{R}'';i\right\rangle \\ &= e^{i\Phi(\mathbf{R},\mathbf{R}',\mathbf{R}'',i)}U_{\mathbf{R}+\mathbf{R}'}\left|\mathbf{R}'';i\right\rangle \end{aligned}$$

in which

$$\Phi\left(\mathbf{R},\mathbf{R}',\mathbf{R}'',i\right):=\phi\left(\mathbf{R}',\mathbf{R}'',i\right)+\phi\left(\mathbf{R},\mathbf{R}'+\mathbf{R}'',i\right)-\phi\left(\mathbf{R}+\mathbf{R}',\mathbf{R}'',i\right). \tag{C.1}$$

$\left(U_{\mathbf{R}+\mathbf{R}'}\right)^{-1}U_{\mathbf{R}}U_{\mathbf{R}'}$ must map any state to itself up to a phase factor [74], and we have

$$\begin{aligned} &\left(U_{\mathbf{R}+\mathbf{R}'}\right)^{-1}U_{\mathbf{R}}U_{\mathbf{R}'}\left(\left|\mathbf{R}'';i\right\rangle+\left|\mathbf{R}'''';i'\right\rangle\right) \\ =\ & e^{i\Phi(\mathbf{R},\mathbf{R}',\mathbf{R}'',i)}\left|\mathbf{R}'';i\right\rangle+e^{i\Phi(\mathbf{R},\mathbf{R}',\mathbf{R}'''',i')}\left|\mathbf{R}'''';i'\right\rangle, \end{aligned}$$

so $\Phi\left(\mathbf{R},\mathbf{R}',\mathbf{R}'',i\right)$ must be independent from $\mathbf{R}''$ and i, and then we use the notation $\Phi\left(\mathbf{R},\mathbf{R}'\right)$.

Let $\mathbf{R}=\mathbf{R}'=\mathbf{0}$ in Eq. (C.1) and we get

$$\Phi\left(\mathbf{0},\mathbf{0}\right)=\phi\left(\mathbf{0},\mathbf{R}'',i\right)\equiv const. \tag{C.2}$$

Without loss of generality, we choose $\phi\left(\mathbf{0},\mathbf{R},i\right)\equiv 0$. Note that the phases are defined modulo 2π. Also, we can make a local gauge transformation such that

$$U_{\mathbf{R}}\left|\mathbf{0};i\right\rangle=\left|\mathbf{R};i\right\rangle.$$

Equivalently speaking

$$\phi\left(\mathbf{R},\mathbf{0},i\right)=0, \tag{C.3}$$

under which Eq. (C.1) becomes

$$\Phi\left(\mathbf{R},\mathbf{R}'\right)=\phi\left(\mathbf{R},\mathbf{R}',i\right), \tag{C.4}$$

such that $\phi\left(\mathbf{R},\mathbf{R}',i\right)$ must also be independent from i. So we can use the notation $\phi\left(\mathbf{R},\mathbf{R}'\right)$.

Also, we note that phase transformation on the $U_{\mathbf{R}}$ matrices, $U_{\mathbf{R}}\rightarrow U_{\mathbf{R}}e^{i\phi(\mathbf{R})}$, will not change the physics and the new $\phi_{\text{new}}\left(\mathbf{R},\mathbf{R}'\right)$ is given by

$$\phi_{\text{new}}\left(\mathbf{R},\mathbf{R}'\right)=\phi_{\text{old}}\left(\mathbf{R},\mathbf{R}'\right)-\phi\left(\mathbf{R}\right)-\phi\left(\mathbf{R}'\right)+\phi\left(\mathbf{R}+\mathbf{R}'\right).$$

So we can always properly choose $\phi\left(\mathbf{R}\right)$ to make

$$\phi_{\text{old}}\left(\mathbf{R},\mathbf{R}\right)-2\phi\left(\mathbf{R}\right)+\phi\left(2\mathbf{R}\right)\equiv 0,$$
$$\phi_{\text{old}}\left(\mathbf{R},-\mathbf{R}\right)-\phi\left(\mathbf{R}\right)-\phi\left(-\mathbf{R}\right)+\phi\left(\mathbf{0}\right)\equiv 0.$$

As a result,

$$\phi\left(\mathbf{R},\mathbf{R}\right)\equiv\phi\left(\mathbf{R},-\mathbf{R}\right)\equiv 0, \tag{C.5}$$

which makes

$$U_{\mathbf{R}}U_{-\mathbf{R}}=e^{i\phi(\mathbf{R},-\mathbf{R})}=1. \tag{C.6}$$

Appendix D

The eigenstates of a lattice model with magnetic translational symmetry

Given the lattice ρ as described under Eq. (3.12), for arbitrary ρ and ρ' in the lattice, both Eqs. (3.12) and (3.13) hold, so

$$\phi\left(\rho,\rho'\right)=0 \text{ or } \pi. \tag{D.1}$$

If we denote $\rho=\sum_{i=1}^{d} y_i\tau_i$, then the matrices

$$U_{\rho}^{\text{lin}}:=\prod_{i=1}^{d}\left(U_{\tau_i}\right)^{y_i} \tag{D.2}$$

form a linear representation of the subgroup of the translational group associated with ρ's as

$$U_{\rho}^{\text{lin}}U_{\rho'}^{\text{lin}}=U_{\rho+\rho'}^{\text{lin}}.$$

It can be show by mathematical induction that U_{ρ}^{lin} is proportional to U_{ρ}:

$$U_{\rho}^{\text{lin}}=\exp\left(-i\rho^2\right)U_{\rho} \tag{D.3}$$

where

$$\rho^2:=\sum_{i=1}^{d}\sum_{i'=i+1}^{d} y_i y_{i'}\phi\left(\tau_i,\tau_{i'}\right), \tag{D.4}$$

which satisfies

$$\left(\rho+\rho'\right)^2=\rho^2+\rho'^2+\phi\left(\rho,\rho'\right). \tag{D.5}$$

Hence, according to the Bloch theorem, the common eigenstate $|\psi_{\mathbf{k},i}\rangle$ of H and U_ρ's satisfies

$$H\,|\psi_{\mathbf{k},i}\rangle = \epsilon_{\mathbf{k},i}\,|\psi_{\mathbf{k},i}\rangle \tag{D.6}$$

$$U_\rho^{\text{lin}}\,|\psi_{\mathbf{k},i}\rangle = e^{-i\rho\cdot\mathbf{k}}\,|\psi_{\mathbf{k},i}\rangle \tag{D.7}$$

$$U_\rho\,|\psi_{\mathbf{k},i}\rangle = e^{-i\rho\cdot\mathbf{k}+i\rho^2}\,|\psi_{\mathbf{k},i}\rangle \tag{D.8}$$

where

$$\mathbf{k} = \sum_{i=1}^{d} k_i\tau^i \tag{D.9}$$

is the pseudo momentum defined on the Brillouin zone $k_i \in [0, 2\pi)$, and τ^i's are the primitive vectors of the reciprocal lattice of the lattice ρ:

$$\tau_i \cdot \tau^j = \delta_{i,j}, \tag{D.10}$$

The index i in $\epsilon_{\mathbf{k},i}$ marks the bands, $i = 1, 2, \ldots, qn_s$. $|\psi_{\mathbf{k},i}\rangle$ is normalized such that

$$\langle\psi_{\mathbf{k},i}|\psi_{\mathbf{k}',i'}\rangle = (2\pi)^d\,\delta\,(\mathbf{k}-\mathbf{k}')\,\delta_{i,i'} \tag{D.11}$$

Because the Hilbert space is divided into invariant subspaces of H with different $\mathbf{k}$'s, we want to find the projectors onto these subspaces. Define local gauge transformation:

$$U^{\mathbf{k}} := \sum_{\mathbf{R},j} e^{i\mathbf{R}\cdot\mathbf{k}}\,|\mathbf{R};j\rangle\,\langle\mathbf{R};j|\,, \tag{D.12}$$

which satisfies

$$\left(U^{\mathbf{k}}\right)^\dagger = \left(U^{\mathbf{k}}\right)^{-1} = U^{-\mathbf{k}} \tag{D.13}$$

and

$$U_{\mathbf{R}}^\dagger U^{\mathbf{k}} U_{\mathbf{R}} = \sum_{\mathbf{R}',j} e^{i\mathbf{R}'\cdot\mathbf{k}}\,|\mathbf{R}'-\mathbf{R};j\rangle\,\langle\mathbf{R}'-\mathbf{R};j| = e^{i\mathbf{R}\cdot\mathbf{k}}U^{\mathbf{k}}, \tag{D.14}$$

$$U^{\mathbf{k}}U_{\mathbf{R}}U^{-\mathbf{k}} = \sum_{\mathbf{R}',j} e^{i\mathbf{R}\cdot\mathbf{k}}e^{i\phi(\mathbf{R},\mathbf{R}'-\mathbf{R})}\,|\mathbf{R}';j\rangle\,\langle\mathbf{R}'-\mathbf{R};j| = e^{i\mathbf{R}\cdot\mathbf{k}}U_{\mathbf{R}}. \tag{D.15}$$

Then we will show that

$$\sum_{\mathbf{r};i} |\mathbf{k},\mathbf{r};i\rangle \langle \mathbf{k},\mathbf{r};i| = \sum_{\rho} U^{\mathbf{k}} U_{\rho}^{\text{lin}} U^{-\mathbf{k}}. \tag{D.16}$$

is the desired projectors, where the momentum state $|\mathbf{k},\mathbf{r};i\rangle$ is given by

$$|\mathbf{k},\mathbf{r};i\rangle = \sum_{\rho} e^{i\mathbf{k}\cdot(\rho+\mathbf{r})} U_{\rho}^{\text{lin}} |\mathbf{r};i\rangle \tag{D.17}$$

where $\mathbf{r}$ is any $\mathbf{R}$ modulo ρ, the position of cells in a single enlarged cell.

First, the momentum state $|\mathbf{k},\mathbf{r};i\rangle$ is indeed having momentum $\mathbf{k}$:

$$\begin{aligned} U_{\rho'}^{\text{lin}} |\mathbf{k},\mathbf{r};i\rangle &= \sum_{\rho} e^{i\mathbf{k}\cdot(\rho+\mathbf{r})} U_{\rho+\rho'}^{\text{lin}} |\mathbf{r};i\rangle \\ &= \sum_{\rho} e^{i\mathbf{k}\cdot(\rho-\rho'+\mathbf{r})} U_{\rho}^{\text{lin}} |\mathbf{r};i\rangle \\ &= e^{-i\mathbf{k}\cdot\rho'} |\mathbf{k},\mathbf{r};i\rangle \end{aligned}$$

Second, $|\mathbf{k},\mathbf{r};i\rangle$'s form a complete orthonormal basis of the Hilbert space:

$$\langle \mathbf{k},\mathbf{r};i|\mathbf{k}',\mathbf{r}';i'\rangle = (2\pi)^d \delta(\mathbf{k}-\mathbf{k}') \delta_{\mathbf{r},\mathbf{r}'} \delta_{i,i'}, \tag{D.18}$$

$$|\mathbf{r}+\rho;i\rangle = \int \frac{d^d\mathbf{k}}{(2\pi)^d} e^{-i\mathbf{k}\cdot(\rho+\mathbf{r})-i\phi(\rho,\mathbf{r})+i\rho^2} |\mathbf{k},\mathbf{r};i\rangle, \tag{D.19}$$

And finally, Eq. (D.16) holds because

$$\begin{aligned} &\langle \mathbf{r}+\rho;i|\mathbf{k},\mathbf{r};i\rangle \langle \mathbf{k},\mathbf{r};i|\mathbf{r}+\rho';i\rangle \\ =&e^{i\mathbf{k}\cdot(\rho-\rho')+i\phi(\rho-\rho',\mathbf{r})+i\rho^2+i\rho'^2} \\ =&e^{i\mathbf{k}\cdot(\rho-\rho')} \left\langle \mathbf{r}+\rho;i|U_{\rho-\rho'}^{\text{lin}}|\mathbf{r}+\rho';i\right\rangle \end{aligned}$$

Now we can map the Hamiltonian into the momentum space. Given that

$$
\begin{aligned}
H = & \sum_{\rho,\mathbf{r},\rho',\mathbf{r}'} \sum_{i,i'} \int \frac{d^d\mathbf{k}}{(2\pi)^d} \frac{d^d\mathbf{k}'}{(2\pi)^d} \\
& h^{i,i'}_{\mathbf{r}+\rho,\mathbf{r}'+\rho'} e^{-i\mathbf{k}\cdot(\rho+\mathbf{r})+i\mathbf{k}'\cdot(\rho'+\mathbf{r}')-i\phi(\rho,\mathbf{r})+i\phi(\rho',\mathbf{r}')+i\rho^2-i\rho'^2} \left|\mathbf{k},\mathbf{r};i\right\rangle \left\langle\mathbf{k}',\mathbf{r}';i'\right| \\
= & \sum_{\rho,\mathbf{r},\rho',\mathbf{r}'} \sum_{i,i'} \int \frac{d^d\mathbf{k}}{(2\pi)^d} \frac{d^d\mathbf{k}'}{(2\pi)^d} h^{i,i'}_{\mathbf{r},\mathbf{r}'+\rho'} e^{-i\mathbf{k}\cdot(\rho+\mathbf{r})+i\mathbf{k}'\cdot(\rho+\rho'+\mathbf{r}')+i\phi(\rho',\mathbf{r}')-i\rho'^2} \left|\mathbf{k},\mathbf{r};i\right\rangle \left\langle\mathbf{k}',\mathbf{r}';i'\right| \\
= & \sum_{\mathbf{r},\rho',\mathbf{r}'} \sum_{i,i'} \int \frac{d^d\mathbf{k}}{(2\pi)^d} h^{i,i'}_{\mathbf{r},\mathbf{r}'+\rho'} e^{i\mathbf{k}\cdot(\rho'+\mathbf{r}'-\mathbf{r})+i\phi(\rho',\mathbf{r}')-i\rho'^2} \left|\mathbf{k},\mathbf{r};i\right\rangle \left\langle\mathbf{k},\mathbf{r}';i'\right|
\end{aligned}
$$

we have

$$
H_{\mathbf{k}} = \sum_{\mathbf{r},\mathbf{r}'} \sum_{i,i'} h^{i,i'}_{\mathbf{r},\mathbf{r}'}(\mathbf{k}) \left|\mathbf{k},\mathbf{r};i\right\rangle \left\langle\mathbf{k},\mathbf{r}';i'\right| \tag{D.20}
$$

$$
h^{i,i'}_{\mathbf{r},\mathbf{r}'}(\mathbf{k}) := \sum_{\rho'} h^{i,i'}_{\mathbf{r},\mathbf{r}'+\rho'} e^{-i\mathbf{k}\cdot(\rho'+\mathbf{r}'-\mathbf{r})+i\phi(\rho',\mathbf{r}')-i\rho'^2} \tag{D.21}
$$

with the inverse transformation

$$
h^{i,i'}_{\mathbf{r},\mathbf{r}'+\rho'} = \int \frac{d^d\mathbf{k}}{(2\pi)^d} e^{i\mathbf{k}\cdot(\rho'+\mathbf{r}'-\mathbf{r})-i\phi(\rho',\mathbf{r}')+i\rho'^2} h^{i,i'}_{\mathbf{r},\mathbf{r}'}(\mathbf{k}) \tag{D.22}
$$

and, according to Eq. (3.7), the symmetry condition

$$
\begin{aligned}
& h^{i,i'}_{\mathbf{r}+\mathbf{r}'',\mathbf{r}'+\mathbf{r}''}(\mathbf{k}) \\
= & \sum_{\rho'} h^{i,i'}_{\mathbf{r},\mathbf{r}'+\rho'} e^{-i\mathbf{k}\cdot(\rho'+\mathbf{r}'-\mathbf{r})+i\phi(\rho',\mathbf{r}'+\mathbf{r}'')-i\rho'^2+i\phi(\mathbf{r}'',\mathbf{r}-\mathbf{r}'-\rho')} \\
= & \sum_{\rho'} h^{i,i'}_{\mathbf{r},\mathbf{r}'+\rho'} e^{-i(\mathbf{k}+\mathbf{k}(\mathbf{r}''))\cdot(\rho'+\mathbf{r}'-\mathbf{r})+i\phi(\rho',\mathbf{r}')-i\rho'^2+i\phi(\mathbf{r}'',\mathbf{r}'-\mathbf{r})} \\
= & h^{i,i'}_{\mathbf{r},\mathbf{r}'}(\mathbf{k}+\mathbf{k}(\mathbf{r}'')) e^{i\phi(\mathbf{r}'',\mathbf{r}'-\mathbf{r})}
\end{aligned} \tag{D.23}
$$

where

$$
\mathbf{k}(\mathbf{r}) := \sum_{i=1}^{d} \left[\phi(\mathbf{r},\mathbf{e}_i) - \phi(\mathbf{e}_i,\mathbf{r})\right] \mathbf{e}^i, \tag{D.24}
$$

given that $\mathbf{e}^i$ is the reciprocal lattice of lattice $\mathbf{R}$

$$
\mathbf{e}_i \cdot \mathbf{e}^j = \delta_{i,j}. \tag{D.25}
$$

If we express $|\psi_{\mathbf{k},i}\rangle$ in the basis of $|\mathbf{k},\mathbf{r};i\rangle$'s,

$$|\psi_{\mathbf{k},i}\rangle = \sum_{\mathbf{r},i'} u^{i',i}_{\mathbf{k},\mathbf{r}} \, |\mathbf{k},\mathbf{r};i'\rangle \,, \tag{D.26}$$

with the normalization condition

$$\sum_{\mathbf{r},i'} \left| u^{i',i}_{\mathbf{k},\mathbf{r}} \right|^2 = 1. \tag{D.27}$$

Then $u^{i',i}_{\mathbf{k},\mathbf{r}}$ diagonalize $h^{i,i'}_{\mathbf{r},\mathbf{r}'}(\mathbf{k})$:

$$h^{i,i'}_{\mathbf{r},\mathbf{r}'}(\mathbf{k}) = \sum_{i''} u^{i,i''}_{\mathbf{k},\mathbf{r}} \epsilon_{\mathbf{k},i''} \left(u^{i',i''}_{\mathbf{k},\mathbf{r}'} \right)^* \tag{D.28}$$

Equation (3.25) requires that $\epsilon_{\mathbf{k},i}$ is periodic in $\mathbf{k}(\mathbf{r})$

$$\epsilon_{\mathbf{k},i} = \epsilon_{\mathbf{k}+\mathbf{k}(\mathbf{r}),i}, \, \forall \, \mathbf{r} \tag{D.29}$$

and

$$u^{i,i'}_{\mathbf{k},\mathbf{r}+\mathbf{r}'} = u^{i,i'}_{\mathbf{k}+\mathbf{k}(\mathbf{r}'),\mathbf{r}} \, e^{i\phi(\mathbf{r},\mathbf{r}')}, \tag{D.30}$$

up to a phase factor depending on $\mathbf{k}$ and i'.

Appendix E

The Hall conductivity of Chern topological band

A Chern topological band has a non-zero Chern number, which is proportional to the Hall conductivity of the band, and is the origin of the quantum Hall effect. Here we compute the Hall conductivity and derive the Chern number.

To compute the Hall conductivity, we define the state $|u_{\mathbf{k},i}\rangle$ in a single enlarged lattice by

$$|u_{\mathbf{k},i}\rangle = \sum_{\mathbf{r},i'} u^{i',i}_{\mathbf{k},\mathbf{r}} |\mathbf{r};i'\rangle . \tag{E.1}$$

$|u_{\mathbf{k},i}\rangle$ with different i's are orthonormal

$$\langle u_{\mathbf{k},i}|u_{\mathbf{k},i'}\rangle = \delta_{i,i'} \tag{E.2}$$

and they are the eigenvectors of the parameterized Hamiltonian restricted to a single enlarged cell:

$$H^{\mathbf{0}}_{\mathbf{k}} := \sum_{\mathbf{r},\mathbf{r}'} \sum_{i,i'} h^{i,i'}_{\mathbf{r},\mathbf{r}'}(\mathbf{k}) |\mathbf{r};i\rangle \langle \mathbf{r}';i'| , \tag{E.3}$$

$$H^{\mathbf{0}}_{\mathbf{k}} |u_{\mathbf{k},i}\rangle = \epsilon_{\mathbf{k},i} |u_{\mathbf{k},i}\rangle . \tag{E.4}$$

Because

$$|\psi_{\mathbf{k},i}\rangle = \sum_{\mathbf{r},i'} u^{i',i}_{\mathbf{k},\mathbf{r}} \sum_{\rho} e^{i\mathbf{k}\cdot(\rho+\mathbf{r})} U^{\mathrm{lin}}_{\rho} |\mathbf{r};i'\rangle = \sum_{\rho} U^{\mathbf{k}} U^{\mathrm{lin}}_{\rho} |u_{\mathbf{k},i}\rangle$$

we have

$$\begin{aligned}
&\left\langle \psi_{\mathbf{k},i} | U^{\delta} | \psi_{\mathbf{k}',i'} \right\rangle \\
=&\sum_{\rho,\rho'} \left\langle u_{\mathbf{k},i} | \left(U^{\mathbf{k}} U^{\mathrm{lin}}_{\rho} \right)^{\dagger} U^{\delta} U^{\mathbf{k}'} U^{\mathrm{lin}}_{\rho'} | u_{\mathbf{k}',i'} \right\rangle \\
=&\sum_{\rho,\rho'} \left\langle u_{\mathbf{k},i} | U^{\mathbf{k}\dagger} U^{\delta} U^{\mathbf{k}'} U^{\mathrm{lin}\dagger}_{\rho} U^{\mathrm{lin}}_{\rho'} | u_{\mathbf{k}',i'} \right\rangle \\
=&\sum_{\rho} e^{-i\rho\cdot(\mathbf{k}-\mathbf{k}'-\delta)} \left\langle u_{\mathbf{k}',i'} \right| U^{\mathbf{k}'} U^{\delta} U^{\mathbf{k}\dagger} \left| u_{\mathbf{k},i} \right\rangle \\
=&(2\pi)^d \, \delta\left(\mathbf{k}-\mathbf{k}'-\delta\right) \left\langle u_{\mathbf{k},i'} | u_{\mathbf{k}-\delta,i} \right\rangle . \qquad \text{(E.5)}
\end{aligned}$$

Thus there can be localized eigenstates of H with energy ϵ_i.

Consider the motion of a wave packet, say, the Wannier state $|W_{\mathbf{0},i}\rangle$ defined in Eq. (3.30), under a constant weak electric field $\mathbf{E}$. The center position of the wave packet $\mathbf{x}_{\mathrm{WP}}$ is given by

$$\mathbf{x}_{\mathrm{WP}} = \sum_{\mathbf{R},j} \langle W_{\mathbf{0},i} | \mathbf{R}; j \rangle \, \mathbf{R} \, \langle \mathbf{R}; j | W_{\mathbf{0},i} \rangle .$$

We want to evaluate the expression using the Bloch waves $|\psi_{\mathbf{k},i}\rangle$'s. However, the position operator $\sum_{\mathbf{R},j} |\mathbf{R}; j\rangle \, \mathbf{R} \, \langle \mathbf{R}; j|$ is ill-defined for the Bloch waves because

$$\begin{aligned}
&\sum_{\mathbf{R},j} \langle \psi_{\mathbf{k},i} | \mathbf{R}; j \rangle \, \mathbf{R} \, \langle \mathbf{R}; j | \psi_{\mathbf{k},i} \rangle \\
=&\sum_{\mathbf{R},j} \langle \psi_{\mathbf{k},i} | \, U^{\mathrm{lin}}_{\rho} \, | \mathbf{R}; j \rangle \, \mathbf{R} \, \langle \mathbf{R}; j | \, U^{\mathrm{lin}\dagger}_{\rho} \, | \psi_{\mathbf{k},i} \rangle \\
=&\sum_{\mathbf{R},j} \langle \psi_{\mathbf{k},i} | \mathbf{R}+\rho; j \rangle \, \mathbf{R} \, \langle \mathbf{R}+\rho; j | \psi_{\mathbf{k},i} \rangle \\
=&\sum_{\mathbf{R},j} \langle \psi_{\mathbf{k},i} | \mathbf{R}; j \rangle \, \mathbf{R} \, \langle \mathbf{R}; j | \psi_{\mathbf{k},i} \rangle - \rho.
\end{aligned}$$

So in calculating the center position of a wave packet using the Bloch waves, the position operator should be replaced by

$$\sum_{\mathbf{R},j} |\mathbf{R}; j\rangle \, \mathbf{R} \, \langle \mathbf{R}; j| = \lim_{\delta \to \mathbf{0}} \frac{U^{\delta} - U^{-\delta}}{2i\delta} \qquad \text{(E.6)}$$

where the limit should be taken after calculating the expectation value of the operator. Then we have

$$\begin{aligned}
\mathbf{x}_{\mathrm{WP}} &= \lim_{\delta\to\mathbf{0}} \langle W_{\mathbf{0},i}| \frac{U^{\delta}-U^{-\delta}}{2i\delta} |W_{\mathbf{0},i}\rangle \\
&= \lim_{\delta\to\mathbf{0}} \int \frac{d^d\mathbf{k}}{(2\pi)^d} \frac{d^d\mathbf{k'}}{(2\pi)^d} \langle \psi_{\mathbf{k},i}| \frac{U^{\delta}-U^{-\delta}}{2i\delta} |\psi_{\mathbf{k'},i}\rangle \\
&= \lim_{\delta\to\mathbf{0}} \int \frac{d^d\mathbf{k}}{(2\pi)^d} \frac{\langle u_{\mathbf{k},i}|u_{\mathbf{k}-\delta,i}\rangle - \langle u_{\mathbf{k},i}|u_{\mathbf{k}+\delta,i}\rangle}{2i\delta} \\
&= \int \frac{d^d\mathbf{k}}{(2\pi)^d} \mathbf{A}_{i,i}(\mathbf{k})
\end{aligned} \tag{E.7}$$

where

$$\mathbf{A}_{i,j}(\mathbf{k}) \equiv \langle u_{\mathbf{k},i}| i\nabla_{\mathbf{k}} |u_{\mathbf{k},j}\rangle , \tag{E.8}$$

is the Berry potential.

With the presence of an electric field $\mathbf{E}$, the Hamiltonian becomes time-dependent:

$$H \to U^{\mathbf{E}t\dagger} H U^{\mathbf{E}t}$$

The velocity $\mathbf{v}_{\mathrm{WP}}$ of the wave packet can be calculated using time-dependent pertur-

bation theory up to $o(\mathbf{E})$:

$$
\begin{aligned}
\mathbf{v}_{\mathrm{WP}} &= \lim_{t\to\infty} \frac{\mathbf{x}_c(t) - \mathbf{x}_c}{t} \\
&= \lim_{t\to\infty} t^{-1} \lim_{\delta\to\mathbf{0}} 2\,\mathrm{Re} \\
&\quad \langle W_{\mathbf{0},i}| \frac{U^{\delta} - U^{-\delta}}{-2i\delta} \left(-i \int_0^t dt' \left(e^{iH(t'-t)} U^{\mathbf{E}t'\dagger} H U^{\mathbf{E}t'} e^{-iH(t'-t)} - H \right) \right) |W_{\mathbf{0},i}\rangle \\
&= \lim_{t\to\infty} t^{-1} \lim_{\delta\to\mathbf{0}} 2\,\mathrm{Re} \\
&\quad \sum_j \int \frac{d^d\mathbf{k}}{(2\pi)^d} \frac{d^d\mathbf{k}'}{(2\pi)^d} \langle \psi_{\mathbf{k},i}| \frac{U^{\delta} - U^{-\delta}}{2i\delta} |\psi_{\mathbf{k}',j}\rangle \\
&\quad \times \langle \psi_{\mathbf{k}',j}| \left(-i \int_0^t dt' \left(e^{iH(t'-t)} U^{\mathbf{E}t'\dagger} H U^{\mathbf{E}t'} e^{-iH(t'-t)} - H \right) \right) |W_{\mathbf{0},i}\rangle \\
&= \lim_{t\to\infty} 2t^{-1}\,\mathrm{Im} \sum_j \int \frac{d^d\mathbf{k}}{(2\pi)^d} \mathbf{A}_{i,j}(\mathbf{k}) \\
&\quad \int_0^t dt' e^{i\epsilon_{\mathbf{k},j}(t'-t)} \sum_{j'} \langle u_{\mathbf{k},j} | u_{\mathbf{k}+\mathbf{E}t',j'} \rangle \, \epsilon_{\mathbf{k}+\mathbf{E}t',j'} \, \langle u_{\mathbf{k}+\mathbf{E}t',j'} | u_{\mathbf{k},i} \rangle \, e^{-i\epsilon_{\mathbf{k},i}(t'-t)} - \epsilon_{\mathbf{k},i}\delta_{i,j} \\
&= \lim_{t\to\infty} 2t^{-1}\,\mathrm{Im} \sum_j \int \frac{d^d\mathbf{k}}{(2\pi)^d} \mathbf{A}_{i,j}(\mathbf{k}) \int_0^t dt' e^{i\left(\epsilon_{\mathbf{k},j} - \epsilon_{\mathbf{k},i}\right)(t'-t)} \langle u_{\mathbf{k},j}| \, \mathbf{E}t' \cdot \nabla_{\mathbf{k}} H^{\mathbf{0}}_{\mathbf{k}} \, |u_{\mathbf{k},i}\rangle \\
&= 2\,\mathrm{Im} \int \frac{d^d\mathbf{k}}{(2\pi)^d} \sum_{j\neq i} \frac{\mathbf{A}_{i,j}(\mathbf{k}) \langle u_{\mathbf{k},j}| \nabla_{\mathbf{k}} H^{\mathbf{0}}_{\mathbf{k}} |u_{\mathbf{k},i}\rangle}{i\left(\epsilon_{\mathbf{k},j} - \epsilon_{\mathbf{k},i}\right)} \cdot \mathbf{E} \\
&= 2\,\mathrm{Im} \int \frac{d^d\mathbf{k}}{(2\pi)^d} \sum_{j\neq i} \mathbf{A}_{i,j}(\mathbf{k}) \, \mathbf{A}_{j,i}(\mathbf{k}) \cdot \mathbf{E} \\
&= -\,2\,\mathrm{Im} \int \frac{d^d\mathbf{k}}{(2\pi)^d} \langle \nabla_{\mathbf{k}} u_{\mathbf{k},i} | \nabla_{\mathbf{k}} u_{\mathbf{k},i} \rangle \cdot \mathbf{E}
\end{aligned}
$$

There is one Wannier function per enlarged unit cell, so the conductivity is given by

$$
\sigma^i = \int \frac{d^d\mathbf{k}}{(2\pi)^d V_c} \mathcal{F}^i_{ab}(\mathbf{k}) \, \tau_a \tau_b
$$

where V_c is the volume of the enlarged unit cell, and

$$
\mathcal{F}^i_{ab}(\mathbf{k}) := i \left[\langle \partial_{k_a} u_{\mathbf{k},i} | \partial_{k_b} u_{\mathbf{k},i} \rangle - \langle \partial_{k_b} u_{\mathbf{k},i} | \partial_{k_a} u_{\mathbf{k},i} \rangle \right] \tag{E.9}
$$

is the Berry curvature. When the lattice is two-dimensional, $V_c = |\tau_1 \times \tau_2|$, and the

Hall conductivity is given by

$$\sigma^i_{\text{Hall}} = \frac{C^i}{2\pi} \tag{E.10}$$

where the first Chern number, an integer topological invariant of the band, is given by

$$C^i := \int \frac{d^2\mathbf{k}}{2\pi} \mathcal{F}^i_{ab}(\mathbf{k}) \tag{E.11}$$

Bibliography

[1] S. M. Brewer, J.-S. Chen, A. M. Hankin, E. R. Clements, C. W. Chou, D. J. Wineland, D. B. Hume, and D. R. Leibrandt, "$^{27}al^{+}$ quantum-logic clock with a systematic uncertainty below 10^{-18}," *Phys. Rev. Lett.*, vol. 123, p. 033201, Jul 2019.

[2] M. H. Anderson, J. R. Ensher, M. R. Matthews, C. E. Wieman, and E. A. Cornell, "Observation of bose-einstein condensation in a dilute atomic vapor," *Science*, vol. 269, no. 5221, pp. 198–201, 1995.

[3] I. I. Rabi, "On the process of space quantization," *Phys. Rev.*, vol. 49, pp. 324–328, Feb 1936.

[4] B. Berche, M. Henkel, and R. Kenna, "Critical phenomena: 150 years since cagniard de la tour," *arXiv preprint arXiv:0905.1886*, 2009.

[5] E. R. Gopal, "Critical opalescence," *Resonance*, vol. 5, no. 4, pp. 37–45, 2000.

[6] R. B. Griffiths, "Thermodynamics near the two-fluid critical mixing point in he^3 - he^4," *Phys. Rev. Lett.*, vol. 24, pp. 715–717, Mar 1970.

[7] E. K. Riedel, "Scaling approach to tricritical phase transitions," *Phys. Rev. Lett.*, vol. 28, pp. 675–678, Mar 1972.

[8] E. K. Riedel and F. J. Wegner, "Tricritical exponents and scaling fields," *Phys. Rev. Lett.*, vol. 29, pp. 349–352, Aug 1972.

[9] A. Hankey, H. E. Stanley, and T. S. Chang, "Geometric predictions of scaling at tricritical points," *Phys. Rev. Lett.*, vol. 29, pp. 278–281, Jul 1972.

[10] R. B. Griffiths, "Proposal for notation at tricritical points," *Phys. Rev. B*, vol. 7, pp. 545–551, Jan 1973.

[11] T. S. Chang, A. Hankey, and H. E. Stanley, "Generalized scaling hypothesis in multicomponent systems. i. classification of critical points by order and scaling at tricritical points," *Phys. Rev. B*, vol. 8, pp. 346–364, Jul 1973.

[12] L. Benguigui and L. Schulman, "Topological classification of phase transitions," *Physics Letters A*, vol. 45, no. 4, pp. 315–316, 1973.

[13] R. B. Griffiths, "Phase diagrams and higher-order critical points," *Phys. Rev. B*, vol. 12, pp. 345–355, Jul 1975.

[14] G. F. Tuthill, J. F. Nicoll, and H. E. Stanley, "Renormalization-group calculation of the critical-point exponent η for a critical point of arbitrary order," *Phys. Rev. B*, vol. 11, pp. 4579–4582, Jun 1975.

[15] T. Chang, D. Vvedensky, and J. Nicoll, "Differential renormalization-group generators for static and dynamic critical phenomena," *Phys. Rep.*, vol. 217, no. 6, pp. 279 – 360, 1992.

[16] K. Hui and A. N. Berker, "Random-field mechanism in random-bond multicritical systems," *Phys. Rev. Lett.*, vol. 62, pp. 2507–2510, May 1989.

[17] Y. Xu and H. Pu, "Emergent universality in a quantum tricritical dicke model," *Phys. Rev. Lett.*, vol. 122, p. 193201, May 2019.

[18] R. H. Dicke, "Coherence in spontaneous radiation processes," *Phys. Rev.*, vol. 93, pp. 99–110, Jan 1954.

[19] H.-J. Zhu, K. Xu, G.-F. Zhang, and W.-M. Liu, "Finite-component multicriticality at the superradiant quantum phase transition," *Phys. Rev. Lett.*, vol. 125, p. 050402, Jul 2020.

[20] D. Campbell, R. Price, A. Putra, A. Valdés-Curiel, D. Trypogeorgos, and I. Spielman, "Magnetic phases of spin-1 spin–orbit-coupled bose gases," *Nat. Commun.*, vol. 7, p. 10897, 2016.

[21] I. Bloch, "Ultracold quantum gases in optical lattices," *Nature physics*, vol. 1, no. 1, pp. 23–30, 2005.

[22] L. Yuan, Q. Lin, M. Xiao, and S. Fan, "Synthetic dimension in photonics," *Optica*, vol. 5, pp. 1396–1405, Nov 2018.

[23] O. Derzhko, J. Richter, and M. Maksymenko, "Strongly correlated flat-band systems: The route from heisenberg spins to hubbard electrons," *International Journal of Modern Physics B*, vol. 29, no. 12, p. 1530007, 2015.

[24] D. Leykam, A. Andreanov, and S. Flach, "Artificial flat band systems: from lattice models to experiments," *Advances in Physics: X*, vol. 3, no. 1, p. 1473052, 2018.

[25] D. Leykam, S. Flach, O. Bahat-Treidel, and A. S. Desyatnikov, "Flat band states: Disorder and nonlinearity," *Phys. Rev. B*, vol. 88, p. 224203, Dec 2013.

[26] M. Goda, S. Nishino, and H. Matsuda, "Inverse anderson transition caused by flatbands," *Phys. Rev. Lett.*, vol. 96, p. 126401, Mar 2006.

[27] R. Chen, D.-H. Xu, and B. Zhou, "Disorder-induced topological phase transitions on lieb lattices," *Phys. Rev. B*, vol. 96, p. 205304, Nov 2017.

[28] A. Zhao and S.-Q. Shen, "Quantum anomalous hall effect in a flat band ferromagnet," *Phys. Rev. B*, vol. 85, p. 085209, Feb 2012.

[29] S. Takayoshi, H. Katsura, N. Watanabe, and H. Aoki, "Phase diagram and pair tomonaga-luttinger liquid in a bose-hubbard model with flat bands," *Phys. Rev. A*, vol. 88, p. 063613, Dec 2013.

[30] M. Bercx, J. S. Hofmann, F. F. Assaad, and T. C. Lang, "Spontaneous particle-hole symmetry breaking of correlated fermions on the lieb lattice," *Phys. Rev. B*, vol. 95, p. 035108, Jan 2017.

[31] R. B. Laughlin, "Anomalous quantum hall effect: An incompressible quantum fluid with fractionally charged excitations," *Phys. Rev. Lett.*, vol. 50, pp. 1395–1398, May 1983.

[32] J. K. Jain, "Composite-fermion approach for the fractional quantum hall effect," *Phys. Rev. Lett.*, vol. 63, pp. 199–202, Jul 1989.

[33] H. L. Stormer, D. C. Tsui, and A. C. Gossard, "The fractional quantum hall effect," *Rev. Mod. Phys.*, vol. 71, pp. S298–S305, Mar 1999.

[34] W. Maimaiti, S. Flach, and A. Andreanov, "Universal $d = 1$ flat band generator from compact localized states," *Phys. Rev. B*, vol. 99, p. 125129, Mar 2019.

[35] A. Ramachandran, A. Andreanov, and S. Flach, "Chiral flat bands: Existence, engineering, and stability," *Phys. Rev. B*, vol. 96, p. 161104, Oct 2017.

[36] M. Röntgen, C. V. Morfonios, and P. Schmelcher, "Compact localized states and flat bands from local symmetry partitioning," *Phys. Rev. B*, vol. 97, p. 035161, Jan 2018.

[37] L. Morales-Inostroza and R. A. Vicencio, "Simple method to construct flat-band lattices," *Phys. Rev. A*, vol. 94, p. 043831, Oct 2016.

[38] W. Maimaiti, A. Andreanov, H. C. Park, O. Gendelman, and S. Flach, "Compact localized states and flat-band generators in one dimension," *Phys. Rev. B*, vol. 95, p. 115135, Mar 2017.

[39] E. Kapit and E. Mueller, "Exact parent hamiltonian for the quantum hall states in a lattice," *Phys. Rev. Lett.*, vol. 105, p. 215303, Nov 2010.

[40] H. Atakişi and M. O. Oktel, "Landau levels in lattices with long-range hopping," *Phys. Rev. A*, vol. 88, p. 033612, Sep 2013.

[41] J. Dong and E. J. Mueller, "Exact topological flat bands from continuum landau levels," *Phys. Rev. A*, vol. 101, p. 013629, Jan 2020.

[42] K. Hepp and E. H. Lieb, "On the superradiant phase transition for molecules in a quantized radiation field: the dicke maser model," *Annals of Physics*, vol. 76, no. 2, pp. 360–404, 1973.

[43] Y. K. Wang and F. T. Hioe, "Phase transition in the dicke model of superradiance," *Phys. Rev. A*, vol. 7, pp. 831–836, Mar 1973.

[44] L. Bakemeier, A. Alvermann, and H. Fehske, "Quantum phase transition in the dicke model with critical and noncritical entanglement," *Phys. Rev. A*, vol. 85, p. 043821, Apr 2012.

[45] T. Holstein and H. Primakoff, "Field dependence of the intrinsic domain magnetization of a ferromagnet," *Phys. Rev.*, vol. 58, pp. 1098–1113, Dec 1940.

[46] N. Lambert, C. Emary, and T. Brandes, "Entanglement and the phase transition in single-mode superradiance," *Phys. Rev. Lett.*, vol. 92, p. 073602, Feb 2004.

[47] N. Lambert, C. Emary, and T. Brandes, "Entanglement and entropy in a spin-boson quantum phase transition," *Phys. Rev. A*, vol. 71, p. 053804, May 2005.

[48] J. Vidal, S. Dusuel, and T. Barthel, "Entanglement entropy in collective models," *J. Stat. Mech. Theory Exp.*, vol. 2007, pp. P01015–P01015, jan 2007.

[49] A. J. Maciejewski, M. Przybylska, and T. Stachowiak, "Full spectrum of the rabi model," *Physics Letters A*, vol. 378, no. 1, pp. 16–20, 2014.

[50] S. J. Masson, M. D. Barrett, and S. Parkins, "Cavity qed engineering of spin dynamics and squeezing in a spinor gas," *Phys. Rev. Lett.*, vol. 119, p. 213601, Nov 2017.

[51] Z. Zhiqiang, C. H. Lee, R. Kumar, K. J. Arnold, S. J. Masson, A. S. Parkins, and M. D. Barrett, "Nonequilibrium phase transition in a spin-1 dicke model," *Optica*, vol. 4, pp. 424–429, Apr 2017.

[52] F. Dimer, B. Estienne, A. S. Parkins, and H. J. Carmichael, "Proposed realization of the dicke-model quantum phase transition in an optical cavity qed system," *Phys. Rev. A*, vol. 75, p. 013804, Jan 2007.

[53] K. Rzażewski, K. Wódkiewicz, and W. Żakowicz, "Phase transitions, two-level atoms, and the A^2 term," *Phys. Rev. Lett.*, vol. 35, pp. 432–434, Aug 1975.

[54] I. Bialynicki-Birula and K. Rzążewski, "No-go theorem concerning the superradiant phase transition in atomic systems," *Phys. Rev. A*, vol. 19, pp. 301–303, Jan 1979.

[55] J. Keeling, "Coulomb interactions, gauge invariance, and phase transitions of the dicke model," *Journal of Physics: Condensed Matter*, vol. 19, p. 295213, jun 2007.

[56] P. Nataf and C. Ciuti, "No-go theorem for superradiant quantum phase transitions in cavity qed and counter-example in circuit qed," *Nature communications*, vol. 1, no. 1, pp. 1–6, 2010.

[57] A. Vukics and P. Domokos, "Adequacy of the dicke model in cavity qed: A counter-no-go statement," *Phys. Rev. A*, vol. 86, p. 053807, Nov 2012.

[58] K. Baumann, C. Guerlin, F. Brennecke, and T. Esslinger, "Dicke quantum phase transition with a superfluid gas in an optical cavity," *Nature*, vol. 464, no. 7293, p. 1301, 2010.

[59] F. Gerbier, A. Widera, S. Fölling, O. Mandel, and I. Bloch, "Resonant control of spin dynamics in ultracold quantum gases by microwave dressing," *Phys. Rev. A*, vol. 73, p. 041602, Apr 2006.

[60] S. R. Leslie, J. Guzman, M. Vengalattore, J. D. Sau, M. L. Cohen, and D. M. Stamper-Kurn, "Amplification of fluctuations in a spinor bose-einstein condensate," *Phys. Rev. A*, vol. 79, p. 043631, Apr 2009.

[61] E. M. Bookjans, A. Vinit, and C. Raman, "Quantum phase transition in an antiferromagnetic spinor bose-einstein condensate," *Phys. Rev. Lett.*, vol. 107, p. 195306, Nov 2011.

[62] C. Cohen-Tannoudji and J. Dupont-Roc, "Experimental study of zeeman light shifts in weak magnetic fields," *Phys. Rev. A*, vol. 5, pp. 968–984, Feb 1972.

[63] L. Santos, M. Fattori, J. Stuhler, and T. Pfau, "Spinor condensates with a laser-induced quadratic zeeman effect," *Phys. Rev. A*, vol. 75, p. 053606, May 2007.

[64] K. Jensen, V. M. Acosta, J. M. Higbie, M. P. Ledbetter, S. M. Rochester, and D. Budker, "Cancellation of nonlinear zeeman shifts with light shifts," *Phys. Rev. A*, vol. 79, p. 023406, Feb 2009.

[65] A. de Paz, A. Sharma, A. Chotia, E. Maréchal, J. H. Huckans, P. Pedri, L. Santos, O. Gorceix, L. Vernac, and B. Laburthe-Tolra, "Nonequilibrium quantum magnetism in a dipolar lattice gas," *Phys. Rev. Lett.*, vol. 111, p. 185305, Oct 2013.

[66] T. Misumi and H. Aoki, "New class of flat-band models on tetragonal and hexagonal lattices: Gapped versus crossing flat bands," *Phys. Rev. B*, vol. 96, p. 155137, Oct 2017.

[67] H. Tasaki, "Ferromagnetism in the hubbard models with degenerate single-electron ground states," *Phys. Rev. Lett.*, vol. 69, pp. 1608–1611, Sep 1992.

[68] B. Sutherland, "Localization of electronic wave functions due to local topology," *Phys. Rev. B*, vol. 34, pp. 5208–5211, Oct 1986.

[69] L. Chen, T. Mazaheri, A. Seidel, and X. Tang, "The impossibility of exactly flat non-trivial chern bands in strictly local periodic tight binding models," *J. of Phys. A: Math. and Theor.*, vol. 47, p. 152001, mar 2014.

[70] A. M. Perelomov, "On the completeness of a system of coherent states," *Theor. Math. Phys.*, vol. 6, pp. 156–164, Feb 1971.

[71] D. R. Hofstadter, "Energy levels and wave functions of bloch electrons in rational and irrational magnetic fields," *Phys. Rev. B*, vol. 14, pp. 2239–2249, Sep 1976.

[72] R. Zhao, G.-D. Xie, M. L. N. Chen, Z. Lan, Z. Huang, and W. E. I. Sha, "First-principle calculation of chern number in gyrotropic photonic crystals," *Opt. Express*, vol. 28, pp. 4638–4649, Feb 2020.

[73] S. Hassani, *Mathematical Physics: A Modern Introduction to Its Foundations*. Springer International Publishing, 2013.

[74] S. Weinberg, *The Quantum Theory of Fields*, vol. 1. Cambridge University Press, 1995.